

# **The Use of Stable Isotope Chronologies in Cephalopod Beaks and Eye Lenses in Trophic Ecology Studies: Among-Tissue Fractionation Patterns and Among-Species Isotopic Niche Overlaps**

**Felix Florida Astejada**

A thesis submitted to the University of Essex in accordance with the requirements for award of the degree of Masters by Research in the School of Life Sciences.

October 2024

Word count:29,832

## Thesis Abstract

This thesis explores the trophic ecology of *Sepia officinalis* in the English Channel using stable isotope analysis (SIA) of  $\delta^{13}\text{C}$  and  $\delta^{15}\text{N}$  to investigate inter-tissue fractionation patterns and potential niche overlap with other marine species. As isotopes of carbon and nitrogen,  $\delta^{13}\text{C}$  reflects the primary sources of carbon in the diet, while  $\delta^{15}\text{N}$  provides insight into an organism's trophic level. Together, these isotopic values allow for feeding habits and habitat use throughout an individual's life to be investigated. *S. officinalis*, an ecologically and commercially important cephalopod, plays a critical role in the English Channel ecosystem. However, its populations face increasing pressure due to overfishing and environmental changes, therefore a deeper understanding of its trophic ecology is essential to the resilience of this species. Chapter 2 focuses on the isotopic differences between various tissues of *S. officinalis*, including archival tissues like eye lenses and beaks, alongside metabolically active muscle tissue. Eye lenses effectively track ontogenetic changes in isotope ratios, while beaks display lower  $\delta^{15}\text{N}$  values, likely influenced by chitin and its morphology. Cross-tissue comparisons allowed for the development of correction factors, enabling more accurate and standardized isotopic measurements across tissues. The study also investigates isotopic niche overlap between *S. officinalis* and co-occurring species (*Cancer pagurus* and *Homarus gammarus*). Significant isotopic overlap could suggest shared dietary and habitat resources, with variability also be linked to differences in their ecology such as life cycles and foraging. These findings provide new insights into tissue-specific isotopic variation and ecological interactions, enhancing our understanding of the role of *S. officinalis* in marine ecosystems and which may help support sustainable fisheries management in the English Channel.

## Acknowledgements

I would like to extend my deepest gratitude to my primary supervisor, Dr Anna Sturrock, whose guidance and support have been instrumental in the completion of this thesis project. I have always admired her drive and accomplishments in our field, and I sincerely hope she continues to excel and inspire others in her future work. I also wish to thank all my co-supervisors and the members of my lab group for their unwavering support throughout my time as a master's student. Your encouragement has meant a great deal to me, and I wish you all continued success in your respective paths.

## **Author's declaration**

I declare that this thesis is an original report of my research, has been written by me and has not been submitted for any previous degree. The experimental work is almost entirely my own work; the collaborative contributions have been indicated clearly and acknowledged

Signed: Felix Astejada

Date: 15/10/2024

## Table of Contents

### Contents

<b>Thesis Abstract</b> .....	2
<b>Acknowledgements</b> .....	3
<b>Author's declaration</b> .....	4
<b>Table of Contents</b> .....	5
Chapter 1 Literature review .....	8
1.1 Introduction.....	8
1.2 Species of interests.....	10
1.2.1 <i>Sepia officinalis</i> .....	10
1.2.2 <i>Sepia elegans</i> .....	12
1.3 Fisheries context.....	13
1.4 Cephalopod response to temperature.....	15
1.4.1 Development and growth .....	16
1.4.2 Distribution .....	17
1.5 Stable isotope analysis (SIA).....	18
1.5.1 Introduction to SIA.....	18
1.5.2 Limitations .....	18
1.5.3 Fractionation, Isotopic Discrimination Factors and Turnover rates.....	19
1.6 Tissues of Interest.....	22
1.6.1 Eye Lenses .....	22
1.6.2 Beaks.....	24
1.6.3 Muscle .....	26
1.7 Research objectives .....	28
Chapter 2: Investigating Among-Tissue Fractionation Patterns in <i>Sepia officinalis</i> from The English Channel .....	31
Abstract.....	31
2.1 Introduction .....	32
2.2 Material and methods.....	39
2.2.1 Cephalopod Samples and Study Site .....	39
2.2.2 Sample Dissection .....	40

2.2.3 Morphological measurements and cuttlebone lamellae counts .....	41
2.2.4 Tissue preparation .....	42
2.2.4.1 Eye lens delamination.....	42
2.2.4.2 Beak sectioning .....	43
2.2.4.3 Muscle preparation .....	44
2.2.5 Stable Isotope Analysis.....	45
2.2.6 Data processing and statistical tests.....	45
2.2.6.1 Cohort and age assignment .....	45
2.2.6.2 Time matching recent growths of archival tissues across individuals ....	46
2.2.6.3 Mixed-effects non-linear (GAMMs) and linear (LMMs) models .....	47
2.2.6.4 Spline model .....	49
2.3 Results.....	49
2.3.1 Relationships between archival tissue size, body size and age .....	50
2.3.2 Lifetime isotopic chronologies.....	52
2.3.3 Multi-tissue isotopic discrimination.....	56
2.4 Discussion .....	61
2.4.1 Relationships between archival tissue size, body size and age .....	61
2.4.2 Trends and comparison of isotope ratios through life .....	62
2.4.3 Multi-tissue isotopic discrimination.....	65
2.4.4 Limitations and caveats.....	67
2.4.5 Conclusion.....	69
Chapter 3: Isotopic Niche Overlap Among Species of Cephalopods and Crustaceans in the English Channel .....	72
Abstract.....	72
3.1 Introduction .....	73
3.2 Material and methods .....	77
3.2.1 Study organisms .....	77
3.2.2 Study site.....	78
3.2.3 Sample collection.....	79
3.2.4 Sample preparation.....	80
3.2.4.1 Cephalopods .....	80
3.2.4.2 Crustaceans .....	81

3.2.5 Stable isotope analysis .....	81
3.2.6 Data analysis .....	83
3.3 Results.....	85
3.3.1 Isotope ratios and body size relationships .....	85
3.3.2 Isotopic niche overlap .....	86
3.3.3 Isotopic niche width and diversity .....	90
3.4 Discussion .....	91
3.4.1 Body size relationships .....	92
3.4.2 Isotopic niche overlap .....	93
3.4.3 Limitations .....	95
3.4.4 Conclusions .....	97
Chapter 4 Future Directions .....	100
Appendices .....	105
References .....	108

# Chapter 1 Literature review

## 1.1 Introduction

Due to high economic interests and non-quota stocks (NQS) status of various cephalopods, such as the Common cuttlefish (*Sepia officinalis*) in the UK, risks of overexploitation are of major concerns (Blue Marine Foundation, 2022). On the other hand, with many commercially important fish stocks already at irreversibly low levels of abundance (Sumaila and Tai, 2020), the importance of cephalopods to a growing global population will become prevalent (Rodhouse et al., 2014). Borges et al. (2023) reports that as a food source, cephalopods is an effective supplementary marine protein source or even as an alternative to fish. In instances of a rapidly shifting environments into warmer conditions favourable to some cephalopods species, further predictions claim that these rapidly adapting and highly proliferating organisms could potentially fill the ecological vacancies left by overexploited fish species (Arkhipkin, 2016).

Cephalopods in general are voracious consumers with most species demonstrating short life cycle, fast growth rates and can reach sexual maturity relatively quickly. These life cycle characteristics are considered to be advantageous in sustaining fishing pressures (Barrett et al., 2022), provided that catch composition rules (e.g. minimum landing size) are implemented and adhered to. Halting the use of destructive fishing methods such as bottom trawling that are commonly used for cuttlefish species and opting to use pots and traps instead would not only be beneficial to sustaining healthy stock levels but also to the conservation of their habitats (Ganias et al., 2021). All this in combination with research-backed management strategies, for example fishery closures, could create a well-balanced fisheries that align with the objectives



of stakeholders including fishers, conservationists, policy makers and the wider general public (Barrett et al., 2022).

Cephalopods are also expected to demonstrate greater plasticity and a faster response to environmental change, especially to temperature, and as such making them good indicators of a changing climate (Boavida-Portugal et al., 2022). Climate change is today's greatest drivers of change in marine ecosystem processes and extending to cephalopod populations and their ecological functions (Boavida-Portugal et al., 2022). As temperatures rise, cephalopod growth rates and abundance are expected to have an overall positive trend in higher latitudes such as the English Channel, potentially leading to proliferation in these regions (Boavida-Portugal et al., 2022). Species like *S. officinalis* could potentially be one of the species to benefit from increasing water temperatures. However, warmer temperatures have also been attributed to negatively impact key life stages such as embryogenesis, as observed with *Octopus vulgaris* (Repolho et al., 2014), and which could later have detrimental effects on growth and recruitment.

Cephalopods have also been documented to partake in large scale movements, from movements between feeding and wintering grounds (Gibson, Atkinson and Gordon, 2016), as response to changes in habitat conditions or tracking the movements of their prey fields. These movements could be key drivers of nutrient connectivity between environments, as they involve the transfer of high biomass from location to location. Notable examples include the migratory patterns of Humboldt squid (*Dosidicus gigas*), which have undergone significant range expansions in the northern California Current System over the past decade, adapting to varying marine oxygen conditions across the Eastern Pacific (Stewart et al., 2012). Additionally, the role of cephalopods in the trophic structure (usually both as predator and prey) and their generalist feeding

behaviour could regard some cephalopod species as a 'keystone' species (Rosa et al., 2013).

In summary, the significance of studying cephalopods, such as *S. officinalis*, extends beyond their economic value, highlighting their role in maintaining marine ecosystem health. The threats of overexploitation and the impact of destructive fishing practices, necessitate immediate conservation efforts. Implementing measures like minimum landing sizes and halting harmful fishing practices are essential steps toward sustainable management. The adaptability of cephalopods and position in the food web not only make them key indicators of environmental change but also potential substitutes for overfished species. Lastly, their migratory patterns potentially enhance ecosystem connectivity, further underscoring their ecological importance.

## 1.2 Species of interests

### 1.2.1 *Sepia officinalis*

The ecology and mode of life of Sepiids such as *S. officinalis* are well-established and documented (Bloor, Attrill and Jackson, 2013). *S. officinalis* exhibits a nekto-benthic lifestyle and typically inhabits subtropical to temperate waters at depths of up to 200 meters (Boletzky, 1983; Jereb and Roper, 2010). They can inhabit a wide range of temperatures, from the Mediterranean Sea to the English Channel. As ectotherms, regional populations exhibit latitudinal differences as predominantly controlled by water temperature and also some indications of dependence on the local climatic conditions, such as hydrological regimes (Keller et al., 2014). However, overall, the subtropical and temperate populations of *S. officinalis* commonly have different life spans as a result of latitudinal differences in temperature (Gras et al., 2016).

Within subtropical climates, *S. officinalis* may exhibit annual life cycles (Goff and Daguzan, 1991). The newly spawned cohorts replace one-year-old adults after mass mortality post-spawning. In subtropical waters, such as the Mediterranean and the Bay of Biscay in Southern Spain, migration patterns are less complex due to relatively constant high temperatures, remaining above 10 °C throughout the year (Guerra and Castro, 1988). Movements and distributions within these habitats seem to be more dependent on the stage of their life cycle instead of seasonal changes in temperature (Hanlon and Messenger, 2018), as spawning can occur all year round, again, due to relatively constant high temperatures (Guerra and Castro, 1988). For example, hatchlings were present in coastal nursery grounds at any point of the year in Mediterranean waters (Basuyaux and Legrand, 2013).

The English Channel is commonly regarded as the northernmost viable habitat for *S. officinalis* (Royer et al., 2006). *S. officinalis* thrives within an optimal temperature range between (15 – 20 °C) (Boyle and Rodhouse, 2008), and while sub-tropical populations tend to exhibit less seasonal variation, those inhabiting the English Channel may be subject to harsher and more unpredictable conditions as a consequent of seasonal fluctuations (Royer et al., 2006).

An extensive review by Bloor et al. (2013) suggests the migration behaviours of populations in the English Channel exhibit a higher degree of complexity, driven primarily by seasonal parameters, such as water temperature, photoperiod lengths, and cyclic food availability that are found in temperate regions. In addition, water currents, salinity, nutrient fluctuations, and trophic interactions can also contribute to the migratory patterns of all populations within its geographic range. In general migration cues are linked to intrinsic behaviours, such as the need to reproduce and

grow, resulting in movements between spawning and feeding grounds (Pierce et al., 2008). However, in the English Channel, these migrations are further mediated by seasonal changes and necessitate over-wintering grounds in deeper waters with higher winter temperatures, particularly in the Western English Channel (Wang et al., 2003).

English Channel *S. officinalis* follow a biannual life cycle, reaching spawning stages after two years (Gras et al., 2016). The Eastern English Channel is a preferred location for their nursery grounds due to the high nutrient input from the terrestrial environment and prevailing currents from west to east (Wang et al., 2003). The spring and summer months provide high productivity due to longer photoperiods, resulting in rapid growth (Koueta and Boucaud-Camou, 2003). In contrast, during autumn and winter, metabolism may slow down in preparation for prey resource scarcity, as they migrate to the Western English Channel, where over-wintering occurs in deeper waters. This slowed metabolism relating to overwintering performance have been mainly observed and studied on other organisms such as Brown trout (Auer et al., 2016) but is likely applicable for other ectotherms such as cuttlefish. The migration between spawning and winter grounds has an estimated duration of two weeks (Bloor et al., 2013). The following spring, individuals that have returned show the first signs of sexual maturation. Between this time and their emigration back to the Western English Channel in autumn, rapid growth and sexual maturation continue. Finally, fully mature adults return to shallow waters to spawn, and mass mortality occurs throughout most of the two-year-old cohorts (Dunn, 1999; Wang et al., 2003).

### 1.2.2 *Sepia elegans*

Like *S. officinalis*, the elegant cuttlefish (*S. elegans*) inhabits subtropical to temperate climates (Mediterranean Sea to the Northeast Atlantic), where it adopts a nekto-benthic

lifestyle in depths of up to 494m. Its range of depth and distribution is also limited by its cuttlebone, similar to *S. officinalis*. It can also generally be found on sandy and muddy substrates (Jereb and Ragonese, 1991; Ragonese and Jereb, 1991).

Reproduction in *S. elegans* occurs all year round in warmer waters, allowing for continuous population recruitment, although there are seasonal peaks. In temperate climates seasonal peaks are likely more exaggerated, however there are few evidence to support this (Gibson, Atkinson and Gordon, 2016).

Eggs are attached to hard substrates like coral or alcyonarian shells, with hatchlings quickly adopting a benthic lifestyle, crucial for their survival and growth (Guerra, 1984). Growth and lifespan are largely influenced by temperature, but other environmental factors also play a role. Males can reach up to 75 mm in mantle length and females up to 89 mm. Sexual dimorphism is likely due to large egg clutch sizes produced by females (Adam, 1952; Ciavaglia and Manfredi, 2009). As small demersal species that reproduce relatively quickly, *S. elegans* exhibit opportunistic diet consisting of small crustaceans, fish, and polychaetes, which is consistent through different life stages.

In fisheries, *S. elegans* is mostly caught as bycatch in the Mediterranean and West Africa. Despite not being a primary target, it forms a large percentage of catch in some areas (Gibson, Atkinson and Gordon, 2016) .

### 1.3 Fisheries context

In the absence of interventions, population collapse of important fisheries species is a major concern, according to Barrett et al. (2022). To mitigate the effects of years of intensive fishing and the global climate crisis, regulatory bodies in the UK have developed plans and initiatives. For instance, the Fisheries Act 2020 outlines sustainability, ecosystem, and climate change objectives and The Channel demersal

non-quota species fisheries management plan (MMO, 2022) is another intervention with a greater emphasis on demersal species from the English Channel such as *S. officinalis*.

Despite clear ecological and economical importance of *S. officinalis*, there are currently no total allowable catch, minimum landing size, or fisheries closures implemented for *S. officinalis* (ICES, 2023). The annual landings of in the EU have reached 40,000t (Jereb et al., 2015) and an annual average of 4,000t in the UK (MMO, 2021). The same MMO report claims that the decrease of *S. officinalis* commercial value from £25.4 million in 2017 to £8.2 million in 2020 could be due to declines in the population abundance rather than reduced fishing efforts. Moreover, neither Covid-19 restrictions nor BREXIT which drastically reduced fishing activities have had a positive influence on stock recovery, further supporting claims that declining commercial values is likely due to decrease in their population rather than changes in fishing practices, as per the MMO report (2021).

In the past, *S. officinalis* was mainly caught as by-catch, but with growing demand, they have become a target species, with the majority of the catch primarily from four countries (UK, France, Spain, and Portugal) (ICES, 2023). As a result of a lack of proper structure such as quotas and species-level identification, catch data are generally misreported and thus underinflated (ICES, 2023). Consequently, assessing these stocks accurately is complex due to insufficient catch data, and additionally, the complex and understudied mode-of-life of cephalopods have made this even more difficult (Gibson et al., 2016).

In the interest of management, a two-stage biomass model was developed by Gras et al. (2014) for assessing the stock of English Channel *S. officinalis*. Their findings

reported a general biomass reduction in recent years and a significant effect of spawning stock biomass and environmental conditions such as water temperature on recruitment. A case study in the Galician waters in the northwest of Spain has drastically improved reports into catch per unit effort based on effective reporting and communication of fishers. In the grand scheme, major fisheries could possibly learn from the practices of these small-scale fisheries (Rocha et al., 2006). A more commercial approach such as the 'Sustainability Toolkit for Cephalopod Fisheries' has also been developed. This document aids fisheries in achieving and maintaining sustainable practices and, in turn, achieving a Marine Stewardship Council (MSC) certification (Roumbedakis et al., 2021). This approach engages environmental sustainability while maintaining a balance with the economic viability of fisheries.

## 1.4 Cephalopod response to temperature

Increasing water temperatures and the rapidly changing conditions brought forth by climate change has a complex effect that is widely debated among researchers. While it is now a general consensus for different fish species that the rapidly changing climate has had detrimental effects on population dynamics and ecological functioning, for cephalopods, it is still currently not understood whether they are benefiting from increasing global temperatures. Fisheries projections such as Doubleday et al. (2016) suggest a general positive correlation of cephalopod catch through time, further adding that increase is not solely related to developing fisheries but higher temperatures also has an effect. On the other hand, in some areas a declining biomass trend related to changing conditions is observable such as *L. forbesii* in the Iberian sea (Chen et al., 2006). A more recent study by Chen et al. (2021), discusses that considering other environmental parameters (such as prey availability and oceanographic processes) alongside temperature could explain distribution and abundance.

### 1.4.1 Development and growth

Temperature is one of the most critical abiotic factors that affects cephalopod recruitment during the early life stages. It plays a crucial role in regulating the timing of embryonic development, physiological and biochemical response. The direct effect of temperature on metabolism determines the duration of egg development and yolk utilization efficiency, which ultimately affects the fitness of pre-recruits (Vidal et al., 2002).

However, it should be noted that individual performance (linked to metabolism) does not seem to be always positively correlated with increasing temperature. In laboratory studies, high temperatures accelerated embryonic development to the point that yolk utilisation was reduced, resulting in smaller and lighter individuals upon hatching (Boletzky, 1975). They concluded that optimum temperature range is required during egg development to produce healthy recruits.

Field studies suggest that intermittent high temperatures can lead to beneficial variability in the timing of hatching. For example, individuals hatched earlier as a result of higher temperature (July), which consequently also hatched at a smaller size, may be released into favourable conditions (August), which results in higher growth rates. On the other hand, individuals that were exposed to lower spring-summer temperatures can maximize yolk utilization and hatch at a good weight and size, this allows the individual to survive for longer in between feeding (Boletzky, 1994; Vidal et al., 2002). Overall, the diversity of hatching timings can counteract and buffer the effects of disturbances. Therefore, temperature plays a crucial role in the early life stages of cephalopods, and its effects are complex and context dependent.



Temperature plays a crucial role in the growth and development of cephalopods. Experimental studies have showcased evidence of a longer lifespan and greater growth of reared *S. officinalis* at lower temperatures (Domingues et al., 2002). In the wild, populations of *S. officinalis* display this difference in physiological attributes depending on the locality, where populations in the English Channel grow larger and for an additional year compared to their Mediterranean counterparts (Gras et al., 2016). Increasing ocean acidification, as a result of warming waters, may affect the development of *S. officinalis* and related species more detrimentally than the direct effects of water temperature alone. Dorey et al. (2013) explored the effects of ocean acidification on the calcification rates of *S. officinalis* cuttlebones. In acidified environments, cuttlebones during embryonic and adult development showed significant growth, consequently negatively affecting both buoyancy and sensitivity to pressure. Squid species are characterized by their extreme sensitivity to acidified environments, related to their blood oxygen transport system, which is intrinsically linked to their high metabolic rates. Potential disruptions to this biochemical process may have adverse effects on their growth and reproduction (Pörtner et al., 2004).

#### 1.4.2 Distribution

Range expansion is the common consensus among cephalopod studies, as evidenced by Borges et al. (2023) and Xavier et al. (2016). These studies examined the effects of a warming climate; moreover, the correlations in distribution shifts can already be observed within the seasonal changes in the spatial distribution of *S. officinalis* egg masses (Laptikhovsky et al., 2023). This study discusses the northward expansion of spawning zones around the UK, which corresponds with seasonal shifts in water temperature. Although *S. officinalis* could potentially expand its range, its physiology and life cycle might still play a role in constraining its distribution. Factors such as

suitable substrates for egg laying and depth limitations could restrict populations of cuttlefish. However, for pelagic squid, expansion may be both rapid and widespread (van der Kooij et al., 2016)

## 1.5 Stable isotope analysis (SIA)

### 1.5.1 Introduction to SIA

Stable isotope analysis (SIA) has emerged as a powerful tool for reconstructing life histories, addressing knowledge gaps in the life cycles of various species, particularly migratory animals like *S. officinalis*, which exhibit variable feeding and habitat use. Analyses of carbon and nitrogen stable isotope ratios ( $\delta^{13}\text{C}$  and  $\delta^{15}\text{N}$  respectively) offer valuable insights into the ecology of organisms (Fry, 2006a). Depending on the specific animal tissue examined, researchers can assess either the most recent a broader spatio-temporal window by studying incrementally growing tissues that archive stable isotope ratios throughout an individual's lifespan.

Life experiences or exposure to different environmental conditions may be influenced by an organism's behaviour or ontogeny. Consequently, SIA can provide crucial information on aspects such as natal origin, migratory pathways, phenology, dietary preferences, and population dynamics (Franzoi, 2016). Compilation of these information enables researchers to reconstruct historical data for various reasons including constructing an ecosystem-based management approach for conservation or for predicting and assessing future and current status of stocks- particularly useful for fisheries management.

### 1.5.2 Limitations

While SIA of animal tissue offers numerous applications, it is not without its limitations and challenges that may hinder the accurate interpretation of stable isotope ratios.

Tissue-specific concerns involve variable turnover rates and fractionation values influenced by factors such as an individual's metabolism, protein synthesis, amino acid pathways, and nutrient allocation (Martinez et al., 2009). These can be further complicated by an organism's physiological parameters, including age, sex, and reproductive status.

In addition to these challenges, variations in environmental conditions and isotopic baseline values also present obstacles for researchers. Factors such as temperature and nutrient availability can alter the ratios by impacting an organism's metabolism and other physiological response to stressors (Martinez et al., 2009). Isotopic baseline values, which can vary both spatially and temporally, are derived from primary productivity in the area at the time of specimen collection (Fry, 2006). These values serve as a crucial starting reference point for stable isotope ratios obtained from animal tissue and are essential for studies focusing on food webs and trophic levels (Post, 2002). Overcoming these limitations is vital for accurately employing SIA to investigate the complex ecological relationships of various organisms.

### 1.5.3 Fractionation, Isotopic Discrimination Factors and Turnover rates

Fractionation refers to the preferential uptake or exclusion of stable isotopes due to differences in atomic mass during physical, chemical, or biological processes (Fry, 2006). Lighter isotopes ( $^{12}\text{C}$  and  $^{15}\text{N}$ ), having fewer neutrons and thus lower atomic mass, react more readily due to weaker bonds and higher vibrational frequencies compared to their heavier counterparts ( $^{13}\text{C}$  and  $^{15}\text{N}$ ). Consequently, heavier isotopes disproportionately accumulate in consumer tissues during assimilation or excretion (Koch et al., 2007), causing shifts in isotopic ratios along trophic and metabolic pathways (Minagawa & Wada, 1984). Fractionation processes can be classified as either kinetic or equilibrium. Kinetic fractionation occurs during incomplete or

unidirectional reactions, where lighter isotopes react faster and heavier isotopes become enriched (Fry, 2006), this is observed during amino acid deamination and ammonia excretion, leading to  $^{15}\text{N}$  enrichment in animal tissues (Martinez del Rio et al., 2009). Equilibrium fractionation, on the other hand, describes isotope partitioning under reversible equilibrium conditions, such examples include the bicarbonate-carbon dioxide exchanges (Peterson & Fry, 1987). Both types of fractionations are influenced by metabolic activity and nutrient rerouting within organisms (Martinez et al., 2009).

Isotopic discrimination factors (IDFs), also referred to as trophic fractionation, quantify the predictable differences in isotope ratios between a consumer's tissues and its diet ( $\Delta = \delta_{\text{tissue}} - \delta_{\text{diet}}$ ) (DeNiro & Epstein, 1981), helping to determine the organism's trophic level. In marine organisms, an enrichment factor of  $<1\text{‰}$  for  $\delta^{13}\text{C}$  and an average of  $3.4\text{‰}$  for  $\delta^{15}\text{N}$  corresponds to a one trophic level increase (Post, 2002; Fry, 2006). This has been supported by studies on cephalopods, including *S. officinalis* (Cherel and Hobson, 2005; Hobson and Cherel, 2006). In a feeding experiment of captive *S. officinalis*, a  $3.3\text{‰}$  enrichment of the  $\delta^{15}\text{N}$  ratio in muscle tissue compared to the diet indicated a slightly above one trophic level increase. Meanwhile,  $\delta^{13}\text{C}$  values adhered to the general rule. Interestingly, no differences between diet and beaks were observed due to chitin effects contributing to  $\delta^{15}\text{N}$  depletion in beak tissue. Changes to  $\delta^{13}\text{C}$  in relation to trophic position are small compared to  $\delta^{15}\text{N}$ , primarily due to its strong association with environmental baseline values. However,  $\delta^{15}\text{N}$  enrichment rules do not always apply to cephalopods. This is because they can supplement their diet from various trophic levels, often through scavenging (Navarro et al., 2013).

Limited information is available on tissue-specific turnover rates for cephalopods, likely due to the challenges in obtaining these results through laboratory feeding experiments. In one such study, Hobson and Cherel (2006) found that muscle tissue in *S. officinalis* displayed a one-trophic-level enrichment compared to the diet fed over 30-60 days. They concluded that the diet was integrated into the muscle within this period. However, the most recently formed regions of beaks (wings) showed no difference, suggesting that the diet was not integrated into this tissue within the same timeframe. Currently, no studies have explored the assimilation length of dietary isotopic ratios into beaks, posing a significant limitation for future research attempting to accurately interpret isotope data. To gain an indicative understanding, recent studies have looked to examples in other organisms, such as fish. According to Sweeting et al. (2005), muscle tissue can have a turnover rate ranging from days to weeks, while harder structures may take months or even years to turn over.

The influence of variables such as temperature, size, and reproductive status on cephalopod muscle tissue is well-established, but less is known about their impact on beaks and eye lenses. In reared European sea bass, tissue-specific fractionation in muscle is affected by temperature, which in turn alters the metabolic pathways for  $\delta^{13}\text{C}$  and  $\delta^{15}\text{N}$  (Barnes et al., 2007). At higher temperatures,  $\delta^{15}\text{N}$  ratios were lower and  $\delta^{13}\text{C}$  ratios were higher due to nitrogen excretion and carbon allocation, respectively. The same study also revealed that lower food intake led to decreased  $\delta^{13}\text{C}$  and  $\delta^{15}\text{N}$  ratios compared to higher intake levels. Moltschaniwskyj and Carter (2013) investigated protein turnover in cephalopod muscle and found that growth and reproductive status influenced turnover rates. Tissue turnover decreased due to reduced somatic growth upon reaching maturity, which may partly explain the short lifespan of cephalopods.

In summary, understanding fractionation and isotopic discrimination factors is vital for assessing their trophic levels and ecological roles for cephalopods including *S. officinalis*. While significant progress has been made, further research on factors influencing beaks and eye lenses, as well as tissue-specific turnover rates, is essential to enhance our knowledge of cephalopod biology and their contributions to marine ecosystems.

## 1.6 Tissues of Interest

Although fish compared to cephalopods have received greater scientific interest and as a result, innovative methods for studying fish throughout ontogeny have been developed, including the use of trace elements and SIA in various tissues such as otoliths and eye lenses (Tzadik et al., 2017; Bell-Tillcock et al., 2021), these techniques have also helped advanced cephalopod research. Stable isotope techniques are transferable to cephalopod tissues like eye lenses, beaks, muscle and statolith and have been used in various successful studies such as the ones reviewed by Xavier et al. (2022). Specific methods mainly used on fish such as eye lens delamination have also allowed researchers to better understand the lifetime trends of stable isotope ratios in cephalopods. Onthank (2013) demonstrated their utility by investigating the isotopic values of Humboldt squid eye lenses and how these values were associated with their ecology.

### 1.6.1 Eye Lenses

The crystalline fibre cells within the eye lenses contain metabolically inert proteins that can record stable isotopic signatures of the environment and diet through sequential deposition of layers (Quaeck-Davies et al., 2018). Eye lenses offer advantages over other cephalopod tissues used in SIA, such as statoliths, which have a smaller amount of organic material and are not ideal for diet reconstruction (Hunsicker et al., 2010;

Chung et al., 2020). In comparison to beaks, muscle, and statoliths, eye lenses offer an all-rounded set of attributes, ideal for lifetime dietary history reconstruction.

Studies on age estimation using eye lenses have mainly been conducted on *O. vulgaris*, and these studies suggest daily growth of lens laminae (Canali et al., 2011). From an SIA perspective, this suggests that eye lens layers are sensitive to diet shifts and movements between habitats and thus may provide a more accurate representation of true isotopic signatures throughout the different life stages of cephalopods. This has been observed in recent studies by Liu et al. (2020) and Zhang et al. (2022), which show that eye lenses may provide an accurate representation of ecological niche through isotopic niche studies. The use of sequential lifetime isotopic signatures also can eliminate the need to sample multiple sizes of the same species, which in turn reduces the potential variations introduced by sampling individuals at different life stages.

Although eye lenses offer an excellent opportunity for sequential lifetime isotopic signatures and diet reconstruction, their use comes with a downside. In most cases, obtaining eye lenses is only possible through lethal sampling, which can be problematic for protected and rare species. Eye lenses are advantageous in that they preserve relatively well, allowing for sampling from decaying carcasses of marine organisms, within a certain timeframe (Osés, 2017). This method has been advantageous for some salmonids that undergo mass mortality post spawn. However, for species like *S. officinalis* (also a terminal spawner), this approach has yet to be used.

Cephalopod eye lenses are formed in two semi-circular halves: the bigger posterior lens and the smaller anterior lens. The posterior lens is the target for delamination

(Onthank, 2013). The eye lenses of *S. officinalis* and *S. elegans* share similar textures and appearances. The outer layers of these lenses are less compact and more prone to flaking, unlike the inner layers, which are more cohesive and can be peeled off in a single piece.

### 1.6.2 Beaks

The beaks of cephalopods, also known as mandibles or jaws, are an essential tool for generalist mode of feeding. These beaks are composed of chitin, a type of polysaccharide, and a complex structure of cross-linked proteins. As a result of this unique combination, cephalopod beaks are renowned for their hardness and rigidity, while also maintaining enough flexibility (Miserez et al., 2008). The formation of beaks begins during embryogenesis and continues throughout a cephalopod's life as successive layers are secreted (Armelloni et al., 2020). Recent research suggests that these layers may serve as a useful tool for age validation of *Octopus vulgaris* (Armelloni et al., 2020) and jumbo squid (*Dosidicus gigas*) (Liu et al., 2017).

An advantage of using beaks for SIA is their ability to provide lifetime chronologies of diet which could be used to infer on trophic dynamics and habitat. Unlike soft tissues, which only provide a snapshot of feeding and habitat isotopic signatures, beak formation chronology can reveal information about an animal's isotopic history throughout its life. In addition, beaks are metabolically inert, meaning that the material is not replaced as the animal grows, making them particularly useful for SIA (Perales-Raya et al., 2014).

Cherel and Hobson (2005) described the three main chronological formations of the lower beaks: the rostrum, the lateral wall, and the tip of the wing. The rostrum, which is the hardest and darkest part of the beak is also the oldest, it signifies the early life stages of cephalopods, while the tip of the wing corresponds to more recent isotopic



signatures. The lateral wall is the intermediate region between the two. These known chronological formations have been used extensively to describe isotopic patterns through life, however they provide low temporal resolutions.

Recently, the hood of upper beaks was used to study the isotopic chronology from birth to death at higher temporal resolutions by sectioning the hood along its growth chronology more frequently. This method leverages the relatively linear growth of the hood, unlike the rostrum, lateral wall, and wing, which exhibit a more complex formation pattern and don't grow on the same plane. However, the chronology of the beak hood also presents challenges, potentially addressed during tissue preparation. The hood grows in a pattern similar to radial propagation, expanding from a small circular point and forming curved growth. The study by Queirós et al. (2020) minimized the overlapping of different time periods by trimming the curved edges, resulting in a strip that represents a more linear growth pattern. Conversely, growth patterns near the rostrum that may contain overlapping time periods (similar to overplating present in fish scales), cannot be easily trimmed (Queirós et al., 2018)

In previous studies, beaks have distinguished ontogenetic patterns in movement and diet. Research analysed beaks from predator stomachs, revealing geographic variations in beak signatures, which helped track albatross foraging and assess its feeding ecology (Alvito et al., 2015). In another study the beak hood facilitated investigation of fine-scale isotopic chronology of elusive giant squids (Guerra et al., 2010). Hobson and Cherel (2006) explored diet signature integration into muscle by comparing it with recent isotopic signatures from the lower beak wing in *S. officinalis*. Despite feeding individuals with prey with known isotopic signatures, limitations in the periodicity of feeding prevented a better understanding of diet integration into muscle tissues.

The chitin present in beaks presents a challenge to accurately interpret the undarkened regions such as the posterior region of the hood, an area of higher chitin concentration. Chitin is naturally depleted in  $\delta^{15}\text{N}$ , which can lower the  $\delta^{15}\text{N}$  values. Several studies have proposed methods to account for the reduced  $\delta^{15}\text{N}$ . One such method is Compound-Specific Isotope Analysis (CSIA), which focuses on analysing individual compounds, such as chitin, to study their different isotopic properties separately. Bulk SIA, on the other hand, measures the average ratio within a single sample (Chere et al., 2019). Although CSIA is much rarer than bulk SIA and requires specialized instruments, it has shown promise in eliminating the effect of chitin.

Another method to account for the effect of chitin is to use correction factors by  $\delta^{15}\text{N}$  of recent growth regions with muscle tissue  $\delta^{15}\text{N}$ , assuming that muscle tissue signatures were integrated within the same time. However, evidence to support this is limited and only has been used in earlier studies such as Cherel and Hobson (2005). On the other hand, Jackson et al. (2006) suggested that the effect should not prevent the comparison of isotopic ratios between individuals. This means that cephalopods collected from the same location and time can still be used to compare variations in their isotopic ratios with the assumption that chitin concentrations do not change among individuals.

### 1.6.3 Muscle

Muscle tissue is widely used in SIA for many terrestrial and marine organisms due to its ease of collection and non-lethal sampling methods for most animal sizes. In contrast, beaks can only be obtained non-lethally from predator droppings or stomachs, whereas eye lenses - another tissue of interest in this review - require lethal sampling. Muscle tissue also requires minimal preparation compared to eye lenses which must undergo delamination (Onthank, 2013). The process of water and lipid

extraction is essential before muscle tissue can be used for SIA. This involves drying, homogenizing, and acid washing to remove excess lipids, which is a relatively straightforward process.

Lipids are known to vary significantly within and between individuals, which can introduce bias in  $\delta^{13}\text{C}$  values. The depletion of  $^{13}\text{C}$  isotopes in lipids compared to proteins is the reason why lipid extraction is commonly performed before SIA (Sweeting et al., 2006). Removing lipids minimises variation and allows for better comparisons of tissue within and among individuals (Post et al., 2007).

However, there is still debate about whether lipid extraction is necessary. Some studies have suggested that the use of solvents in extraction can leech nitrogen isotopes, leading to misleading  $\delta^{15}\text{N}$  values (Sotiropoulos et al., 2004). Other studies have found that lipid extraction can normalise values across the cohort (Post et al., 2007). To determine whether lipid extraction is necessary, researchers have suggested analysing the C:N ratios of samples. A ratio greater than 4 indicates that lipid extraction is advised, while ratios between 2.9 and 3.7 are considered acceptable for marine organisms (Kiljunen et al., 2006).

Muscle tissue is a useful tool for studying the isotopic signatures of feeding and habitat, providing a snapshot of ecological processes occurring prior to the time of sample collection. However, the temporal window available for observation largely depends on the isotopic turnover rate of the tissue, which varies depending on the tissue type, species, age, sex, reproductive status, and environmental conditions (Jackson et al., 2006). Muscle tissue is metabolically active and affected by these biological factors, making it important to consider turnover rates when analysing isotopic signatures. For cephalopods, turnover rates vary greatly, but it is generally agreed that due to their

rapid growth and short lifespan, the isotopic ratios of their diets can be represented in tissue over a period of weeks to months. Unfortunately, specific turnover rates for most cephalopod species are not well understood. Currently, the only available information is from a study by Stowasser et al. (2006) which suggests that the muscle turnover rate of *Lolliguncula brevis* is around four weeks or longer. However, it is important to note that *L. brevis* is a smaller species compared to *S. officinalis* which can grow to more than twice its size.

## 1.7 Research objectives

Firstly, we will explore variations in Carbon and Nitrogen stable isotopes ratios ( $\delta^{13}\text{C}$  and  $\delta^{15}\text{N}$ , respectively) in *S. officinalis*. The goal is to understand the degree of isotopic discrimination in these tissues, especially in recent life stages, by comparing archival tissues to muscle. Such comparisons could potentially uncover tissue-specific fractionations, as well as important correction factors if eye lenses and beaks exhibit significant isotopic discrimination. Muscle isotopic turnover rates are not currently established; thus, supporting evidence for potential turnover rates is vital for advancing future research in this field. Comparing lifelong isotopic chronologies between eye lenses and beaks is also essential for advancing methodological approaches, such as standardising beak sectioning techniques, and for effectively utilising these tissues to reconstruct ecological parameters. This includes improving interpretations of trophic dynamics, community structure, ecological niche, and migration patterns.

Second, muscle  $\delta^{13}\text{C}$  and  $\delta^{15}\text{N}$  of *S. officinalis* collected in 2020 and other cephalopod species with crabs and lobsters collected in 2020 from Lyme Bay marine protected area. The isotopic niche of between these groups could indicate potential resource and habitat similarities if isotopic ratios significantly overlap. In this study levels of

interactions between conspecifics and taxonomic groups could be better understood which may have implications for future studies regarding connectivity and trophic studies within an environmentally and economically important region of the English Channel.



## Chapter 2: Investigating Among-Tissue Fractionation Patterns in *Sepia officinalis* from The English Channel

### Abstract

*Sepia officinalis*, an ecologically and commercially significant cephalopod, has notable gaps in knowledge concerning the variation of  $\delta^{13}\text{C}$  and  $\delta^{15}\text{N}$  isotopic values across different tissues (muscle, beaks, and eye lenses) and how these values align across the life of *S. officinalis*. This study aims to address these gaps by comparing long-term isotopic records preserved in archival tissues with those in metabolically active muscle tissue to understand ontogenetic changes in  $\delta^{13}\text{C}$  and  $\delta^{15}\text{N}$  throughout life. The findings reveal that eye lenses effectively capture non-linear patterns in  $\delta^{13}\text{C}$  isotope profiles, aligning more closely with the expected lifelong movement or dietary history of *S. officinalis*. In contrast, beak profiles displayed unexpected trends. Cross-tissue comparisons of recent growth layers enabled the development of age-based correction factors, offering the potential to standardize isotopic values between beaks and eye lenses across studies. Furthermore, analysis of the full life chronology identified minimal differences in isotope values between individuals of different ages and sampling years, with evidence of discrimination factors through life supporting the gradual diminishing effect of chitin on  $\delta^{15}\text{N}$  values from early to later life stages. This study provides preliminary estimates of correction factors and highlights the differences in isotope values across tissues, offering a framework for translating isotopic data from one tissue type to another. These insights could enhance the understanding of *S. officinalis* trophic ecology and support future research, conservation efforts, and fisheries management strategies.

## 2.1 Introduction

Cephalopods, including cuttlefish, squid, and octopuses, are believed to play a central role in marine ecosystems and are considered 'keystone' species, as they have a vital influence on the ecological functions of their habitats (Pierce and O'dor, 2013). They occupy a central position in the food web as both prey and predators, which is essential for maintaining the balance of food web dynamics and trophic connectivity (Boyle and Rodhouse, 2008). Their rapid growth within a short life cycle of typically two years is driven by their voracious feeding behaviour (Bloor et al., 2013). Economically, they also contribute substantially to global fisheries, highlighting their importance beyond ecological roles (Bobowski et al., 2023).

Since the 1950s, cephalopod landings have risen from 580,500 metric tonnes, peaking at 4 million tonnes in 2007 (Jereb and Roper, 2010). Although global landings have slowed, cephalopods, particularly the common cuttlefish (*Sepia officinalis*), remain commercially exploited in many European countries, including the UK. In 2017, the commercial value of *S. officinalis* reached £25.4 million, but this declined to £8.2 million in 2020 (MMO, 2021). The Marine Management Organisation (2021) suggests this reduction may reflect population declines rather than decreased fishing effort. However, stock assessments for *S. officinalis* and other cephalopods are fraught with uncertainties, largely due to the lack of structured management measures such as quotas and species-level identification, often resulting in misreported catch data (ICES, 2023). In the UK, there are no total allowable catches, minimum landing sizes, or fisheries closures in place for *S. officinalis* (ICES, 2023).

While evidence suggests that rising temperatures may correlate with increased cephalopod abundance (Doubleday et al., 2016), other studies indicate that ocean



acidification, another consequence of warming, could negatively impact cuttlebone development—a critical component for cuttlefish buoyancy control. This, in turn, may affect their migration capabilities and have detrimental consequences for population health (Dorey et al., 2013).

Understanding the complex responses of cephalopods to climate change requires a detailed exploration of their trophic ecology. This is particularly relevant for *S. officinalis*, as their life cycle and population dynamics are highly sensitive to temperature fluctuations (Domingues, Sykes and Andrade, 2002; Gras et al., 2016). In this context, stable isotope analysis (SIA) has proven invaluable, providing insights into the movement and dietary habits of both terrestrial and marine organisms (Post, 2002; Hobson, 2008; Layman et al., 2012; Hobson and Wassenaar, 2018).

$\delta^{13}\text{C}$  and  $\delta^{15}\text{N}$  isotopes in organism tissues can be traced back to their diet, providing insights into trophic level positioning and habitat primary production (Post, 2002; Fry, 2006a; Trueman, MacKenzie and Palmer, 2012). Carbon and nitrogen isotopes undergo fractionation during biochemical processes, such as nutrient assimilation and excretion, in consumer tissues (Fry, 2006a; Martínez del Río et al., 2009). Ratios of heavier to lighter isotopes vary depending on tissue formation and metabolic processes and can yield predictable values in relation to dietary sources (Martínez del Río et al., 2009). Typically,  $\delta^{13}\text{C}$  reflects primary carbon sources with an enrichment factor between 0.5‰ to 1.5‰ per trophic level, while  $\delta^{15}\text{N}$  increases by approximately 3.4‰ with each step up the trophic hierarchy, making  $\delta^{15}\text{N}$  a reliable proxy for trophic level (DeNiro and Epstein, 1978; Minagawa and Wada, 1984) (DeNiro and Epstein, 1978; Minagawa and Wada, 1984). However,  $\delta^{13}\text{C}$  and  $\delta^{15}\text{N}$  fractionation can vary between species. Several factors, such as prey availability and isotope routing, can

contribute to differences among consumers, even within conspecifics (Koch, 2007; Martínez del Río et al., 2009).

Multi-tissue comparisons within species improve our understanding of isotopic discrimination factors and tissue-specific fractionation. Muscle tissues, being metabolically active, provide a snapshot of recent diet and environmental conditions due to their continuous turnover during growth (Cherel et al., 2009). The rapid growth and short lifespan of cephalopods are linked to their high metabolism, which drives the rapid replacement of muscle tissue, reflecting dietary isotopic ratios over shorter timeframes (Fry and Arnold, 1982). In contrast, species with slower growth and lower metabolic rates may integrate isotope ratios over longer periods (Carter, Bauchinger and McWilliams, 2019). Unfortunately, specific turnover rates for most cephalopod species remain poorly understood. The only available data, from Stowasser et al. (2006), suggests that the muscle turnover rate of *Lolliguncula brevis* is approximately four weeks or more. Archival tissues, such as eye lenses and cephalopod beaks, provide lifelong isotopic records, making them invaluable for reconstructing ontogenetic dietary shifts (Meath et al., 2019; Xavier et al., 2022).

The crystalline fibre cells within eye lenses contain metabolically inert proteins that record stable isotopic signatures of the environment and diet through the sequential deposition of layers throughout the individual's life (Quaeck-Davies et al., 2018). Eye lenses offer a key advantage over calcified structures such as statoliths, which are used to study trace elements in some cephalopods (Chung et al., 2021). Unlike calcified structures, the proteins in eye lenses are enriched with  $^{15}\text{N}$  isotopes, facilitating the interpretation of ecological processes related to nitrogen, such as an organism's trophic level (Hunsicker et al., 2010).

Cephalopod beaks are composed of chitin (a polysaccharide), cross-linked proteins, and water (Miserez et al., 2008). Like eye lenses, beak formation begins during embryogenesis and continues throughout the cephalopod's life as successive layers are secreted (Armelloni et al., 2020). Once formed, beak tissues become metabolically inert, providing a chronological record of isotopic variations over the cephalopod's lifespan (Cherel and Hobson, 2005; Xavier et al., 2022). However, beaks undergo structural changes unrelated to metabolism. Dopa-rich proteins at the beak tip repel water, stiffening the tip by becoming predominantly protein, while the rostral tip enriches in chitin (Miserez et al., 2008). This chitin-to-protein gradient is also visible as a darkening of the beak from tip to base (Miserez et al., 2008). Since chitin is naturally depleted in  $^{15}\text{N}$ ,  $\delta^{15}\text{N}$  values are lower in the more pigmented sections of the beak, while the lighter sections are enriched (Hobson and Cherel, 2006; Cherel et al., 2009). Previous studies, such as Cherel and Hobson (2005) used correction factors based on the assumption that muscle tissue isotopic signatures reflect recent growth in the beak and can correct for the  $\delta^{15}\text{N}$  depletion. Compound-Specific Isotope Analysis (CSIA) is a promising method for examining individual compounds, such as protein, separately from others like chitin and lipids (Cherel, Bustamante and Richard, 2019). In this study, we used bulk SIA, which measures the average isotopic ratio within a single sample, emphasising the importance of comparing beak tissue to other tissues that are established to be more reflective of isotopic resources in *S. officinalis* (i.e. muscle and potentially, eye lenses, supported by other work on fish species: e.g. Bell-Tilcock et al. (2021) and Curtis et al. (2020)).

To sample beaks along their chronological growth, careful preparation is required to avoid sampling across different time periods. While the delamination of eye lenses is well-established and relatively simple, achieved by removing consecutive layers and

measuring the diameter throughout, beak sectioning is more delicate and less precise. In this study, the upper beak hood was utilised and sectioned from the rostral tip to the posterior edge. Similar methods were used for the beaks of *Kondakovia longimana*, where changes in feeding habits and trophic position were observed as they grew, with recent sections displaying higher  $\delta^{15}\text{N}$  values compared to older sections closer to the rostral tip (Queirós et al., 2018). The same study suggested that the rostral tip exhibited vertical deposition of beak material, whereas the rest of the hood showed horizontal deposition, indicating that sampling of beak chronology may encapsulate both older and recent growths, especially near the rostral tip. For simplicity, the term ‘overplating’ will be used to describe these overlapping depositions in beak chronology.

By comparing archival tissues, which provide a lifelong isotopic record, with metabolically active tissues, researchers can reconstruct a more comprehensive dietary history. Muscle tissue reflects recent isotopic signals, while eye lenses and beaks offer insights into long-term isotopic patterns. Muscle is widely used in trophic ecology, serving as a reference for recent isotopic ratios due to its well-understood properties. This supports the use of muscle as a proxy for habitat baseline values, with the assumption that it reflects prey recently consumed by *S. officinalis*. This approach minimises potential isotopic variations across years, allowing for comparisons of individuals from different life stages and collection years. Together, these tissues provide a synergistic tool for building accurate historical accounts of an individual’s diet and movement, integral for understanding population dynamics and trophic interactions.

In this study, we explored variations in the morphology and isotopic composition ( $\delta^{13}\text{C}$  and  $\delta^{15}\text{N}$ ) of different tissues from the common cuttlefish (*Sepia officinalis*), including archival tissues (beaks and eye lenses) and metabolically active tissues (mantle

muscle). Our first objective was to describe the relationships between archival tissue size, increment counts, and body size, to assess the utility of each archival tissue for back-calculating size and age through ontogeny.

Secondly, we compared muscle  $\delta^{13}\text{C}$  and  $\delta^{15}\text{N}$  values with those measured in the most recent growth layers of eye lenses and beaks. We hypothesised that  $\delta^{13}\text{C}$  values would be similar among the three tissue types in recent growths and across the entire isotopic chronology, and that the  $\delta^{15}\text{N}$  of recent eye lens laminae would match that of muscle, while beak  $\delta^{15}\text{N}$  would be lower than muscle due to the presence of chitin in beaks and its associated  $^{15}\text{N}$ -reducing effects. Furthermore, we compared lifelong isotopic chronologies between eye lenses and beaks to understand the underlying factors driving variation in  $\delta^{13}\text{C}$  and  $\delta^{15}\text{N}$  and to estimate tissue-specific isotopic fractionation factors. We also examined recent growth chronology in comparison to muscle. We hypothesised that the  $^{15}\text{N}$ -reducing effects of chitin would result in increased fractionation early in the chronology of eye lenses and beaks, with this effect diminishing through life due to the described chitin-to-protein gradient.

Investigating the relationship between archival tissues and body size allows attribution of characteristics of isotopic chronologies from beak and eye lens tissues to specific size and age-classes of *S. officinalis*. These measurements are particularly helpful for studies aiming to track migration or dietary shifts through ontogeny and provenance. In fish, eye lenses have been used to discern size at out-migration and their nursery habitats (Tilcock, 2019). A recent study by Sakamoto et al. (2023) described the movement of *Thysanoteuthis rhombus* from the western North Pacific by estimating mantle length (body size), derived from linear models of intact lens diameter vs. mantle length, for each sampled lamina. Beak relationships with mantle lengths could improve size estimation of cephalopods from beaks preserved in predator stomachs,

consequently improving biomass estimation of species such as *Illex argentinus* (Chen et al., 2012).

Isotopic chronologies in *S. officinalis* beaks have primarily been studied by analysing the rostral tip, lateral wall, and wing to explore early, intermediate, and recent life stages, respectively (Cherel et al., 2009). Our study aims to achieve finer temporal resolution, which has generally been carried out on larger beaks of bigger cephalopod species (Tonder et al., 2021), while also making these chronologies directly comparable to those derived from eye lenses within the same individual. To our knowledge, this study represents the first comparison of isotopic chronologies between beaks and eye lenses in *S. officinalis*. While similar isotope fractionation assessments have been performed in other species, comparisons between archival tissues are rare. Previous studies using metabolically active tissues to observe isotopic values at end of life of fish species and assess tissue fractionation often required sampling the same individual multiple times or using individuals of varying sizes across different sampling events (MacNeil, Skomal and Fisk, 2005; Suring and Wing, 2009). By sampling archival tissues, size biases and the variability in turnover rates related to increasing size or environmental changes can potentially be reduced.

MacNeil et al. (2005) aimed to use different muscle, blood and liver to reveal a more complete understanding of dietary switching in Elasmobranchs and Suring and Wing (2009) used their better understanding of fractionations to improved generic fractionation values to be more tissue-specific. In the case of this study the use of incremental archival tissue can reveal ontogenetic changes, and the fractionations observed between tissues enables a better interpretation of trophic ecology through ontogeny by providing isotopic fractionation factors, which can be specific to different tissues and age (Hobson and Clark, 1992; Carleton and Del Rio, 2010).

Understanding the morphological characteristics of beak and eye lens tissues, such as beak overplating, and how these features can inform future methodological approaches is essential for effectively addressing ecological questions about *S. officinalis* and other cephalopods. For example, while eye lenses are generally considered to provide more detailed isotopic signatures throughout life (Onthank, 2013), the methods used to sample beak chronologies in this study suggest that beaks may offer more reliable isotopic data than previously assumed.

The overall objective of this study is to refine the tools needed to reconstruct the life histories and trophic ecology of *S. officinalis* and other cephalopods through tissue analysis. By improving methods for assessing isotopic variations in beaks, eye lenses, and muscle, we aim to enhance the ability to track dietary shifts throughout ontogeny. The improved understanding of multi-tissue isotopic discrimination will facilitate comparisons across studies of *S. officinalis* from the English Channel, with potential applicability to other populations and species. This enhanced knowledge can contribute to broader ecological and conservation efforts. Ultimately, this research seeks to establish a framework for utilising isotopic data from *S. officinalis* tissues to answer fundamental ecological questions and support the sustainable management of its populations, particularly in the context of climate change and fishing pressures.

## 2.2 Material and methods

### 2.2.1 Cephalopod Samples and Study Site

This study focuses on the analysis of tissues of *Sepia officinalis*, utilising individuals previously obtained in the English Channel through routine CEFAS monitoring surveys conducted from 2017 to 2021 (Table 1). The collection methods involved both trawl

nets and procurement from local fisheries (all samples of *S. officinalis* from 2020 were commercially obtained). Samples (whole animals) were stored at -20°C.

The English Channel, a crucial study area, spans approximately 750 km from the Western English Channel to the Eastern English Channel covering a total surface area of 77,000 km<sup>2</sup> (Dauvin, 2019). Distinguished by its diverse benthic habitats, the Western Channel, with a maximum depth of 174 meters, differs notably from the shallower Eastern channel, which has a depth of about 50 meters (Larsonneur et al., 1982).

### 2.2.2 Sample Dissection

Mantle length was measured, then a longitudinal incision was made along the mantle's ventral side to expose the internal organs. Sex and maturity stage were estimated based on the appearance of the reproductive organs and the *S. officinalis* scale outlined in ICES (2010).

Mantle muscle samples were extracted from the underside of the body, near the head and adjacent to the gill area with subsequent removal of the skin and thorough washing with milli-Q water to eliminate residues.

The upper and lower beaks were excised and separated, followed by the careful removal of any residual soft tissue, and then were thoroughly washed in MQ before freezing. Both left and right eye lenses were removed from the eyes and collected. Subsequently, muscle samples, beaks, and eye lenses were promptly stored at -20°C. Cuttlebones were extracted, air dried, and stored at room temperature.



### 2.2.3 Morphological measurements and cuttlebone lamellae counts

Cephalopod eye lenses form as two hemispherical sections (Fig. 3). The smaller anterior section (Fig. 3) was removed and discarded, and eye lens diameter was estimated by measuring the diameter of the larger posterior half using a stereoscope at X magnification and GXcapture-T software. Upper beak hood measurements (Fig. 1) were collected using a two-decimal-place calliper.

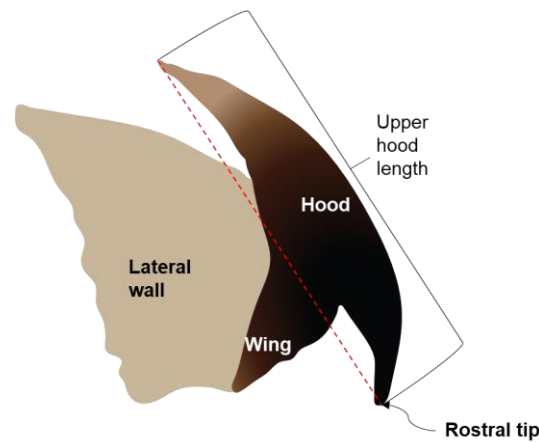


Fig. 1: A diagrammatic representation illustrating morphometric measurements of the upper beak in *S. officinalis*. Both measurements were taken from the rostral tip to the free corner for lateral wall length and to the posterior edge of the hood for upper hood length.

For cuttlebone lamellae counts, images of the cuttlebone were captured by stitching images taken from the anterior (edge) to the posterior (core) regions at varying magnifications to achieve higher image resolution, especially for thinly spaced lamellae closer to the core (Fig. 2). Subsequently, these images were stitched together using Hugin, an image stitching software. Finally, employing a tree ring counting tool on Image J, each lamella was diligently counted (Fig. 2). Figure 2 shows blue pen marks, dotted from the edge to the core, which were applied during the manual counting of each lamella. This method was replicated on four additional

cuttlebones to validate and confirm the accuracy of digital lamellae counting.

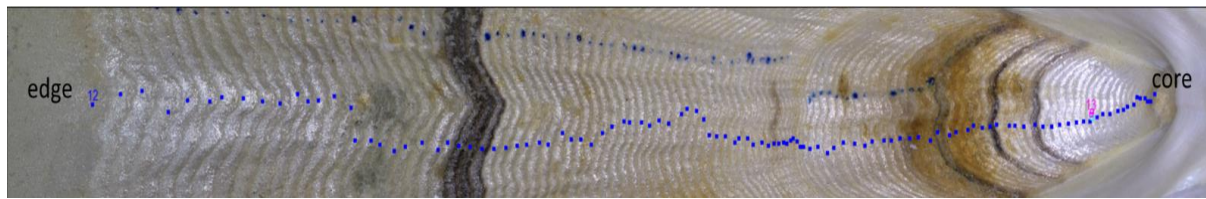


Fig. 2: Stitched image of *S. officinalis* cuttlebone. Each blue square represents a counted lamella.

## 2.2.4 Tissue preparation

### 2.2.4.1 Eye lens delamination

Both eye lenses and beaks were subsampled to reconstruct changes in  $\delta^{13}\text{C}$  and  $\delta^{15}\text{N}$  over each individual's lifespan using the methods outlined below. Eye lens delamination is the process of peeling layers of sequentially deposited crystallin fibre cells or laminae (Fig. 3). The delamination method employed in this study is an adaptation of the approach outlined by Wallace et al. (2014), originally designed for teleost eye lenses.

Given the challenges associated with peeling one layer at a time, the cost associated with each sample, and the necessity to meet mass requirements for stable isotope analysis, multiple laminae were often combined into a single analysis, particularly for layers closer to the core that have a smaller diameter and less material. The outermost lamina is characterised by a gelatinous consistency and greater thickness compared to consecutive layers. Subsequent laminae are more compacted and easier to peel, particularly when kept hydrated using droplets of milli-Q water. After the removal of each lamina or group of laminae, the lens diameter was re-measured until eye lens measured approximately 1000  $\mu\text{m}$  diameter. 1000  $\mu\text{m}$  was decided to be the target diameter to stop lens delamination to ensure the innermost lamina did not weigh below 0.0002g. Samples were air-dried in tin capsules, weighed to the nearest 0.00001g,

then crimped (sealed closed, pressed and shaped into a ball) and sent off for isotope analysis. Notably, only one eye lens was utilised per individual to allow archiving of the second lens for other purposes.

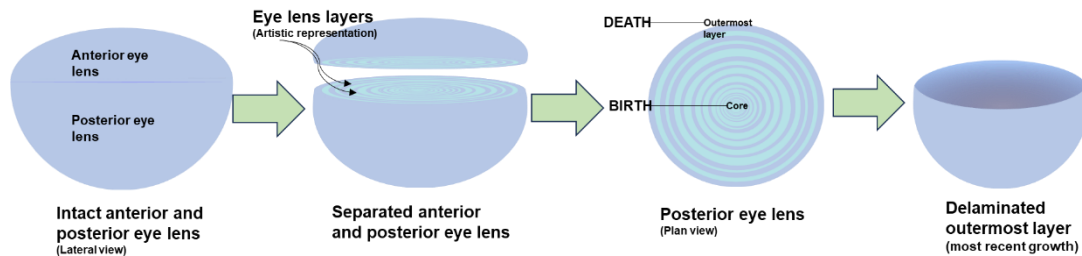


Fig. 3: Preparation of *S. officinalis* eye lens for stable isotope analysis. The posterior eye lens is separated from the anterior eye lens. Group layers are delaminated from the intact posterior lens. This is repeated until ~1mm eye lens diameter is reached.

#### 2.2.4.2 Beak sectioning

For stable isotope analysis, only the upper beak hoods were utilised adapted from the previous work of Queirós et al. (2018). The sectioning process began by separating the upper hood from the rest of the upper beak using a thin stainless-steel saw for the harder, darkened parts and a stainless steel nail clipper for the softer, undarkened regions. Once separated, the hood was shaped into a long rectangular strip by clipping off either side of the longest plane, maintaining symmetry throughout (Fig. 4). Extra care was taken for the darkened regions, especially those close to the rostrum, as they are harder and more likely to crack or shatter. Trimming the hood was carried out to minimise integration of different time periods due to the curved growth pattern of the beak (Fig. 4C), similar to the methods from Queirós et al. (2018) and expert advice from J. Queirós pers. comm. (2023).

The upper hood was sectioned from the darker rostral tip (start of life) to the posterior undarkened region (most recent growth) (Fig. 4). Starting with the undarkened region (most recent growth), sections progressed towards the rostral tip (oldest growth). Planned sections lengths were estimated based on eye lens samples (see time

matching section below) then measured using callipers, marked with a scalpel, and cut using nail clippers, all within a clear plastic bag to prevent the loss of clippings. Each section was chronologically arranged in a drying container then dried in an oven for 24-28 hours at 65°C. Larger sections were homogenised using an agate pestle and mortar then added to tin cups and crimped then weighed. The pestle and mortar were cleaned with ethanol and milli-Q water after each use. Smaller sections were added directly to tin cups, crimped and weighed.

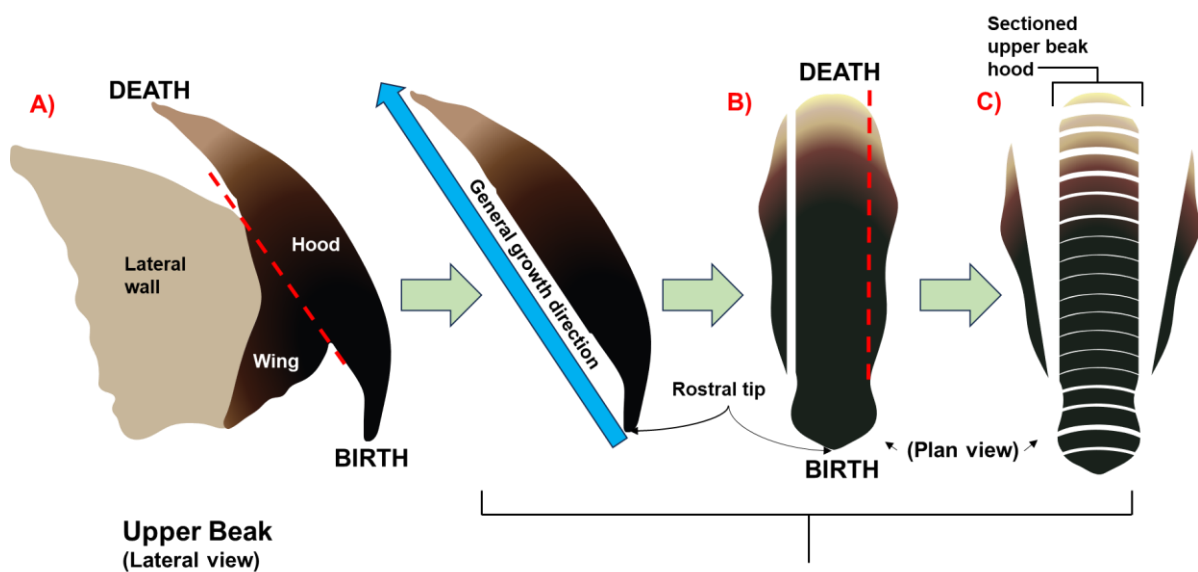


Fig. 4: Preparation of *S. officinalis* upper beak hood for stable isotope analysis. The hood is separated from the upper beak along the dashed red line (A) and further trimmed down on both sides (B) to reduce overlap of different growth periods, the trimmed areas are discarded. The trimmed hood is then sectioned from the undarkened posterior towards the rostral tip (C).

#### 2.2.4.3 Muscle preparation

To prepare muscle samples for isotopic analysis, the muscle tissues were defrosted, cleaned again with MQ water, then dried for 24-48 hours at 65°C. A portion of muscle approximately 1cm<sup>3</sup> was broken off and homogenised using an agate pestle and mortar, ensuring that the equipment was cleaned with 28.5% ethanol then MQ water then dried thoroughly after every use. The homogenised tissue was then added to tin cups, crimped and weighed.

## 2.2.5 Stable Isotope Analysis

Stable isotope ratio analysis was performed at the Laboratório de Isótopos Estáveis LIE - Stable Isotopes Analysis Facility, at the Faculdade de Ciências, Universidade de Lisboa - Portugal.  $\delta^{13}\text{C}$  and  $\delta^{15}\text{N}$  in the samples were determined by continuous flow isotope mass spectrometry (CF-IRMS) (Preston and Owens, 1983), on a Sercon Hydra 20-22 (Sercon, UK) stable isotope ratio mass spectrometer, coupled to a EuroEA (EuroVector, Italy) elemental analyser for online sample preparation by Dumas-combustion. Delta Calculation was performed according to  $\delta = [(R_{\text{sample}} - R_{\text{standard}})/R_{\text{standard}}] \times 1000$ , where R is the ratio between the heavier isotope and the lighter one.  $\delta^{15}\text{N}_{\text{Air}}$  values are referred to Air and  $\delta^{13}\text{C}_{\text{VPDB}}$  values are referred to PDB (Pee Dee Belemnite). The reference materials used were IAEA N1, IAEA N2 and USGS26, and Glucose BCR no. 657, IAEA-CH7 and IAEA-C3 (Coleman and Meier-Augenstein, 2014); the laboratory QC check used was Rice Flour. Uncertainty of the isotope ratio analysis, calculated using values from 6 to 9 replicates of laboratory standard interspersed among samples in every batch of analysis, was  $\leq 0.2\text{‰}$ . The major mass signals of N and C were used to calculate total N and C abundances, using Wheat Flour Standard OAS (Elemental Microanalysis, UK, with 1.47%N, 39.53%C) as elemental composition reference materials.

## 2.2.6 Data processing and statistical tests

### 2.2.6.1 Cohort and age assignment

Given that stable isotope baselines can vary among years (Fry, 2006b) and life stages (Hobson, 1999), we estimated capture age and hatch year (cohort) for each individual to maximise time matching across individuals and tissue samples. To estimate the age of each *S. officinalis* individual we assumed a maximum lifespan of 24 months, with most individuals around the UK thought to exhibit a 24-month life cycle with some

exhibiting 12 (Dunn, 1999; Gras et al., 2016). Given that all individuals were caught in March or June, and peak spawning occurs between May and July (Bloor, Attrill and Jackson, 2013), we inferred June as the peak spawning month because it falls in the middle of this range. Consequently, we assumed that these individuals were either in their first or second year of life. Density distributions (normalmixEM function from mixtools R package) of mantle length, eye lens diameter, upper beak hood and cuttlebone laminae counts were generated, confirming bimodal distributions across all metrics. Given that ageing *S. officinalis* is complex and difficult, and only have seen some success in juveniles by using beak microstructures (Guerra-Marrero et al., 2023), we instead used the cuttlebone lamellae counts (as a proxy for age) to assign individuals as year 1 or year 2 age-class based on whether their counts were above or below the root of the superimposed density lines of the bimodal distribution. To help refine individual ages, we assumed a uniform hatch month of June thus an individual caught in June and assigned as year 1 was categorised as age 1 class while an individual caught in March and assigned as year 1 was categorized as age 0.75 class (Table 1). In contrast, individuals assigned to the second mode were exclusively collected in June and were thus all assigned age 2 class, suggesting that they were all nearing the end of their life.

#### 2.2.6.2 Time matching recent growths of archival tissues across individuals

To compare isotope chronologies among tissue types, we temporally aligned the samples from two archival tissues: eye lens laminae and upper beak hood sections. Approximately the last four months of growth were estimated for beaks and eye lenses by calculating the difference in mean size (lens diameter and hood length) between 0.75- and 2-year-olds and dividing this value by the difference in age (15 months). Individuals were excluded if their most recent growth layer exceeded four months.

$\delta^{13}\text{C}$  and  $\delta^{15}\text{N}$  values from all layers within the last four months were averaged or retained their original value if a single growth layer spanned four months. These isotope values were compared to investigate tissue isotopic fractionations (Fig. 8 and 9).

#### 2.2.6.3 Mixed-effects non-linear (GAMMs) and linear (LMMs) models

Initial visual inspections of all combinations of archival tissues, sampling years (SY), and isotopes suggested that non-linear models were appropriate for  $\delta^{13}\text{C}$ , while linear models were more suitable for  $\delta^{15}\text{N}$  (Fig. 7). Therefore, mixed-effects non-linear (GAMMs) and linear (LMMs) models were used to investigate differences in  $\delta^{13}\text{C}$  and  $\delta^{15}\text{N}$  between eye lenses, beaks and muscle among SY (2017, 2020 and 2022). Further examination of model outputs supported the use of non-linear models for  $\delta^{13}\text{C}$  and linear models for  $\delta^{15}\text{N}$ . The inclusion of archival tissue as a term in each GAMM and LMM allowed the model to assess and compare the distinct isotopic trends in beak versus eye lens tissues, while the nested structure captured random individual-specific variability across repeated measurements. All assumptions for the models, including homoscedasticity and normality of residuals, were tested and confirmed through Q-Q and residual plots.

Additionally, several model variations were formulated for both  $\delta^{13}\text{C}$  and  $\delta^{15}\text{N}$  data sets. First, each sample year and tissue type were modelled separately. Next, a combined model including sample year and archival tissue as fixed effects was developed. However, no significant differences were found among sample years, indicating that this variable could be removed. This simplified model was confirmed as the most parsimonious based on both the Corrected Akaike Information Criterion (AICc) and degrees of freedom. Additional model variations, incorporating smoothing variables with and without random-effect terms, were also tested, and the final model

presented below provided the best overall fit. AICc was selected due to the relatively small sample size, but standard AIC also confirmed this result.

The general formula for the GAMMs used to analyse  $\delta^{13}\text{C}$  was:

$$y \sim \text{archival tissue} + s(x, \text{by} = \text{archival tissue}) + s(x, \text{Individual ID}, \text{bs} = \text{"re"}) + s(\text{Individual ID}, \text{bs} = \text{"re"})$$

where  $y$  represents isotope values,  $x$  is a continuous variable indicating a relative age scale used as a predictor for both *archival tissue* (beak and eye lens), and *Individual ID* represents the unique identifier for each individual. The term “re” stands for random effect and is used to model the random individual-specific variability across repeated measurements (nested data).

The general formula for the LMMs used to analyse  $\delta^{15}\text{N}$  was:

$$y \sim x + \text{archival tissue} + (x \mid \text{Individual ID})$$

where  $y$  represents  $\delta^{15}\text{N}$  values,  $x$  is a continuous variable reflecting relative age, and archival tissue refers to either beak or eye lens. The model included repeated measures within individuals, with random effects assigned to each *Individual ID*, allowing for the comparison of  $\delta^{15}\text{N}$  trends between *archival tissues* while accounting for variability at the individual level.

Additionally, LMs were fitted for the isotope ratios of muscle through increasing mantle length (body size) for all samples and was also separately fitted for each SY (Fig. 7e, 7h). This analysis aims to capture population-level isotope trends through ontogeny, similar to individual-level trends observed in archival tissues. However, while individual trends theoretically begin at age 0, population-level trends are constrained by the



smallest available size (mantle length = 7.5 cm, corresponding to age class 0.75). As a result, the analysis does not reflect the earliest life stages of the population.

#### 2.2.6.4 Spline model

Initially, a capture age was estimated using the capture date and lamellae count. Growth layers were then assigned a relative age based on the tissue size relative to its final size at capture, allowing a relative age scale to be used as a common predictor for both beak and eye lens. Using the “smooth.spline” function in the splines R package, a spline model was fitted to predict  $\delta^{13}\text{C}$  and  $\delta^{15}\text{N}$  values for beak and eye lens lifetime chronology. Each set of 21 predicted isotope data points for beak tissue was subtracted from eye lens values for the same individual, and these differences were analysed to investigate lifetime isotopic fractionations across all individuals (Fig. 10). Similarly to other analysis as mentioned in 2.6.3, GAMMs were fitted for  $\delta^{13}\text{C}$  and LMMs for  $\delta^{15}\text{N}$ .

## 2.3 Results

The isotopic composition of  $\delta^{13}\text{C}$  and  $\delta^{15}\text{N}$  was measured across beak, eye lens, and muscle tissues of *Sepia officinalis* collected in 2017, 2020, and 2022. The samples spanned estimated age classes of 0.75, 1, and 2 years, with mantle lengths ranging from 7.5 cm to 24 cm (Table 1). While individual layers were sometimes combined in order to reach the minimum mass requirements, the maximum number of chronological layers successfully analysed from a single individual was 21 eye lens laminae and 14 beak segments from a one year old individual and 21 and 24 from a two year old individual. The range of observed  $\delta^{13}\text{C}$  values were consistently higher in the archival tissue types, ranging from -22.30‰ to -13.44‰ (beak), and -22.41‰ to -13.76‰ (lens) compared to -18.75‰ to -17.05‰ for muscle (Table 1).

Similarly, the minimum  $\delta^{15}\text{N}$  values were consistently lower in the archival tissues, but the maximum values more similar, ranging from 5.5‰ to 14.3 ‰ (beak), and 9.8‰ to 14.6‰ (lens) compared to 11.9‰ to 14.5‰ for muscle (Table 1).

Table 1: Summary information of all *Sepia officinalis* samples analysed in this study. For each tissue type (beak, eye lens and muscle) the mean number of layers (laminae in eye lenses and segments of beak) analysed per individual are shown, alongside their  $\delta^{13}\text{C}$  and  $\delta^{15}\text{N}$  ranges.

Sampling month & year	Estimated age	N samples	Mantle length range (mm)	Tissue type	Mean N layers	$\delta^{13}\text{C}$ range	$\delta^{15}\text{N}$ range
March 2017	0.75	8	7.5 - 11.5	beak	6	-20.503 - -13.443	6.003 - 9.785
				eye lens	5	-22.071 - -15.669	9.845 - 12.888
				muscle	N/A	-18.751 - -17.051	11.878 - 13.566
June 2020	1	8	11 - 15	beak	12	-22.295 - -14.414	5.521 - 11.197
				eye lens	11	-22.409 - -13.757	10.227 - 14.514
				muscle	N/A	-18.358 - -17.308	12.224 - 13.646
June 2022	1	3	14 - 15	beak	11	-20.953 - -14.178	7.198 - 11.931
				eye lens	19	-21.369 - -14.333	12.116 - 14.602
				muscle	N/A	-18.472 - -17.341	14.013 - 14.109
June 2022	2	6	20.5 - 24	beak	18	-21.212 - -13.662	6.929 - 14.312
				eye lens	20	-21.613 - -14.099	10.568 - 13.862
				muscle	N/A	-18.668 - -17.694	13.208 - 14.506

### 2.3.1 Relationships between archival tissue size, body size and age

Strong positive relationships were observed between body size (mantle length), eye lens diameter, and upper beak hood length (Fig. 5). Eye lens diameter explained 89% of the variability in mantle length ( $F_{1,30} = 251.4$ ,  $p < 0.001$ ), while upper hood length explained 95% of the variation in mantle length ( $F_{1,24} = 417.9$ ,  $p < 0.001$ ) (Fig. 5).

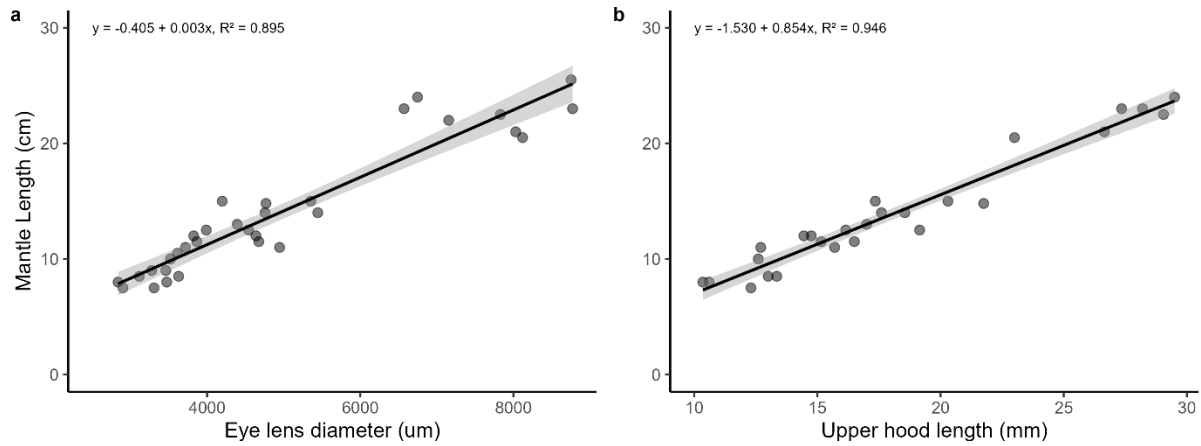


Fig. 5: Measurements of mantle length versus (a) eye lens diameter and (b) upper hood length for *Sepia officinalis*.

Mantle length was also positively related to cuttlebone lamellae count ( $F_{1,740} = 13,190$ ,  $p < 0.001$ ) with an adjusted  $R^2$  value of 95% (Fig. 6a). The bimodal distribution in body size and cuttlebone lamellae counts were used to divide samples into two age classes by fitting two mixture curves (Fig. 6b). The root of the two distributions (92.3 lamellae) was used as the breakpoint to classify individuals as age 1 and age 2, with individuals assigned as age 1 that were caught in March (3 months before the mean hatch date) then reassigned to 0.75 years old. As described in the methods, we then assigned each lens and upper hood growth layer a relative age assuming linear growth between birth (lens core and beak first segment) and its final assigned age (outermost lens diameter and beak segment).

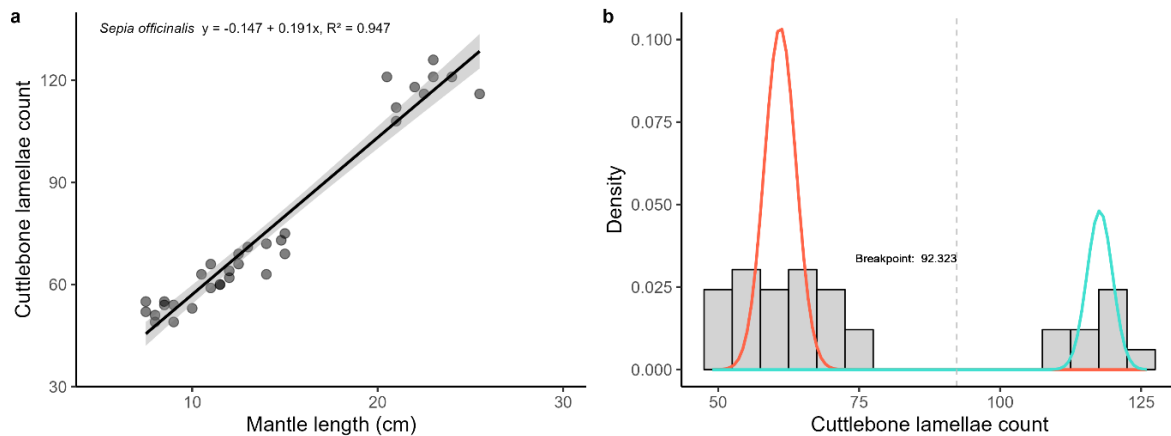


Fig. 6: Measurements of mantle length versus cuttlebone lamellae count (a) and a mixture model for cuttlebone lamellae count of *S. officinalis* samples (b). Results of the linear regression model ( $\pm 95\%$  CI, grey shading) and the root between the bimodal distribution (breakpoint) are displayed within the plots. Distribution of younger and older age classes are indicated by red and turquoise curves, respectively.

### 2.3.2 Lifetime isotopic chronologies

$\delta^{13}\text{C}$  and  $\delta^{15}\text{N}$  profiles through life were plotted using mixed-effects GAMs and LMs, for each isotope respectively. 2017 and 2020 groups are comprised of 0.75- and 1-year-olds for each sampling year (SY), and 2022 are comprised of 1- and 2-year-old age classes.

Overall, clear ontogenetic patterns were observed in beak and eye lens  $\delta^{13}\text{C}$  and  $\delta^{15}\text{N}$  values (Fig. 7a-c, e-g). Beak  $\delta^{13}\text{C}$  generally decreased from birth to death, with the exception of two-year-olds from the 2022 sampling year (SY), where this trend deviated (Fig. 7c). In contrast, eye lens  $\delta^{13}\text{C}$  followed a unimodal pattern, typically peaking around 5 months. During this peak, eye lenses and beaks showed similar  $\delta^{13}\text{C}$  values across all SYs, with both tissues nearing or falling within the muscle  $\delta^{13}\text{C}$  range. However, for age-2 individuals in 2022,  $\delta^{13}\text{C}$  values began to diverge around one year, with eye lenses and beaks displaying noticeable differences at the end of life (Fig. 7c).

For  $\delta^{15}\text{N}$ , eye lens values were relatively stable, showing minimal change over time, with a  $\delta^{15}\text{N}$  range of 4.757‰ (Fig. 7e-g; Table 1). In contrast, beak  $\delta^{15}\text{N}$  showed a strong positive increase throughout life across all SYs, with a  $\delta^{15}\text{N}$  range of 8.791‰ (Fig. 7e-g; Table 1). For more detailed isotope profiles, see the appendix for individual lifetime  $\delta^{13}\text{C}$  and  $\delta^{15}\text{N}$  values in beaks and eye lenses (Fig. 11).

Across all samples, mantle length had no significant effect on  $\delta^{13}\text{C}$  but did influence  $\delta^{15}\text{N}$ , with ratios increasing as body size increased. Separate linear models for each SY indicated no significant effect of mantle length on either  $\delta^{13}\text{C}$  or  $\delta^{15}\text{N}$  (Fig. 7d-h). To determine whether lifetime ontogenetic trends in  $\delta^{13}\text{C}$  and  $\delta^{15}\text{N}$  isotope ratios differed between beak and eye lens tissues of *S. officinalis*, interaction terms for archival tissue type were included in the models.

For  $\delta^{13}\text{C}$ , GAMMs indicated that the ontogenetic trends differed between the two archival tissues across all SYs. Smooth terms for both beak and eye lens tissues were statistically significant, suggesting different ontogenetic trajectories for each tissue type (e.g., SY 2022: beak edf = 3.03,  $F = 5.83$ ,  $p < 0.001$ ; eye lens edf = 4.38,  $F = 7.85$ ,  $p < 0.001$ ). Beak tissues often showed linear trends, with edf values close to 1 (e.g., SY 2017: edf = 1.00,  $F = 39.52$ ,  $p < 0.001$ ), while eye lens tissues exhibited more complex, non-linear relationships, as indicated by higher edf values ( $> 2$ ) in all SYs (e.g., SY 2020: edf = 4.74,  $F = 9.53$ ,  $p < 0.001$ ). In terms of changes in  $\delta^{13}\text{C}$  (green highlights), beak isotope profiles in SY 2017 and 2020 showed significant decreases, whereas SY 2022 exhibited an increase later in life (Fig. 7a-c). Eye lens isotope profiles, by contrast, showed significant increases early in life (before age 0.75) for all SYs (Fig. 7a-c).

The inclusion of archival tissue in the models allowed for comparisons of intercepts between beak and eye lens tissues. The parametric coefficient for eye lens was statistically significant across all SYs (e.g., SY 2022: Estimate = -1.02,  $p < 0.001$ ), therefore  $\delta^{13}\text{C}$  values compared to reference beak tissues were consistently lower. LMMs for  $\delta^{15}\text{N}$  revealed significant differences between beak and eye lens tissues across all SYs. The fixed effect for eye lens versus beak was consistently significant, indicating higher  $\delta^{15}\text{N}$  values in eye lenses (e.g., SY 2022: Estimate = 2.99,  $p < 0.001$ ). A significant positive relationship in  $\delta^{15}\text{N}$  through ontogeny was observed in beak tissues across all SYs ( $p < 0.05$ ), but no such relationship was detected in eye lenses ( $p > 0.05$ , Fig. 7e-g).

Furthermore, the LMMs for  $\delta^{15}\text{N}$  showed statistically significant linear relationships between age and  $\delta^{15}\text{N}$ , with significant fixed effects (e.g., for beak in 2017:  $t = 6.998$ ) and high conditional  $R^2$  values ( $R^2_{\text{c}} > 0.5$ ). Random effects accounted for differences between individuals (e.g., variance for individuals in SY 2022 beaks: 0.204). This indicated that the linear models adequately captured the variation in  $\delta^{15}\text{N}$ . However, low marginal  $R^2$  values ( $R^2_{\text{c}} < 0.5$ , Fig. 7e-g) suggest a low explanatory power of fixed effects (age relative scale).

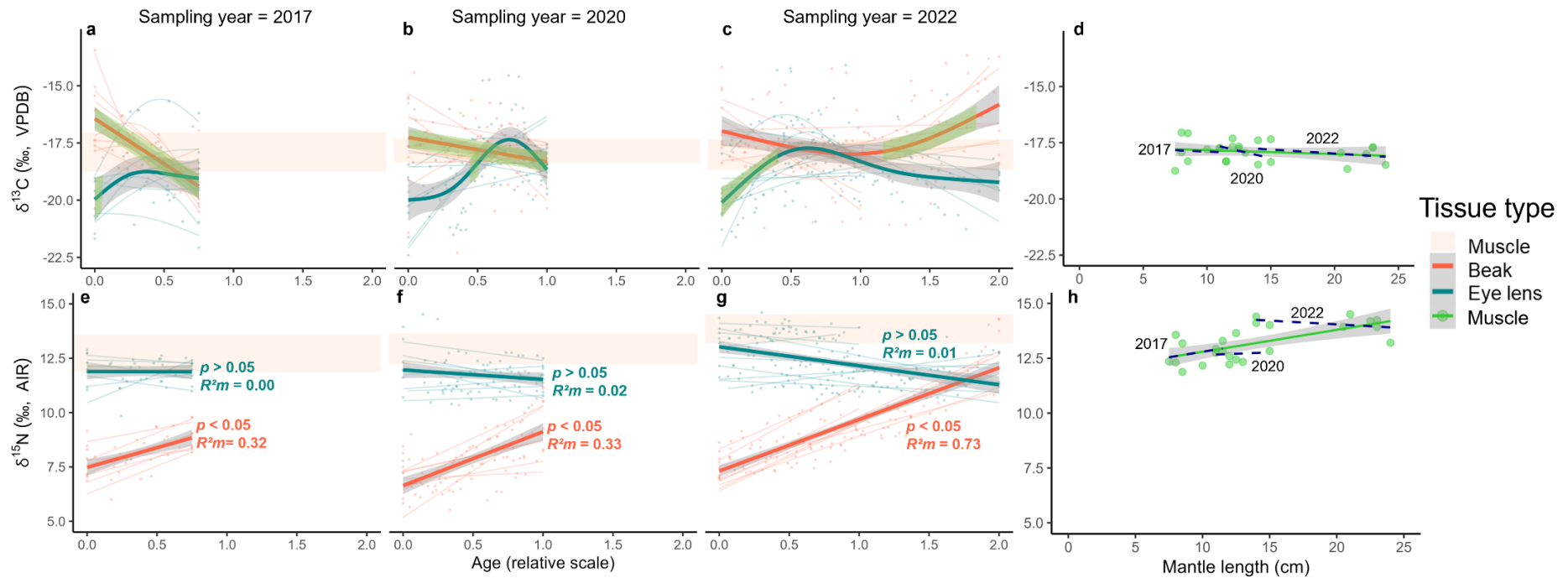


Fig. 7: *S. officinalis* lifetime chronological records of  $\delta^{13}\text{C}$  (a-c) and  $\delta^{15}\text{N}$  (e-g) (linked within individual by fine lines) from beak (red) and eye lens (turquoise) sequential layers for three groups from three different sampling year (2017, 2020 and 2022), showing the range of muscle values at capture in beige. A GAMM was added for each tissue and sampling year group for  $\delta^{13}\text{C}$  and LMM for  $\delta^{15}\text{N}$  ( $\pm 95\%$  CI in grey). Green highlights on the plot indicates significant change in  $\delta^{13}\text{C}$  through age. Age predictor values of the highlighted regions are as follows: a) beak (0-0.75) and eye lens (0-0.17), b) beak (0-1) and eye lens (0.44-0.56), c) beak (1.33-178) and eye lens (0-0.44). Linear mixed-effects models were annotated with their  $p$  and  $R^2_c$  (variance explained by mixed-effects) values in the same colour as their corresponding tissue. An LM was fitted ( $\pm 95\%$  CI, grey shading) for *S. officinalis* muscle  $\delta^{13}\text{C}$  (d) and  $\delta^{15}\text{N}$  (h). LMs were fitted separately for each sampling year groups comprising the *S. officinalis* samples (2017, 2020, 2022) and displayed as the dashed dark blue lines along with the solid green line on both *S. officinalis* plot window. Capture age was estimated using capture date and lamellae count, then growth layers assigned a relative age based on the tissue size relative to its final size at capture.

### 2.3.3 Multi-tissue isotopic discrimination

The last four months of growth for beak and eye lens tissues were averaged for  $\delta^{13}\text{C}$  and  $\delta^{15}\text{N}$  values and subtracted from the corresponding muscle isotope values for the same individual (Fig. 8). Differences between muscle and archival tissues were tested using a one-sample  $t$ -test and its non-parametric equivalent to determine if the means differed significantly from zero, with zero indicating no difference compared to muscle isotope values.

The Wilcoxon signed-rank test found no significant difference between  $\delta^{13}\text{C}$  values of beak and muscle tissues ( $V = 161$ ,  $p = 0.979$ ). The median  $\delta^{13}\text{C}$  for beak was  $-17.83\text{‰}$ , while for muscle it was  $-17.79\text{‰}$ , indicating minimal variation between the two tissues. In contrast, the one-sample  $t$ -test showed that eye lens  $\delta^{13}\text{C}$  values were significantly lower than muscle ( $t = -3.87$ ,  $df = 24$ ,  $p < 0.001$ ), with a median  $\delta^{13}\text{C}$  of  $-18.82\text{‰}$  for the eye lens, representing a  $0.54\text{‰}$  lower median value compared to muscle.

For  $\delta^{15}\text{N}$ , the Wilcoxon signed-rank test revealed a significant difference between beak and muscle tissues ( $V = 0$ ,  $p < 0.001$ ), with beak  $\delta^{15}\text{N}$  being lower. The median  $\delta^{15}\text{N}$  for beak was  $8.90\text{‰}$ , compared to  $13.18\text{‰}$  for muscle, showing a difference of  $4.28\text{‰}$ . Similarly, a one-sample  $t$ -test for eye lens  $\delta^{15}\text{N}$  revealed a significant difference from muscle ( $t = -9.20$ ,  $df = 24$ ,  $p < 0.001$ ), with a median  $\delta^{15}\text{N}$  of  $12.08\text{‰}$  for the eye lens, which was  $1.10\text{‰}$  lower than muscle.



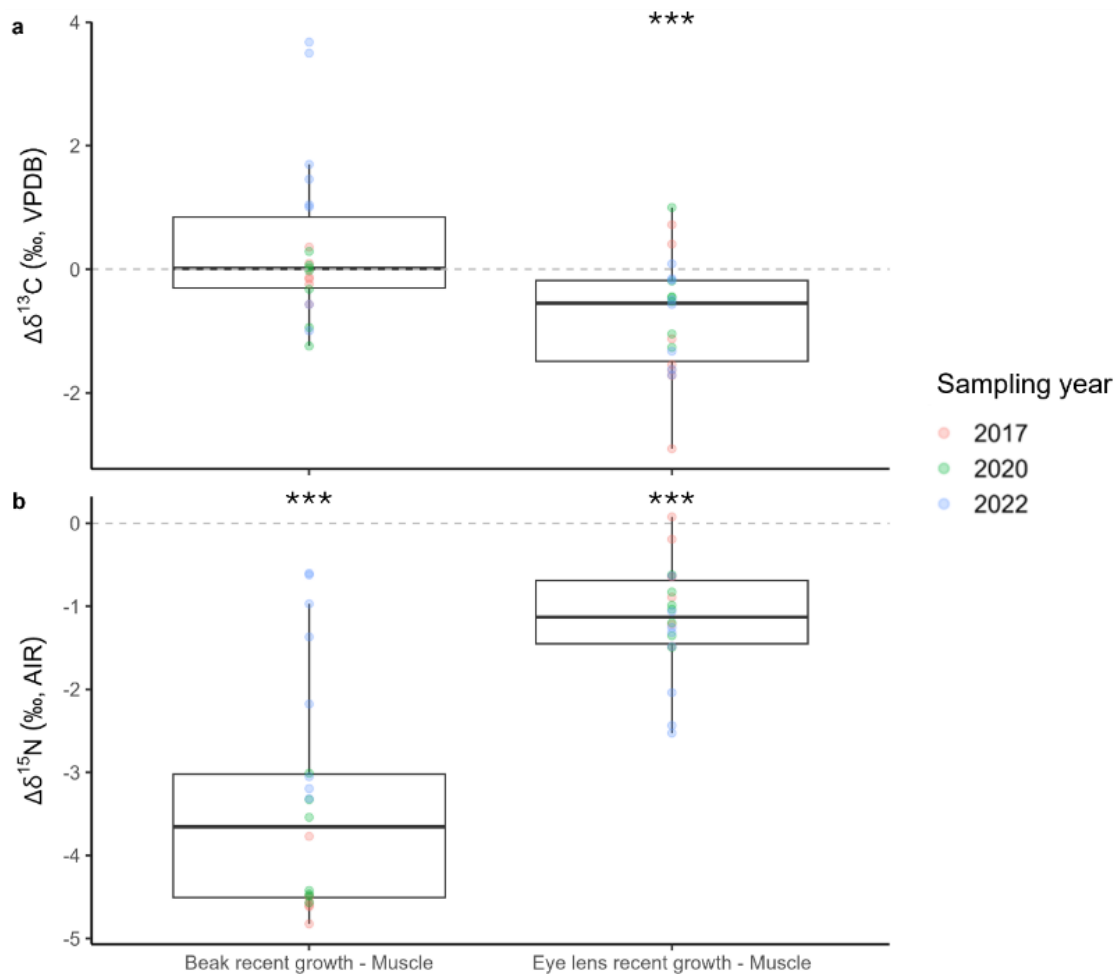


Fig 8: The difference between muscle vs. beak and eye lens for  $\delta^{13}\text{C}$  and  $\delta^{15}\text{N}$  over approximately the last four months of growth for both archival tissues and across all samples. For individuals with multiple beak and eye lens layers within the last four months of growth, layers were averaged before being subtracted from the muscle isotope value for the same individual. Stars above the boxplots indicate the degree of significant difference between beak and eye lens. The grey dashed line on  $y=0$  marks the point of no difference with muscle isotope values.

Age classes (0.75, 1 and 2) as a predictor was chosen over mantle lengths (body size) in this analysis as AIC comparisons across all combination of isotope and tissue isotope discriminations suggested a lower AIC value and therefore more parsimonious fit. In most cases, sampling year did not have a significant effect on discrimination factors, apart from  $\Delta\delta^{13}\text{C}_{\text{beak-muscle}}$ . Kruskal-Wallis tests on ranked residuals of LM model indicated a marginal effect of SY on  $\Delta\delta^{13}\text{C}_{\text{beak-muscle}}$  ( $p = 0.041$ ).

The linear model assessing the influence of age on  $\Delta\delta^{13}\text{C}_{\text{beak-muscle}}$  indicated a significant positive effect of age ( $\beta = 2.05$ ,  $p < 0.001$ ). ANOVA models using age showed no significant effect on  $\Delta\delta^{13}\text{C}_{\text{lens-muscle}}$  ( $p = 0.961$ ). The linear model assessing the influence of age on  $\Delta\delta^{15}\text{N}_{\text{beak-muscle}}$  showed a significant positive effect ( $\beta = 2.44$ ,  $p < 0.001$ ). For the eye lens, the Anova for  $\Delta\delta^{15}\text{N}_{\text{lens-muscle}}$  a significant negative effect of age ( $p < 0.001$ ).

Indication of a significant influence of age, requires correction factors for  $\delta^{13}\text{C}$  and  $\delta^{15}\text{N}$  differences between beak and muscle, with positive adjustments required for both isotopes as age increases.  $\delta^{13}\text{C}$  differences in eye lens tissue did not show a significant trend with age, while  $\delta^{15}\text{N}$  differences in eye lens tissue did show an increasing trend. The detailed correction values can be found in Table 2.

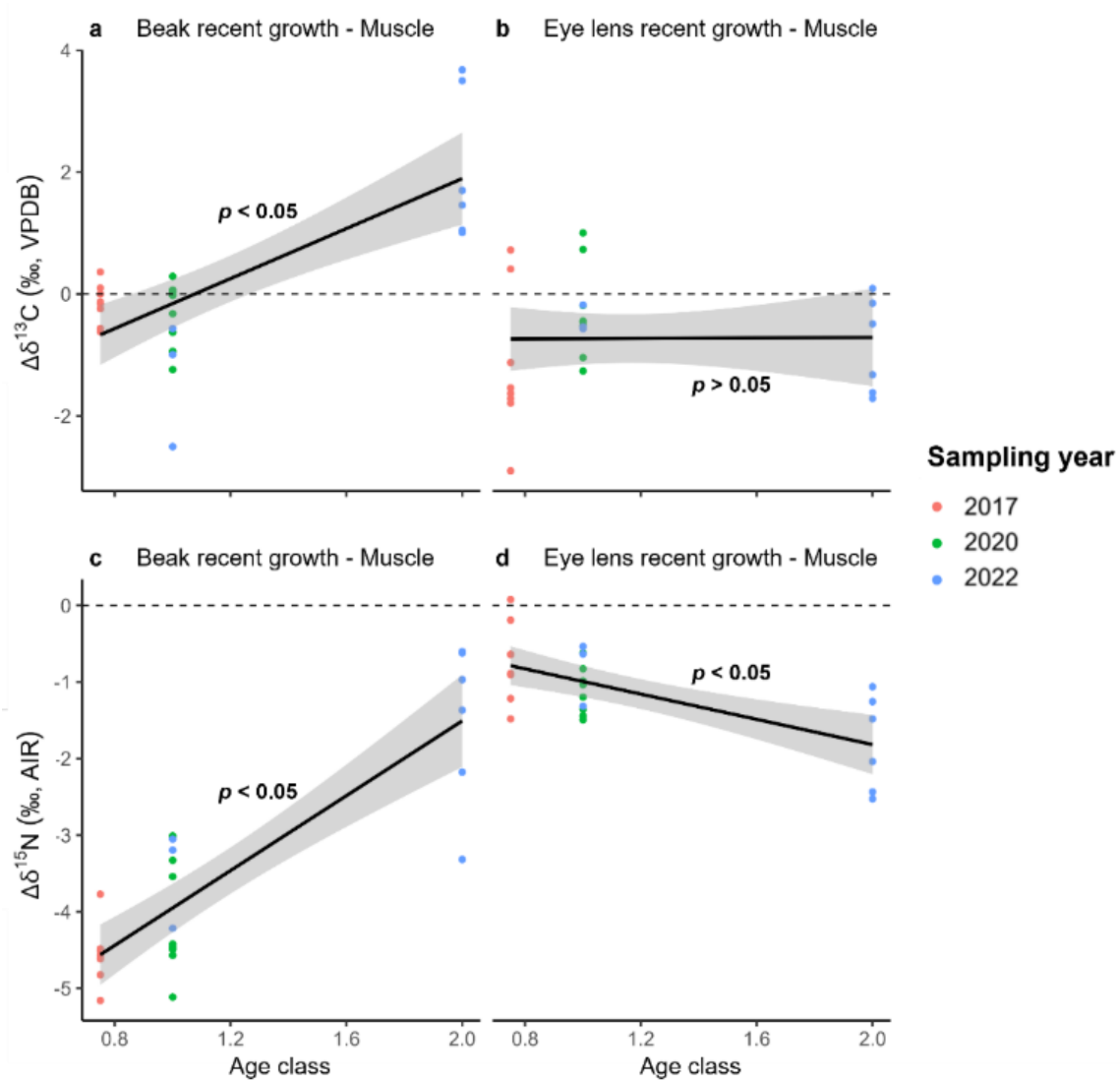


Fig. 9: The differences between muscle and archival tissues (beak and eye lens) for  $\delta^{13}\text{C}$  and  $\delta^{15}\text{N}$  over approximately the final four months of growth are presented, grouped by age classes. Each point represents an individual, with colours indicating sampling year. The grey dashed line at  $y = 0$  represents no difference compared to muscle isotope values. The main age classes are 0.75, 1, and 2 years. Significance values for each regression model are shown, with all models being significant except for  $\Delta\delta^{13}\text{C}_{\text{beak-muscle}}$ . Capture age was estimated using capture date and lamellae count, then growth layers assigned a relative age based on the tissue size relative to its final size at capture.

The difference between beak and eye lens lifetime  $\delta^{13}\text{C}$  and  $\delta^{15}\text{N}$  for *S. officinalis* (expressed as  $\Delta\delta^{13}\text{C}_{\text{beak-lens}}$  and  $\Delta\delta^{15}\text{N}_{\text{beak-lens}}$ ) was explored (Fig. 10).

For  $\Delta\delta^{13}\text{C}$ , GAMM explained 96.3% of the deviance (adjusted  $R^2 = 0.959$ ). The smooth term for age relative scale ( $\text{edf} = 7.3$ ,  $F = 91.47$ ,  $p < 0.001$ ) and the random effects for

individual variation (edf = 23.4,  $F = 28,754.78$ ,  $p < 0.001$ ) were both significant which captures non-linear patterns in  $\Delta\delta^{13}\text{C}$  differences over time.

For  $\Delta\delta^{15}\text{N}$ , LMM demonstrated a strong fit, with a highly significant linear relationship between age relative scale and  $\Delta\delta^{15}\text{N}$  differences (Estimate = 4.8,  $t = 43.5$ ). The model explained 69.3% of the variance of fixed effects alone ( $R^2m = 0.69$ ), and 89.6% when considering both fixed and random effects ( $R^2c = 0.9$ ). The overall residual variation was small, accounting for most of the linear variation in  $\Delta\delta^{15}\text{N}$  differences through life (Std. Dev. = 0.46).

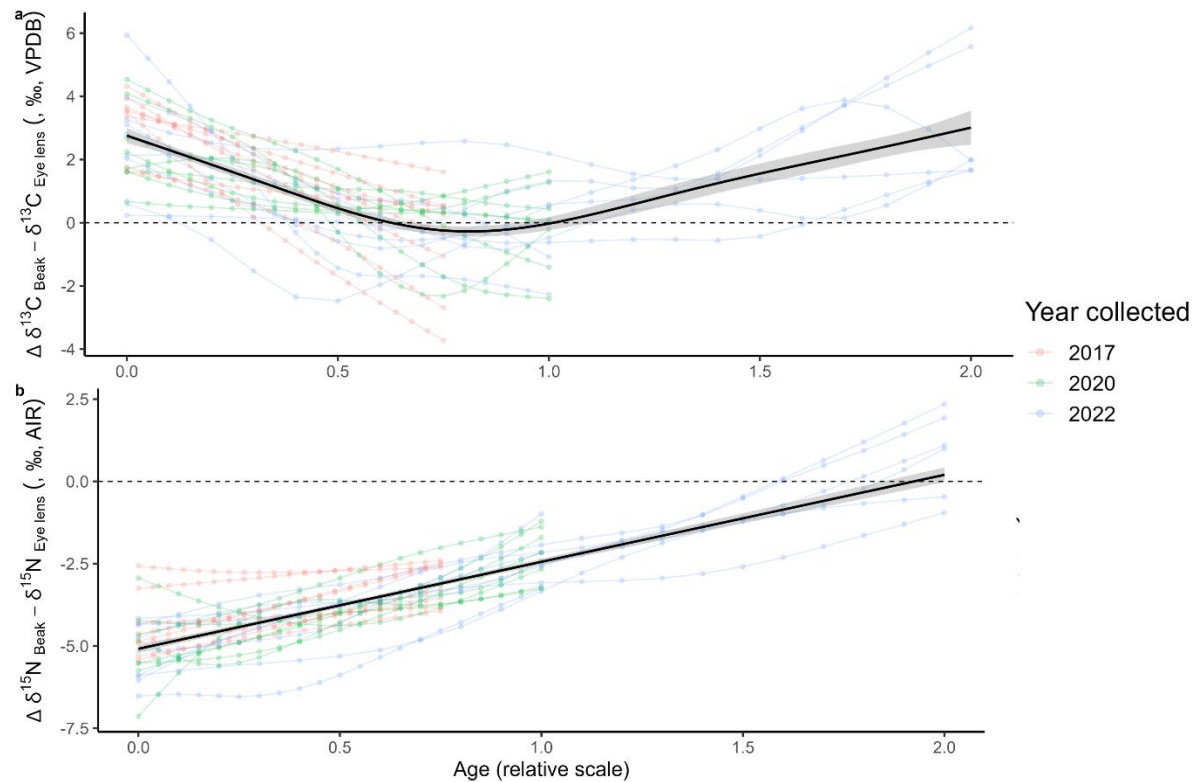


Fig. 10: Difference between beak and eye lens  $\delta^{13}\text{C}$  and  $\delta^{15}\text{N}$  for *S. officinalis*.  $\delta^{13}\text{C}$  and  $\delta^{15}\text{N}$  data was predicted using a spline model, then beak-eye differences per individual within each sampling year groups (2017 in red, 2020 in green and 2022 in blue) for *S. officinalis* were fitted with a GAMM ( $\pm 95\%$  CI, grey shading). Each faint lines represent an individual and each data point within each individual are predicted  $\delta^{13}\text{C}$  and  $\delta^{15}\text{N}$  values. A fine dashed line is shown at  $y=0$  to mark the point of no difference between eye lens and beaks. Capture age was estimated using capture date and lamellae count, then growth layers assigned a relative age based on the tissue size relative to its final size at capture.

## 2.4 Discussion

### 2.4.1 Relationships between archival tissue size, body size and age

The relationships observed between archival tissue size, such as eye lens diameter ( $\mu\text{m}$ ) and beak hood length (mm), and mantle length (cm) demonstrate that both tissues reliably estimate body size, with beak hood length showing slightly greater explanatory power as a predictor (Fig. 5b). These relationships are essential for linking isotopic chronologies from beak and eye lens tissues to specific size and age classes, which improves ecological interpretations when studying their trophic ecology throughout life.

The valuable traits offered by archival tissues, such as the higher temporal resolution typically provided by eye lenses in isotopic chronology reconstructions (Onthank, 2013) and the preservation of beaks in predator stomachs or faeces (Alvito et al., 2015), offer natural sampling opportunities that enhance our understanding of predator-prey interactions. Relating these traits to body size could further improve stock assessments by allowing researchers to discern isotopic resources utilised at key life stages, such as recruitment.

The correlation between cuttlebone lamellae counts and mantle length (Fig. 6) also suggests that cuttlebone lamellae can serve as a useful determinant of age in cuttlefish (Chung et al., 2020). However, the number of lamellae does not perfectly correspond to true age, as it may be influenced by temperature, as established in cuttlebone structure studies (Bettencourt and Guerra, 1999). Despite this, it provides a useful estimate of age class cohorts, as demonstrated in this study. Models testing the

influence of age showed significant results and yielded a more parsimonious model structure than those based on body size.

Aging studies using beak microstructure have proven effective for squid and are likely transferable to other cephalopods (Agus et al., 2024). Cross-referencing such beak readings in *S. officinalis* with our results would enhance age classification. Statoliths, previously used to age *S. officinalis* (Bettencourt and Guerra, 2001), struggle to determine age beyond 240 days but are still valuable for early life studies. Future research could combine aging methods using both beaks and statoliths, then compare chemical archives from beaks, eye lenses, and statoliths, as seen in Stounberg et al. (2022) comparison of element concentration between fish eye lenses and otoliths. This combined approach, along with body size interpolation, could offer deeper insights into population structure and trophic ecology.

#### 2.4.2 Trends and comparison of isotope ratios through life

The expected lifetime  $\delta^{13}\text{C}$  and  $\delta^{15}\text{N}$  values of *S. officinalis*, informed by their mode of life and trophic ecology (Bloor, Attrill and Jackson, 2013) provide insights into the isotope patterns observed in this study. Initially,  $\delta^{13}\text{C}$  values may be enriched due to inshore hatching during summer, although maternal nutrient use during egg development may deplete early life isotope ratios in archival tissues (Ziegler, Miller and Nagelmann, 2021), as the mothers likely spend more time in deeper waters near the end of their life. This maternal influence has been documented in other species using isotopic analyses of eye lenses and otoliths (Ben-Tzvi et al., 2007; Quaeck-Davies et al., 2018). As individuals migrate offshore with rising temperatures and overwinter in deeper waters,  $\delta^{13}\text{C}$  values are expected to decline. A return to nutrient-rich inshore environments during warmer summer temperatures, typical of the English Channel, would result in  $\delta^{13}\text{C}$  enrichment. This cycle marks the first year and a half of

life, with sexually mature individuals returning inshore for spawning during their final year. Consequently, the isotopic profile is expected to exhibit two peaks in  $\delta^{13}\text{C}$ , corresponding to periods of inshore residency during the summer. This interpretation is based on established patterns of  $\delta^{13}\text{C}$  depletion in offshore waters and enrichment in inshore regions (Hobson, 1999). An increase in  $\delta^{15}\text{N}$  with ontogeny, commonly observed in cephalopods (Sajikumar et al., 2020; Sakamoto et al., 2023) is expected in *S. officinalis*, with larger individuals feeding at higher trophic levels. This trend is supported by Chouvelon et al. (2011), who found a positive relationship between body size and  $\delta^{15}\text{N}$ . However, Vinagre et al. (2011) reported no significant relationship between  $\delta^{15}\text{N}$  and body size in *S. officinalis* from the Bay of Cascais.

The isotope profiles of beaks and eye lenses throughout life, as showcased in Fig. 7, somewhat reflect the expected values, particularly for  $\delta^{13}\text{C}$  in eye lenses and  $\delta^{15}\text{N}$  in beak chronologies. The  $\delta^{13}\text{C}$  profiles showed non-linearity, especially evident in the eye lenses, which capture the summer peaks predicted by the literature. However, only one peak is observed, corresponding to age classes 0.75 and 1, while this pattern is absent in age class 2. Near the end of life, depleted  $\delta^{13}\text{C}$  values, likely reflecting offshore overwintering phases, were observed. In contrast, beak  $\delta^{13}\text{C}$  did not align with expectations, showing a negative relationship over time in age 0.75 and 1 (highlighted in green). Larger individuals exhibited increasing  $\delta^{13}\text{C}$  later in life, which may correspond to a second summer peak not captured in eye lenses. This discrepancy could be attributed to the finer temporal resolution observed in beaks at recent life. During sectioning, the most recent beak layers were more easily distinguished, potentially allowing for more detailed isotope variability to be captured (from firsthand experience). Conversely, the thicker, more saturated, and irregular outer layers of eye lenses in larger individuals (also observed firsthand) may have

affected  $\delta^{13}\text{C}$  readings in recent life stages. Further investigation into this phenomenon could be valuable. For instance, freeze-drying eye lenses before delamination, as attempted by Quaeck-Davies et al. (2018) in fish, may enhance the clarity of the outer layers and help achieve better resolution for comparison with beak profiles.

The significant increase in beak  $\delta^{15}\text{N}$  aligns with the rise in trophic levels, however, the  $^{15}\text{N}$ -reducing effect of chitin, particularly prominent in early life and decreasing with age, likely influenced the overall  $\delta^{15}\text{N}$  profile (Miserez et al., 2008; Guerra et al., 2010). Mixed-effects linear models fitted to both archival tissues revealed differing isotope profiles, confirming linearity but showing key differences, especially in intercepts, indicating that beaks and eye lenses display significantly different  $\delta^{15}\text{N}$  values at the start of life. Throughout life stages and across sampling years, eye lens  $\delta^{15}\text{N}$  remained stable and consistently higher than beak  $\delta^{15}\text{N}$ , except in the most recent values of larger individuals.

The relationship between muscle  $\delta^{13}\text{C}$  (Fig. 7d) and  $\delta^{15}\text{N}$  (Fig. 7h) and body size was investigated to explore potential similarities between individual-level isotope variations and population-level trends through ontogeny. Muscle  $\delta^{13}\text{C}$  was independent of body size, which was reflected in the stable  $\delta^{13}\text{C}$  profiles of eye lenses after age 0.5. Similarly,  $\delta^{15}\text{N}$  showed no significant relationship with body size across different sampling years, mirroring the trends observed in eye lens  $\delta^{15}\text{N}$ . Based on these findings, it lends more credibility to the eye lens isotope chronology, which leads to the conclusion that the significant increase in beak  $\delta^{15}\text{N}$  is likely attributed to the chitin gradient that diminishes over time and not due to trophic level increase over time. While this gradient is recognised in cephalopod trophic ecology studies involving beaks (Miserez et al., 2008; Cherel, Bustamante and Richard, 2019), it is rarely showcased as a steadily increasing  $\delta^{15}\text{N}$  trend throughout life, as most studies rely on



only three sections of the beak (rostrum, lateral wall, and wing) (Xavier et al., 2022). Additionally, a direct comparison between eye lens and beak  $\delta^{15}\text{N}$  chronologies has not been performed before. If the population-level  $\delta^{15}\text{N}$  trends in muscle align with the observed eye lens  $\delta^{15}\text{N}$  profile, this could offer the first correction factor estimates to account for the nitrogen-reducing effect of chitin through life. While similar discrimination factors have been evaluated in cephalopods and other species, these studies typically focus on specific life stages rather than considering an individual's entire life. (Hobson and Cherel, 2006).

### 2.4.3 Multi-tissue isotopic discrimination

To assess the differences among muscle, eye lenses, and beaks, isotope ratios from recent growth layers in archival tissues were compared to muscle by subtracting muscle isotope values from those of the archival tissues (Fig. 8). This method facilitated the development of potential correction factors, allowing the isotopic data from archival tissues to be more comparable to muscle, which is often considered a reliable reference tissue for quantifying  $\delta^{13}\text{C}$  and  $\delta^{15}\text{N}$  ratios. Using muscle isotope ratios as a baseline minimised the effects of baseline variability, as muscle ratios effectively become the reference point. This enables the isotope variability of eye lenses and beaks to be quantified relative to muscle, facilitating their comparison even in the absence of diet isotope ratios, which are typically used in other research to quantify diet-tissue discrimination (Hewitt et al., 2021).

When all samples were pooled,  $\delta^{13}\text{C}$  values in beaks were the closest to muscle  $\delta^{13}\text{C}$ , whereas the other tissues and isotope combinations showed significant differences (Fig. 8). While the results from this initial analysis could be used as a quick way to translate isotope ratios between tissues, more variable-specific correction factors would offer a more nuanced understanding. Therefore, the effects of age and body

size were explored to see which better explained the differences between archival tissues and muscle. Both factors significantly influenced these differences, suggesting a strong relationship with ontogeny. The more parsimonious model, which included age (Fig. 9), was selected to calculate an age-based correction factor. This refinement likely improved precision, as metabolism, which varies through life stages in many marine organisms, can affect how isotope ratios are routed or assimilated into *S. officinalis* tissues (Fry and Arnold, 1982; Shipley and Matich, 2020).

The isotopic trends with age and their consistency (or lack thereof) with individual-level isotopic trends (Fig. 7) provide insights into which archival tissue shows more reliable patterns. For instance,  $\delta^{13}\text{C}_{\text{lens-muscle}}$  exhibited no significant age-related changes, consistent with the  $\delta^{13}\text{C}$  profile for eye lenses. Similarly,  $\delta^{15}\text{N}_{\text{beak-muscle}}$  followed a pattern consistent with the  $\delta^{15}\text{N}$  individual-level profile. In contrast,  $\delta^{13}\text{C}_{\text{beak-muscle}}$  and  $\delta^{15}\text{N}_{\text{lens-muscle}}$  with age did not align with their corresponding individual-level isotope profiles (Fig. 7a-c and 7e-g, respectively). Thus, it remains inconclusive which archival tissue offers the most reliable individual-level isotopic trends.

The analysis of isotopic differences between beak and eye lens ( $\delta^{13}\text{C}_{\text{beak-lens}}$  and  $\delta^{15}\text{N}_{\text{beak-lens}}$ ) throughout life revealed consistent individual isotopic patterns across the lifespan (Fig. 10). A substantial variation in  $\delta^{13}\text{C}$  and  $\delta^{15}\text{N}$  was explained using non-linear and linear mixed-effects models, allowing us to highlight the differences between the lifetime isotopic chronologies of beak and eye lens tissues. Notably, the isotopic chronologies were not uniform throughout life, with beak tissues generally exhibiting higher  $\delta^{13}\text{C}$  values than eye lenses, except for a brief period around age 1, where no difference ( $\delta^{13}\text{C}_{\text{beak-lens}} = 0$ ) was observed (Fig. 10a). In terms of  $\delta^{15}\text{N}$ , eye lenses consistently showed more enriched  $\delta^{15}\text{N}$  compared to beaks. This pattern may provide the first quantifications of the chitin-to-protein gradient, assuming no significant change

in  $\delta^{15}\text{N}$  throughout life. The lack of difference ( $\delta^{15}\text{N}_{\text{beak-lens}} = 0$ ) observed at later life stages suggests that  $\delta^{15}\text{N}$  values of eye lenses and beaks converge, which are also relatively similar to muscle isotope values.

#### 2.4.4 Limitations and caveats

Understanding environmental isotope baseline values is essential for interpreting the isotope ratios observed in the tissues of *S. officinalis*. These baseline values provide a means to assess how shifts in environmental conditions influence isotope ratios across different sampling years (Fry and Sherr, 1989; Miller, Millar and Longstaffe, 2008). Quantifying baseline isotope data allows for a clearer understanding of how variations in the environment affect the isotope values in *S. officinalis* tissues. Isotopic turnover rates of cephalopod muscles are understudied and lags behind other taxa with numerous studies such as in fish (Perga and Gerdeaux, 2005; McIntyre and Flecker, 2006) birds (Hobson and Clark, 1992; Haramis et al., 2007) and mammals (MacAvoy, Arneson and Bassett, 2006; Miller, Millar and Longstaffe, 2008). Currently, there is no estimate for the timespan over which isotope ratios are integrated into muscle tissues (Jackson et al., 2007). This limits accurate comparisons of short-term dietary shifts. Winter et al. (2019) addressed this issue by conducting diet-switching experiments, where individuals were fed diets with known isotope ratios and then switched to a different diet. The isotopic changes in tissues were tracked over time, offering insight into turnover rates.

Another caveat in this study relates to the use of age as a relative scale for archival tissues. This approach results in the loss of absolute size information for each tissue type and assumes that scaling with age and size is perfectly correlated. Furthermore, archival tissues like beaks and eye lenses may grow at different rates throughout life (Rodríguez-Domínguez et al., 2013). Additionally, the uniformity of growth layers in

these tissues remains relatively unstudied. For instance, the overplating in early beak chronology and the thick outer layers of eye lenses could introduce inaccuracies by sampling across different regions simultaneously (Queirós et al., 2018). While general lifetime isotopic trends were explored in this study, finer-scale isotopic variations were not fully captured. The isotope data exhibited unexpected fluctuations, which restricted the ability to confidently discern anything beyond broad trends such as general increases or decreases in isotope values.

Expanding the range of body sizes sampled would enhance the resolution of population-level variations in isotope changes through ontogeny. A wider range of mantle lengths for *S. officinalis* would provide a more comprehensive understanding of how isotope ratios change across different life stages and would offer a more robust comparison with archival tissue profiles.

Although this study focuses on *S. officinalis*, a species of significant ecological and commercial importance in European waters, it does not extend to other cephalopods, such as pelagic squid. The differences in the mode of life and biology between species may limit the applicability of these findings to other cephalopods, requiring further research to broaden the study's relevance.

While SIA has proven valuable in dietary reconstructions, it presents limitations by averaging isotope ratios over whole tissues. Compound-specific isotope analysis (CSIA) provides a finer resolution by allowing the analysis of individual compounds, such as chitin, independently from other tissue components. CSIA offers a more precise understanding of isotopic composition and dietary trends compared to bulk SIA and could offer significant advantages if applied to cephalopod tissues such as beaks and muscle, reducing biases associated with bulk tissue analysis (Cherel,

Bustamante and Richard, 2019). CSIA may also help uncover some biochemical components within the studied tissues, potentially offering alternative interpretations to those presented here. While we acknowledged that the physiological components of beaks (i.e. chitin) as a factor influencing the observed isotopic values for beak  $\delta^{15}\text{N}$ , and  $\delta^{13}\text{C}$  values generally reflected ecological aspects of *S. officinalis* in both archival tissues, CSIA could help clarify whether additional underlying biochemical processes, such as lipid accumulation or other changes in tissue chemistry through the life cycle can affect  $\delta^{15}\text{N}$  and  $\delta^{13}\text{C}$  values. Aside from the insights CSIA may provide, it is important to recognise that numerous factors can influence isotopic values. Nevertheless, the fundamental principle and often summarised as ‘you are what you eat’ remains robust, continuing to form the basis for interpreting isotopic values in trophic ecology studies.

## 2.4.5 Conclusion

This study offers preliminary estimates for correction factors and reveals previously unexamined discrimination between  $\delta^{13}\text{C}$  and  $\delta^{15}\text{N}$  values across different tissues of *S. officinalis*. These insights could be critical for future research, particularly when comparing studies that use different tissues like eye lenses, beaks, and muscle. The ability to translate isotope values between these tissues not only simplifies comparisons between studies but also expands the relevance of one tissue to others. For example, beaks, which are commonly found in predator stomachs, provide direct evidence of predator-prey interactions, an aspect that muscle or eye lenses alone would not capture as effectively. Additionally, this study introduces new methods for sectioning the beak, providing evidence that the upper beak hood can be reliably used to create lifetime isotopic chronologies. This methodological advancement represents an important step forward, as it enables more precise comparisons with eye lens data,

a previously unattained feat in *S. officinalis* studies. These findings underscore the potential for beaks to be used in future research as a more informative archival tissue.

Confirming the usability of these findings requires reproducibility. Repeated studies should verify that the observed patterns and trends are not limited to this specific sample set. Encouragingly, evidence from this study already supports this reproducibility, as multiple sampling years and age classes demonstrated consistent differences in isotopic values both during recent life stages and throughout the entire lifespan of *S. officinalis*. Establishing reproducibility across multiple cohorts and samples is important to confirm that the results are not coincidental and reflect broader, reliable trends in *S. officinalis* isotope data.

Additional research into the isotopic values presented in this study will contribute to the growing archives of data that are essential for building effective management plans aimed at preserving the ecological and commercial importance of *S. officinalis* in the English Channel. These data archives can be invaluable for both conservation efforts and future fisheries management strategies.



## Chapter 3: Isotopic Niche Overlap Among Species of Cephalopods and Crustaceans in the English Channel

### Abstract

While the isotopic niche is not a direct reflection of the trophic niche and does not fully encompass the complexity of trophic interactions, it serves as a useful proxy for inferring resource competition, particularly in species that co-exist and utilise similar habitats and resources. Using stable isotope analysis ( $\delta^{13}\text{C}$  and  $\delta^{15}\text{N}$ ), the isotopic niche overlap of four demersal species in the English Channel: *Sepia officinalis*, *S. elegans*, *Cancer pagurus*, and *Homarus gammarus*, was assessed. The results indicate significant isotopic niche overlap, especially between the two crustacean species, suggesting shared dietary resources. *S. officinalis* showed greater overlap with *C. pagurus* than with *H. gammarus*, likely due to the use of similar basal resources. In contrast, *S. elegans* demonstrated niche partitioning, reflecting its distinct trophic position. Both *S. officinalis* and *S. elegans* exhibited increasing  $\delta^{13}\text{C}$  and  $\delta^{15}\text{N}$  values with body size, indicating potential ontogenetic dietary shifts, which were not observed in the crustaceans. Overall, the broad isotopic niches observed across all species suggest a diverse prey base, potentially enhancing their resilience to environmental changes. However, the prevalent trophic interactions inferred from the shared use of isotopic resources among commercially important species highlight the need for a holistic approach to conservation and fisheries management in the English Channel.



## 3.1 Introduction

Investigating niche partitioning can help understand interspecific competition for resources such as diet and habitat, trophic dynamics (Costa-Pereira et al., 2019), and food web structure (Ponce et al., 2021). The concept of the ecological niche was first defined by Hutchinson (1978) as a multidimensional space with axes representing different environmental variables, with biotic axes defining the resources that animals use, and abiotic axes describing their habitat and the environmental conditions. Using stable isotope analysis (SIA), ecologists have adapted this concept to use the isotopic niche of different organisms, particularly tissue carbon ( $\delta^{13}\text{C}$ ) and nitrogen ( $\delta^{15}\text{N}$ ) stable isotope ratios, as a proxy for abiotic and biotic axes, respectively (Newsome et al., 2007). In brief, tissue  $\delta^{13}\text{C}$  varies as a function of the carbon sources used by primary producers at the base of the food web (e.g., benthic versus pelagic or inshore versus offshore) (Hobson, 1999), while  $\delta^{15}\text{N}$  exhibits a stepwise enrichment of approximately 3-4‰ per trophic level, and is thus primarily used to estimate trophic position (Minagawa and Wada, 1984). The isotopic niche, while narrower in scope than the broader ecological niche concept, provides valuable insights into trophic dynamics (Layman et al., 2012), species interactions (Cooper and Wissel, 2012), geographic distribution (e.g. marine vs. terrestrial sources) (Hobson, 2008), and ontogenetic shifts (Krumsick and Fisher, 2019). The relative degree of overlap or separation of isotopic niche space can be used to infer interspecific competition or resource partitioning, as it reflects the extent to which species utilise isotopically similar or distinct resources (Marshall et al., 2019; Ogloff et al., 2019; Roughgarden, 1972). Ultimately, these tools can help us understand the basis for species coexistence, which often relies on resource partitioning to prevent competitive exclusion (Pianka, 1974).

Tissue carbon and nitrogen isotope ratios, expressed as  $\delta^{13}\text{C}$  and  $\delta^{15}\text{N}$ , respectively, vary as a function of the organism's diet and the tissue's turnover time (Fry, 2006a).  $\delta^{13}\text{C}$  and  $\delta^{15}\text{N}$  biplots are particularly useful for visualising the isotopic distribution and variability within and among species (Newsome et al., 2007) while statistical tools such as Layman's metrics (Layman et al., 2007) and the Stable Isotope Bayesian Ellipses (Jackson et al., 2011) are useful for quantifying isotopic variability and overlap within and among species (Hayden et al., 2013). Approaches such as stomach content analysis complement isotopic studies by providing direct observations of consumer prey items and their sizes (Ogloff et al., 2019; Sturbois et al., 2022). However, stomach content analysis can be limited by the difficulty of distinguishing partially digested prey items, the relatively narrow spatiotemporal scope, and potential biases caused by variable digestibility of different prey items (Hyslop, 1980). In contrast, stable isotope analysis of muscle tissue can offer insights into assimilated diet information over a relatively broader spatiotemporal scale (Fry, 2006a), for example, reflecting dietary intake over weeks to months for cephalopods (Stowasser et al., 2006) and crustaceans (deVries et al., 2015; Hewitt et al., 2021). Isotopic techniques also typically require less time and fewer samples than more traditional approaches such as stomach content analysis to estimate the full variability in species' resource use (Layman et al., 2012).

Isotopic niche width, reflecting the full range of isotopic values exhibited by a particular species, is akin to its trophic niche width and provides insights into dietary diversity and resource use (Hette-Tronquart, 2019). Put simply, trophic niche width can be visualised as a spectrum occupied by different functional groups, with specialists at the extremes and generalists in the centre. Specialists may focus on a limited number of prey items and/or have a narrow spatial or temporal distribution, while generalists

exploit a wider range of available resources (Dennis et al., 2011). Intraspecific variability also occurs, for example, with some species represented by both omnivorous and strictly carnivorous individuals (Levis et al., 2017). Isotopic niche width can also be used to understand changes in habitat quality. For instance, Pelage et al. (2022) found that demersal fish species in degraded habitats expanded and diversified their resource use, leading to increased interspecific competition. This underscores the importance of isotopic niches for predicting the impacts of environmental change. Similarly, Weber et al. (2023) demonstrated specialisation and diversification in two coexisting turtle species, indicating variable resource use among sympatric species. Dillon et al. (2021) also reported notable differences in  $\delta^{13}\text{C}$  and  $\delta^{15}\text{N}$  values among four commercially important fish guilds, allowing to inform fisheries management through a better understanding of the food web dynamics in their study system.

The ecological niches occupied by marine cephalopods and crustaceans are highly diverse, with different species and life stages encompassing different functional roles, including those of predators, prey, and scavengers (Jurrius and Rozemeijer, 2022; Boyle and Rodhouse, 2008; Lawton, 1989). These roles are crucial for regulating populations, driving nutrient cycling, and facilitating energy transfer within marine ecosystems (Hunsicker et al., 2011; Payne and Moore, 2006). Beyond their ecological value, cephalopods and crustaceans hold economic and societal importance (Blampied et al., 2022; Bobowski et al., 2023). In this study, we explore niche overlap between four species in the English Channel: the common cuttlefish (*Sepia officinalis*), elegant cuttlefish (*Sepia elegans*), brown crab (*Cancer pagurus*), and European lobster (*Homarus gammarus*) (Boudreau and Worm, 2012; Gibson, Atkinson and Gordon, 2016). All four species are distributed throughout the English Channel and S.

*officinalis*, *C. pagurus*, and *H. gammarus* hold substantial economic importance (Rees, Sheehan and Attrill, 2021; Lishchenko et al., 2021). However, it is unclear how much they compete for resources and how resilient they are to future climate change and other perturbations.

This study aims to compare the isotopic niches of four demersal species - *S. officinalis*, *S. elegans*, *C. pagurus*, and *H. gammarus* - to investigate the extent to which they are competing for or partitioning dietary resources, and ultimately to provide baseline data to support ecosystem-based management. First, we assessed whether body size was related to muscle  $\delta^{13}\text{C}$  and  $\delta^{15}\text{N}$  to explore ontogenetic changes in habitat use, diet, and trophic level within each species. We hypothesised that  $\delta^{13}\text{C}$  values would decrease with increasing size due to the age-related offshore movements of *S. officinalis*, *S. elegans*, *C. pagurus*, and *H. gammarus*. We also hypothesized that muscle  $\delta^{15}\text{N}$  values would become enriched with increasing size due to size-related increases in trophic level. Second, we compared the isotopic niche widths and overlap among species to describe resource use and potential competition, respectively. We hypothesized that there would be high levels of isotopic overlap as a result of their opportunistic feeding behaviours and overlapping use of benthic habitats. Due to the higher mobility of the nekto-benthic cephalopod species, we hypothesized that they will display a broader range of  $\delta^{13}\text{C}$  values than the less mobile crustacean species.

## 3.2 Material and methods

### 3.2.1 Study organisms

*S. officinalis* and *S. elegans* are nekto-benthic cephalopods, distributed from the Mediterranean Sea to the Northeast Atlantic shelf (Lishchenko et al., 2021). Both species are generalist and voracious feeders (Bloor, Attrill and Jackson, 2013). Both species have a short life span, with *S. officinalis* living for up to two years and *S. elegans* for up to 18 months in the English Channel (Gibson, Atkinson and Gordon, 2016). *S. officinalis* represents the most profitable cephalopod fishery in the English Channel, with exploitation rates almost doubling between 2007 and 2017 (Davies et al., 2018). Catches have been decreasing since then, but the lack of survey data and their non-quota stock status have led to uncertainties regarding population size and the sustainability of this emerging fishery (ICES, 2023). In 2017, the commercial value of *S. officinalis* reached £25.4 million, but it decreased to £8.2 million in 2020 (MMO, 2021). According to the Marine Management Organisation (2021), this reduction in value may reflect population declines rather than decreased fishing effort. As for *S. elegans*, it is often caught as by-catch and there is almost no commercial demand, which exacerbates the lack of data on its population size and distribution (Barrat and Allcock, 2012).

*C. pagurus* and *H. gammarus* are benthic predators and scavengers (Boudreau and Worm, 2012) distributed widely across the Northeast Atlantic, ranging from intertidal zones to depths of up to 100 meters for *C. pagurus* (Shelton and Hall, 1981) and 150 meters for *H. gammarus* (Binney et al., 2024). They have much longer life spans than the two focal cephalopod species, with *C. pagurus* living for up to 20 years and *H. gammarus* for up to 50 years (McClellan et al., 2014). Habitat and diet shifts associated

with ontogeny are well documented but become less pronounced as the animals grow larger (Harrison, 1997; Onderz. Form. B. et al., 2022). Both species reside in shallow nursery grounds during early life stages before transitioning into deeper waters as they mature, which can help to reduce intraspecific competition (Agnalt et al., 2009). Both species have a generalist diet, primarily preying on bivalves and small crustaceans but occasionally also on larger prey such as fish (Lawton, 1989). *C. pagurus* supports over 250 fishers in the west English Channel, yielding 720 tonnes of landings in 2019 alone, valued at £2.15 million, although there has been a slight decline in recent years (MMO, 2022). In the same year and area, *H. gammarus* landings totalled 84 tonnes, worth £1.3 million, with a historical peak of 147 tonnes recorded in 2007 (MMO, 2022). Collectively, these two species constitute approximately 13% of the UK's total commercial catch. Their economic significance is further underscored by their support of small (under 10m) inshore vessels (Rees, Sheehan and Attrill, 2021), contributing to around 65% of employment in the commercial fishing sector (Stamp et al., 2022).

### 3.2.2 Study site

The English Channel is one of the busiest channels in the world for shipping, recreational and commercial fishing, and aquaculture (Gray, 1996; Glegg, Jefferson and Fletcher, 2015). It is also highly productive and boasts a high diversity of habitats, including biogenic reefs (Dauvin, 2019), maerl beds, seagrass beds, and kelp forests, which provide excellent nursery and feeding grounds for crustaceans and cephalopods (L.Jackson et al., 2001; Hernandez Farinas et al., 2014). However, overfishing and habitat destruction are causing declines in many species and reducing the resilience of marine communities to respond to climate change (Cheung et al., 2012). Given these challenges, implementing an ecosystem-based management approach is increasingly recommended for balancing biodiversity and fisheries targets

(Morissette, Christensen and Pauly, 2012). Food web and niche-based approaches (e.g. using Ecopath) could help develop these strategies by shedding light on inter- and intraspecific competition between ecologically and commercially important species (Chase and Leibold, 2003). Previous studies in this region have indicated dietary niche separation of two crustaceans (*Carcinus maenas* and *Crangon crangon*) using metabarcoding (Siegenthaler et al., 2022), and between *S. officinalis* and various fish species using isotopic methods (Sturbois et al., 2022). Conversely, Stamp et al (2024) observed high levels of isotopic niche overlap between *C. pagurus* and *H. gammarus* suggesting potential for interspecific competition. However, no study to date has examined niche overlap between coexisting cephalopods and crustacea in this important region.

### 3.2.3 Sample collection

This study utilises cephalopods obtained in the Channel through surveys conducted by the Centre for the Environment, Fisheries and Aquaculture Science (Cefas) from 2017 to 2022 using trawling and procured from local fisheries (Fig. 1, Table 1). Samples (whole animals) were stored at -20 °C and defrosted for sex and maturity determination by Cefas. *C. pagurus* and *H. gammarus* were sampled from mussel farms near to and inside the Lyme Bay MPA as detailed in Olczak (2022) and Stamp et al. (2024).

Table 1: Summary information of all cephalopod and crustacean samples collected from various sampling locations in the English Channel, UK. Multiple sampling locations for a species were averaged, therefore longitudes and latitudes shown on the table relate to the general sampling location of that species. Specific locations for *Sepia officinalis* from 2020 are unknown.

Species	Taxonomic group	Year collected	n	Size range (cm)	Sampling locations
<b><i>Sepia elegans</i></b>	Cephalopod	2017	7	3.5 - 7	49.71243°N, 4.22544°W
<b><i>Sepia officinalis</i></b>	Cephalopod	2017	8	7.5-11.5	49.77417°N, 4.07833°W
<b><i>Sepia officinalis</i></b>	Cephalopod	2020	8	11 - 15	Western channel commercial landings
<b><i>Sepia officinalis</i></b>	Cephalopod	2022	8	14 - 24	ICES Rectangle 30E8
<b><i>Cancer pagurus</i></b>	Crustacean	2020	39	8.2-19.9	50.64470°N, 3.10770°W
<b><i>Homarus gammarus</i></b>	Crustacean	2020	34	6.6-16.7	50.64443°N, 3.12484°W

## 3.2.4 Sample preparation

### 3.2.4.1 Cephalopods

Whole samples were stored at -20 °C at Cefas laboratories in Lowestoft. When ready for dissection, the mantle length was measured, then a longitudinal incision made along the mantle's ventral side to expose the internal organs to determine sex and maturity stage. Mantle muscle samples approximately 2 cm<sup>3</sup> were dissected from the underside of the body, near the head and adjacent to the gill area with subsequent removal of the skin and thorough washing with Milli-Q water to eliminate residues before freezing the muscle sample at -20°C.

To prepare samples for isotopic analysis, the muscle plugs were defrosted, cleaned again with Milli-Q water, then dried for 24-48 hours at 65 °C. A portion of muscle



approximately 1 cm<sup>3</sup> was broken off and homogenised using an agate pestle and mortar, ensuring that the equipment was cleaned with ethanol then Milli-Q water then dried thoroughly after every sample. The homogenised tissue was then weighed into clean tin capsules and sealed.

#### 3.2.4.2 Crustaceans

Samples from crustacean species were prepared on the vessels immediately after collection. *C. pagurus* muscle tissues were extracted from the rear right swimming leg, while *H. gammarus* tissues were taken from the endopod of the fourth swimming leg. Each individual was photographed for identification to species level. Key data such as the sampling date, sex, carapace size, weight, general condition, and coordinates of the collection points were recorded. To preserve the specimens for subsequent analysis, liquid nitrogen was used for flash-freezing, followed by storage at -80°C until the tissues were ready for laboratory examination.

At the University of Plymouth Laboratory, tissues were dissected, cleaned, and refrozen. The freeze-drying process involved evaporation and desiccation, using parafilm covers with vent holes and silica gel in a desiccator for 24 hours. The dried tissue samples were homogenised using a pestle and mortar and 0.7 mg of the powdered tissue were weighed into clean tin capsules and sealed.

#### 3.2.5 Stable isotope analysis

Stable isotope ratio analysis for cephalopod samples was performed at the Laboratório de Isótopos Estáveis LIE - Stable Isotopes Analysis Facility, at the Faculdade de Ciências, Universidade de Lisboa – Portugal.  $\delta^{13}\text{C}$  and  $\delta^{15}\text{N}$  measurements were determined by continuous flow isotope mass spectrometry (CF-IRMS) (Preston and Owens, 1983), on a Sercon Hydra 20-22 (Sercon, UK) stable isotope ratio mass spectrometer, coupled to a EuroEA (EuroVector, Italy) elemental analyser for online

sample preparation by Dumas-combustion. Delta Calculation was performed according to  $\delta = [(R_{\text{sample}} - R_{\text{standard}}) / R_{\text{standard}}] * 1000$ , where R is the ratio between the heavier and lighter isotope.  $\delta^{15}\text{N}_{\text{Air}}$  values are referred to air and  $\delta^{13}\text{C}_{\text{VPDB}}$  values are referred to PDB (Pee Dee Belemnite). The reference materials used were IAEA N1, IAEA N2 and USGS26, and Glucose BCR no. 657, IAEA-CH7 and IAEA-C3 (Coleman and Meier-Augenstein, 2014), while the laboratory QC check used was Rice Flour. The uncertainty of the isotope ratio analysis was  $\leq 0.2\text{‰}$ , calculated using values from 6 to 9 replicates of laboratory standard interspersed among samples in every batch of analysis. The major mass signals of N and C were used to calculate total N and C abundances, using Wheat Flour Standard OAS (Elemental Microanalysis, UK, with 1.47%N, 39.53%C) as elemental composition reference materials.

Stable isotope ratio analysis for crustacea muscle samples was performed at the University of Southampton Stable Isotope Ratio Mass Spectrometry Laboratory using an Elementar vario Isotope Select Elemental Analyser, set to CN mode and equipped with a Thermal Conductivity Detector (TCD), interfaced with an Isoprime 100 continuous flow isotope ratio mass spectrometer (IRMS). The samples were combusted at 950 °C with the addition of pure oxygen. The resulting gases, NO<sub>x</sub> and CO<sub>2</sub>, were then reduced to N<sub>2</sub> and CO<sub>2</sub> in the reduction column, maintained at 550 °C. The TCD determined the elemental ratios, while the IRMS was used for isotope ratio analysis. Acetanilide served as the elemental standard for carbon and nitrogen. For normalising the isotope ratios, international reference materials USGS 40 and USGS 41 were used. Additionally, appropriate quality control materials, like the internal fish muscle standard, were employed to ensure the precision of the analysis.

Although two different isotope laboratories were used to analyse the cephalopod and crustacean samples, as previously mentioned, three *S. officinalis* muscle samples

were also analysed at the University of Southampton. The  $\delta^{13}\text{C}$  and  $\delta^{15}\text{N}$  values obtained from these samples differed by no more than  $\pm 0.9\text{‰}$  for  $\delta^{13}\text{C}$  and  $\pm 2.5\text{‰}$  for  $\delta^{15}\text{N}$  from their overall means, remaining within the total range of isotope values for other *S. officinalis* muscle samples observed in this study.

### 3.2.6 Data analysis

Linear regression was used to test for relationships between body size (mantle length for cephalopods and carapace length for crustaceans) and stable isotope ratios ( $\delta^{13}\text{C}$  and  $\delta^{15}\text{N}$ ) for each species. Residuals were checked for normality, independence, and equal variance.

Standard ellipse areas (SEA) of muscle  $\delta^{13}\text{C}$  and  $\delta^{15}\text{N}$  values were used to visualise and compare the isotopic niche space between each species pairing after Jackson et al. (2011). To assess interannual variation, the isotopic niche of *S. officinalis* was also compared between individuals sampled in 2017, 2020 and 2022, however comparisons among *S. officinalis*, *C. pagurus*, and *H. gammarus* collected in 2020 were deemed the most robust, as they are free from potential confounding effects of interannual variability in isotopic baselines. Specifically, SEA corrected for small and unequal sample sizes ( $\text{SEA}_c$ ) was estimated using the SIBER package in R (Jackson et al., 2011) using maximum likelihood estimates. Initially, ellipses were calculated to encapsulate 95% of the data, representing the complete isotopic niche ( $\text{CI} = 0.95$ ), followed by the core isotopic niche ( $\text{CI} = 0.4$ ) to facilitate a more conservative comparison (Jones et al., 2020). Bayesian estimated standard ellipse areas ( $\text{SEA}_B$ ) were calculated from posterior estimates using confidence intervals of 50%, 75%, and 95%, providing a robust estimation of niche area while accounting for uncertainties.  $\text{SEA}_B$  values at upper and lower 95% CI were extracted to compare ellipse size among groups, allowing for their differences to be stated and whether they are significant or

not (Buss et al., 2022). Lastly, the percentage overlap between each species pair was quantified using the "maxLikOverlap" function to estimate SEAc from the original isotope data via the maximum-likelihood estimation approach, similar to the methods used by Planque et al. (2021).

Finally, six niche metrics were applied using the "laymanMetrics" function in the SIBER package to describe the variability in  $\delta^{13}\text{C}$  and  $\delta^{15}\text{N}$  values, enabling comparisons between groups and allowing inferences to be drawn about the structure and distribution of data points within each niche (Layman et al., 2007).

- 1 The  $\delta^{13}\text{C}$  range (CR) observed for each group, which reflects the full extent of basal resources utilised by a group.
- 2 The  $\delta^{15}\text{N}$  range (NR) observed for each group, which indicates the diversity of trophic levels within the group at the species scale.
- 3 The area of the convex hull (TA) that encloses all isotope data points for a group within the isotopic biplot. TA captures the full diversity of isotopic sources supporting the group or species, representing their entire niche.
- 4 The mean distance to the centroid (CD) measures the average deviation of individual data points from the centroid, which is calculated as the bivariate mean of the group's isotopic data. CD provides insight into the variability of isotopic sources used by the group.
- 5 The mean nearest neighbour distance (NND), calculated as the average straight-line distance between each data point and its nearest neighbour. It indicates the density and clustering of isotopic data points within the group.
- 6 The standard deviation of the mean nearest neighbour distance (SDNND). It highlights the variability in evenness of spacing between data points within the group.

### 3.3 Results

Across all species and years, there was a narrow range of  $\delta^{13}\text{C}$  values from -19.0‰ to -17.1‰. The highest  $\delta^{13}\text{C}$  values were observed in *S. officinalis* from 2017 (-17.1‰), while the lowest were recorded in *H. gammarus* from 2020 (-19.0‰). For *S. officinalis*,  $\delta^{13}\text{C}$  values varied across the years from -18.8‰ in 2017 to -17.3‰ in 2020. The  $\delta^{15}\text{N}$  values ranged from 10.6‰ to 14.8‰ (i.e. >1 trophic level), with the lowest  $\delta^{15}\text{N}$  value recorded in *S. elegans* from 2017 and the highest in *C. pagurus* from 2020. For *S. officinalis*,  $\delta^{15}\text{N}$  values ranged from 11.9‰ to 14.5‰, with the highest values observed in 2022. Other species, such as *H. gammarus*, showed a  $\delta^{15}\text{N}$  range of 11.6‰ to 14.6‰, while *C. pagurus* exhibited a  $\delta^{15}\text{N}$  range from 11.8‰ to 14.8‰.

#### 3.3.1 Isotope ratios and body size relationships

In most instances, muscle  $\delta^{13}\text{C}$  and  $\delta^{15}\text{N}$  values were unrelated or weakly positively related to body size (Fig. 1). Muscle  $\delta^{13}\text{C}$  showed no significant relationships with size, except for a positive relationship for *C. pagurus* ( $F_{1, 38} = 13.11$ ,  $p < 0.001$ ). Positive relationships were also observed between muscle  $\delta^{15}\text{N}$  and body size for *S. officinalis* (all years pooled;  $F_{1,23} = 16.97$ ,  $p < 0.001$ ) and *S. elegans* ( $F_{1,6} = 8.905$ ,  $p = 0.0245$ ). However, the relationships were generally weak ( $r^2 = 0.23$  to  $0.60$ ; Fig. 1) and no significant correlations were observed between either isotope and body size for *S. officinalis* when the data were separated by year, with samples collected in 2022 tending to have  $\delta^{15}\text{N}$  values around 2‰ higher than the other two collection years (Fig. 1).

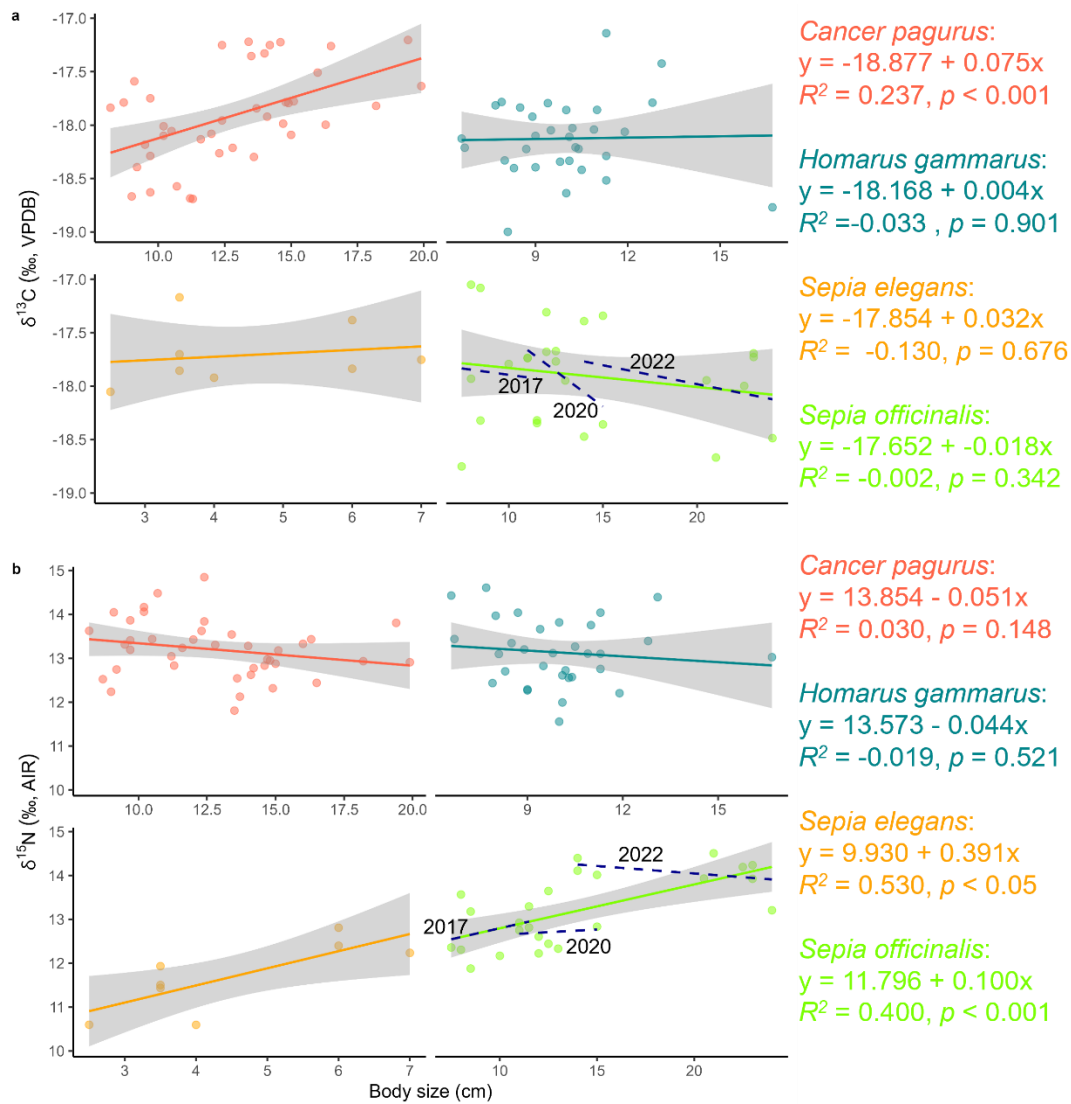


Fig. 1: Body size versus muscle (a)  $\delta^{13}\text{C}$  and (b)  $\delta^{15}\text{N}$  of *Cancer pagurus* (red), *Homarus gammarus* (turquoise), *Sepia elegans* (yellow) and *S. officinalis* (green). Size was defined by mantle length and carapace size for cephalopods and crustaceans, respectively. For each species a linear regression model was fitted ( $\pm 95\%$  CI, grey shading) with the equations displayed on the right of the plots. Linear regression models were fitted separately for each year groups comprising the *S. officinalis* samples (2017, 2020, 2022) and displayed as the dashed dark blue lines along with the solid green line on both *S. officinalis* plot window.

### 3.3.2 Isotopic niche overlap

Although the 2022 *S. officinalis* samples exhibited noticeably enriched  $\delta^{15}\text{N}$  compared to both the 2017 and 2020 samples, high overlap between 95% SEACs (ellipses encapsulating 95% of the data, representing the complete isotopic niche) were observed among years for this species (Fig. 2a). As such, we performed subsequent

niche overlap analyses with *S. officinalis* included with all years combined and with 2020 separated for more direct comparison with *C. pagurus* and *H. gammarus* (also collected in 2020). Overall, 95% SEAc were highly overlapping across groups (Fig. 2b). The least overlap was observed for *S. elegans*, which displayed relatively depleted  $\delta^{15}\text{N}$  values. The core isotopic niche (40% SEAc) exhibited similar trends (Fig. 2c-d; Table 2) with the combined-year *S. officinalis* ellipse showing the largest overlap with *C. pagurus* (74.1%), followed by a 50% overlap between the two crustacean species, followed by a 47.3% overlap between the ellipses of the combined-year *S. officinalis* and *H. gammarus*. Similar to the 95% SEAc, the *S. officinalis* 2020 samples exhibited a smaller ellipse than when all years were combined, and when matching years were compared, *S. officinalis* exhibited a greater overlap with *C. pagurus* (29.4%) than *H. gammarus* (17.6%). The *S. elegans* 40% SEAc ellipse was largely isolated, with no overlap except for a 5% overlap with the *S. officinalis* 2020 group.

Table 2: Sample size-corrected ellipse areas (SEAc) encompassing approximately 40% of data per group are displayed. Overlap of 40% SEAc were generated using SIBER (n=1000 iterations) and ellipse areas (‰<sup>2</sup>) displayed for each group pairs of *S. officinalis* (2020), *S. officinalis* (all years combined), *S. elegans* (2017), *C. pagurus* (2020) and *H. gammarus* (2020). % overlap is the proportion of overlapping sections between ellipse pairs, relative to their non-overlapping sections.

Groups (1) & (2)	Area 1 (‰ <sup>2</sup> )	Area 2 (‰ <sup>2</sup> )	Overlap Area (‰ <sup>2</sup> )	Overlap (%)
<i>S. officinalis</i> (2020) vs <i>C. pagurus</i> (2020)	0.562	0.941	0.342	29.4
<i>S. officinalis</i> (all years) vs <i>C. pagurus</i> (2020)	1.270	0.941	0.941	74.1
<i>S. officinalis</i> (2020) vs <i>H. gammarus</i> (2020)	0.562	0.814	0.206	17.6
<i>S. officinalis</i> (all years) vs <i>H. gammarus</i> 2020	1.270	0.814	0.669	47.3
<i>S. officinalis</i> (2020) vs <i>S. officinalis</i> (all years)	0.562	1.270	0.450	32.6
<i>C. pagurus</i> (2020) vs <i>H. gammarus</i> (2020)	0.941	0.814	0.585	50.0
<i>S. officinalis</i> (2020) vs <i>S. elegans</i> (2017)	0.562	0.700	0.061	5.1
<i>S. elegans</i> (2017) vs <i>S. officinalis</i> (all years)	0.700	1.270	0.000	0.0
<i>S. elegans</i> (2017) vs <i>C. pagurus</i> (2020)	0.700	0.941	0.000	0.0
<i>S. elegans</i> (2017) vs <i>H. gammarus</i> (2020)	0.700	0.814	0.000	0.0



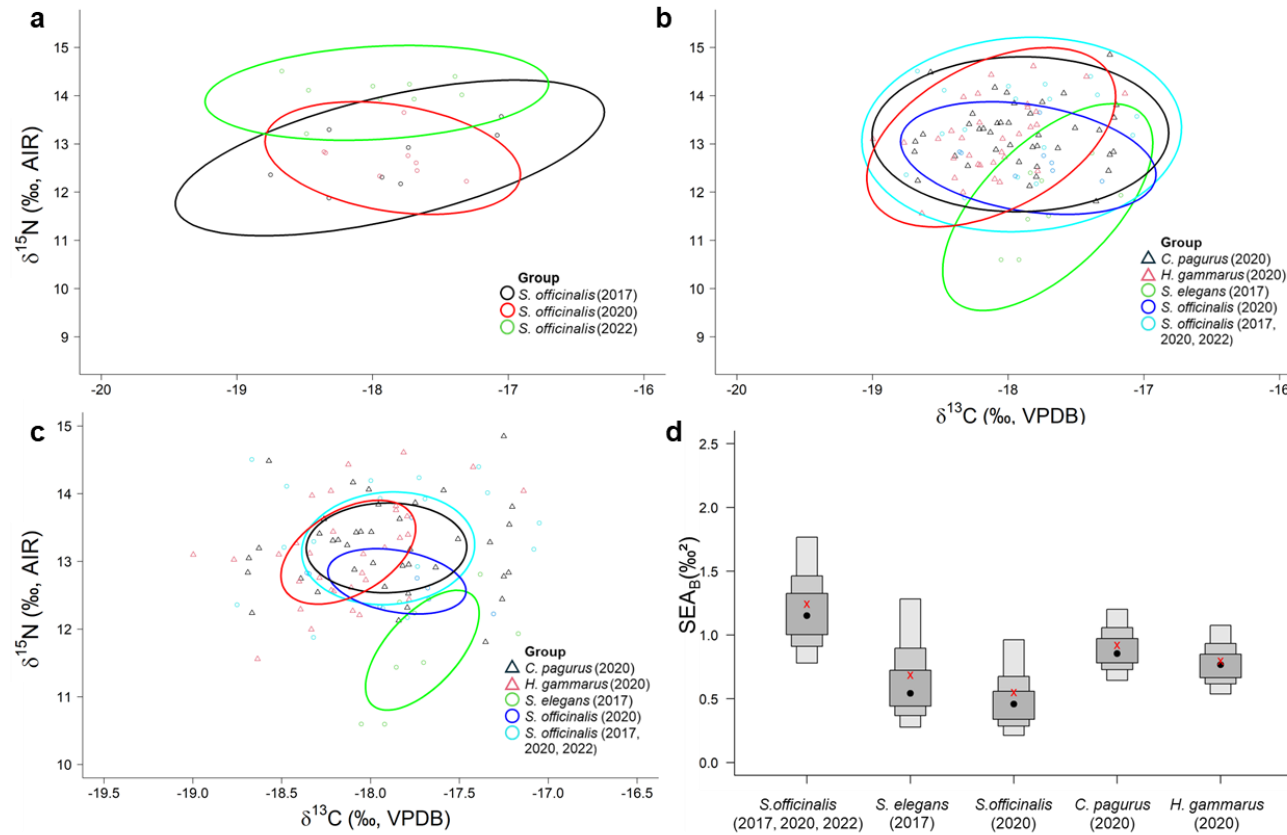


Fig. 2: (a) Sample size-corrected 95% ellipse (SEA<sub>C</sub>) fitted to muscle  $\delta^{13}\text{C}$  and  $\delta^{15}\text{N}$  of *S. officinalis* samples collected from 2017 (black), 2020 (red) and 2022 (green). (b) 95% SEA<sub>C</sub> of *C. pagurus* (black triangles), *H. gammarus* (red triangles), *S. elegans* (green circles), *S. officinalis* from 2020 (dark blue circles) and the combined *S. officinalis* samples from 2017, 2020 and 2022 (light blue circles). (c) 40% SEA<sub>C</sub> of *C. pagurus* (black triangles), *H. gammarus* (red triangles), *S. elegans* (green circles), *S. officinalis* from 2020 (dark blue circles) and the combined *S. officinalis* samples from 2017, 2020 and 2022 (light blue circles). (d) Bayesian standard ellipse areas (SEA<sub>B</sub>) for each group based on posterior estimates after  $n = 1000$  iterations. These estimated areas are plotted on a density plot (d) depicting their confidence intervals. Dark grey box (50% CI), grey (75% CI) and light grey (95% CI). The black dot represents the mode of SEA<sub>B</sub> estimates. Red crosses correspond to the 40% SEA<sub>C</sub>. SIBER was used to generate the ellipses and density plots.

### 3.3.3 Isotopic niche width and diversity

Niche widths (SEAc size) were relatively similar across all groups and Bayesian estimates (SEAB) confirmed that ellipse sizes were not different (Fig. 2d). Among all groups, *H. gammarus* exhibited the widest isotopic niche, with the largest CR (1.859‰) and NR (3.053‰), *C. pagurus* followed closely with a CR of 1.487‰ and NR of 3.041‰. Combined *S. officinalis* displayed a moderately wide niche (CR = 1.701‰, NR = 2.628‰), reflecting a broad but slightly more limited range compared to the crustaceans. In contrast, *S. elegans* 2017 had the smallest CR (0.883‰) and a moderate NR (2.214‰). *S. officinalis* 2020 had a similarly narrow range of isotopic resources (CR = 1.05‰, NR = 1.422‰). In terms of total area (TA), *C. pagurus* had the largest TA (3.735‰<sup>2</sup>), followed closely by combined *S. officinalis* (3.622‰<sup>2</sup>). *H. gammarus* had a slightly smaller TA (3.02‰<sup>2</sup>), while *S. officinalis* 2020 and *S. elegans* 2017 had the smallest TA values (0.745‰<sup>2</sup> and 0.983‰<sup>2</sup>, respectively), indicating narrower niche sizes.

Combined *S. officinalis* had the largest CD (0.862), with *S. elegans* following at 0.721. The crustaceans had lower CD values, with *H. gammarus* and *C. pagurus* at 0.715 and 0.678, respectively. *S. officinalis* 2020 exhibited the lowest CD (0.466). For NND, *S. elegans* showed the largest value (0.28), reflecting the widest spacing between individual data points. Combined *S. officinalis* and *S. officinalis* 2020 followed closely (NND = 0.267 and 0.268). *H. gammarus* and *C. pagurus* had the lowest NND values (0.189 and 0.203), suggesting more tightly clustered data points. In terms of SDNND, *S. officinalis* 2020 showed the highest variability (SDNND = 0.286), followed by *S. elegans* (0.221). Combined *S. officinalis* and *C. pagurus* had moderate SDNND values

(0.164 and 0.169), while *H. gammarus* had the most even distribution of isotopic data points (SDNND = 0.135).

Table 3: Layman's metrics to describe isotopic niche variability per group. Number of samples (n), the total range of carbon isotope ratios (CR, ‰), total range of nitrogen isotope ratios (NR, ‰), total area of the convex hulls (TA, ‰<sup>2</sup>), mean distance to centroid (CD), mean nearest neighbour distance (NND) and standard deviation of nearest neighbour distance (SDNND) are displayed below. Values for CD, NND and SDNND range between 0-1. All metric values were generated using SIBER. See section 2.5.2.1 for explanations of each metrics displayed below.

Group	n	CR (‰)	NR (‰)	TA (‰ <sup>2</sup> )	CD	NND	SDNND
<i>S. officinalis</i> (all years)	24	1.701	2.628	3.622	0.862	0.267	0.164
<i>S. officinalis</i> (2020)	8	1.05	1.422	0.745	0.466	0.268	0.286
<i>S. elegans</i> (2017)	7	0.883	2.214	0.983	0.721	0.28	0.221
<i>C. pagurus</i> (2020)	39	1.487	3.041	3.735	0.678	0.203	0.169
<i>H. gammarus</i> (2020)	34	1.859	3.053	3.02	0.715	0.189	0.135

### 3.4 Discussion

This study revealed high isotopic niche overlap between four coexisting cephalopod and crustacean species in the English Channel. Although the isotopic niche is not synonymous with trophic niche and cannot fully capture the complexity of trophic interactions, it serves as a useful proxy for inferring resource competition, particularly for species such as these that are known to co-exist and use similar habitats and resources (Marshall et al., 2019). Given the ongoing environmental changes driven by both natural and anthropogenic disturbances, including climate change, examining previously unstudied niche overlaps provides insights for species and habitat management. Such insights could improve long-term predictions of potential impacts resulting from modifications to recreational or commercial fisheries (Dillon et al., 2021).

This understanding may have broader implications for food security and employment, both within the English Channel and globally (Stamp et al., 2022). By enhancing the

ability of managers to detect ecological shifts, it provides an opportunity for timely interventions, potentially preventing irreversible population declines. (Anderson et al., 2011; Stamp et al., 2022).

### 3.4.1 Body size relationships

The observation that  $\delta^{13}\text{C}$  and  $\delta^{15}\text{N}$  values in *H. gammarus* did not significantly change with size indicating no clear ontogenetic shifts in diet and so individuals of all sizes will compete for a similar pool of resources. It also suggests that, regardless of body size, some individuals are feeding at the same or higher trophic levels than 2020 *S. officinalis*, as inferred from  $\delta^{15}\text{N}$  values. This same relationship was observed between *C. pagurus* and *S. officinalis*. The independence of  $\delta^{15}\text{N}$  from body size has been documented in other crustaceans, such as *Callinectes sapidus* (Hoeinghaus and Iii, 2007) and may reflect opportunistic feeding behaviour (Siegenthaler et al., 2022).

Conversely, *C. pagurus* may reduce intraspecific competition through habitat differentiation during ontogeny, as suggested by significant enrichment of  $\delta^{13}\text{C}$  with increasing body size. Similarly, *S. elegans* may reduce intraspecific competition through ontogeny, inferred from significant  $\delta^{15}\text{N}$  enrichment, which suggests that it may prefer different prey types as body size increases, while still feeding at the same trophic level within the studied size range.

The different strategies of resource partitioning within species, as revealed by the relationship between isotope ratios and body size, may be necessary to mitigate the high niche overlap observed among species in this study.

### 3.4.2 Isotopic niche overlap

Given the potential isotopic variation at the base of the food web among years, the most robust comparisons of isotopic niche were made between *S. officinalis*, *C. pagurus*, and *H. gammarus* samples collected in 2020, revealing high levels of niche overlap based on muscle  $\delta^{13}\text{C}$  and  $\delta^{15}\text{N}$  values. As expected, the crustacean species showed the highest overlap, suggesting that these sympatric decapods share similarities in diet and habitat (Agnalt et al., 2009; McClellan et al., 2014), but likely partition their niches by using different microhabitats to avoid competitive exclusion and maintain equilibrium. Such behaviour-driven niche partitioning has also been observed by Siegenthaler et al. (2022) in English Channel decapods.

*S. officinalis* exhibited more isotopic overlap with *C. pagurus* than with *H. gammarus*. Both *S. officinalis* and *C. pagurus* displayed slightly more enriched  $\delta^{13}\text{C}$  values, suggesting nearshore benthic environments, while *H. gammarus* exhibited more depleted  $\delta^{13}\text{C}$  values, indicative of offshore carbon sources (Hobson, 1998). This may be related to *H. gammarus* territorial behaviour and limited home range (Smith et al. 2001), with minimal movement into shallower waters compared to *C. pagurus* and *S. officinalis*. Given that these *H. gammarus* individuals were collected in and adjacent to the Lyme Bay MPA, they likely had access to high-quality habitat, reducing the need for extensive movement for foraging. While *C. pagurus* and *S. officinalis* likely have more extensive home ranges (Bloor et al., 2013a; Hunter et al., 2013), this was not reflected in broad-ranging  $\delta^{13}\text{C}$  values, further supported by the similar isotopic niche widths and CR values among species. Similar niche widths (Fig. 2d) suggested that none of the species exploited a significantly greater range of resources than the others, reinforcing their generalist feeding behaviours.

Among all isotopic niche comparisons, the key finding was that the order of overlap remained consistent between the combined-year *S. officinalis* and the crustacean species, even with the increased isotope diversity from other years. This suggests that *C. pagurus* may be in greater competition with *S. officinalis* than *H. gammarus*, likely due to the more depleted  $\delta^{13}\text{C}$  values in *H. gammarus*. The combined-year *S. officinalis* niche also encompassed the full range of the *C. pagurus* trophic niche, with the inclusion of 2022 *S. officinalis* samples widening its  $\delta^{15}\text{N}$  range. This indicates potential competition across different body sizes, indirectly suggesting competition across life stages between *S. officinalis* and the crustacean species. These findings point to complex resource-use dynamics and highlight variations in the mode of life between the studied species, which may facilitate coexistence in the Channel, despite what appears to be high competition inferred from the high overlap (Lancaster, Morrison and Fitt, 2017). *S. officinalis* typically live for two years, while the crustacean species have much longer lifespans, raising questions about how these dynamics may shift with environmental changes or increased fishing pressure.

*S. elegans* exhibited the least overlap with the other groups and demonstrating niche partitioning. While its  $\delta^{13}\text{C}$  values overlapped with those of other species, *S. elegans* showed depleted  $\delta^{15}\text{N}$  values, indicating it feeds at relatively lower trophic levels. This highlights the role of species size in resource partitioning, whereby physiological constraints like gape size limit prey size diversity, as seen in teleost (Eaton, 2019).

All four species exploit overlapping food resources within benthic communities in the English Channel and surrounding northeast Atlantic waters. Crustaceans represent a significant dietary component common to these species. Both *C. pagurus* and *H. gammarus* preferentially prey upon crustaceans such as smaller crabs, shrimps, and

squat lobsters, alongside molluscs like bivalves and gastropods (Lawton, 1995). In contrast, while crustaceans similarly feed on a substantial proportion of the diet of *S. officinalis* (Castro and Guerra, 1990), cuttlefish typically target smaller, more mobile prey, including shrimps, mysids, and juvenile crabs (Blanc and Daguzan, 1998). Although molluscs and echinoderms, such as starfish and urchins, are commonly preyed upon by both crustacean species, they are notably absent in the diets of *S. officinalis* and *S. elegans* (Guerra, 2006; Neves et al., 2009).

Considering dietary overlap, the greatest potential competition likely exists between *C. pagurus* and *H. gammarus* due to their reliance on similar hard-shelled benthic invertebrates. This corresponds with observations in the current study, which found the highest isotopic niche overlap occurred between these two crustacean species. The moderate niche overlap observed between the crustaceans and *S. officinalis* in the results may reflect shared predation on smaller crustaceans like shrimps and juvenile crabs. Therefore, the observed isotopic niche overlaps in the results align with known dietary preferences, suggesting that these species exploit shared resources to varying extents while still maintaining some degree of niche partitioning.

### 3.4.3 Limitations

The combination of *S. officinalis* samples is confounded by highly variable isotope ratios of basal resources attributed to a potentially high turnover rate of their tissue (Post, 2002), which can affect the position of consumers in isotope space. Other factors, such as prey availability, isotope routing, and fractionation, may also contribute to isotope differences among consumers, even within conspecifics (Shipley and Match, 2020). No corrections were applied to the muscle  $\delta^{13}\text{C}$  and  $\delta^{15}\text{N}$  values to align isotope signatures of spatiotemporally separated species and consumers. These

type of corrections would have offset differences in baseline values and accounted for species-, sex-, and tissue-specific isotopic fractionations (Midani, Wynn and Schnell, 2017). The absence of these adjustments presents a limitation that may have influenced the interpretation of isotopic niche data.

Differences among years were largely driven by enriched  $\delta^{15}\text{N}$  values in 2022 *S. officinalis*, which could be attributed to sampling of larger individuals in 2022 compared to 2017 and 2020 who may thus have been feeding at higher trophic levels. Nevertheless, separate analyses for each year suggest no significant relationship between  $\delta^{13}\text{C}$  or  $\delta^{15}\text{N}$  and body size (Fig. 1). Similar findings of trophic enrichment was reported by Vinagre et al. (2011) for *S. officinalis* in the Bay of Cascais, though their study, like this one, was limited by small sample sizes and under-representation of larger body sizes. In contrast, Chouvelon et al. (2011) with comparable body size ranges and sample sizes to the combined *S. officinalis* group in this study, found a positive relationship between body size and  $\delta^{15}\text{N}$ . An increase in  $\delta^{15}\text{N}$  with ontogeny is common in cephalopods (Sajikumar et al., 2020; Sakamoto et al., 2023) and was also observed in *S. elegans* in this study. Therefore, assuming a similar pattern for the combined-year *S. officinalis* samples aligns with trophic trends.

The methods used to quantify stable isotope ratios can also lead to misinterpretations. For instance, standard ellipses among all groups were not significantly different, as shown by overlapping 95% confidence intervals (light grey boxes, Fig. 2d).  $\text{SEA}_\text{C}$  niche sizes were close to the mode of  $\text{SEA}_\text{B}$  predictions but slightly inflated for all groups (red crosses, Fig. 2d), providing some confidence that  $\text{SEA}_\text{C}$  estimates were reasonably accurate. However, Jackson et al. (2011) demonstrated that  $\text{SEA}_\text{C}$  estimates, although corrected, can still be biased by low sample sizes, as seen in the



greater discrepancy between  $SEA_B$  mode and  $SEA_C$  estimates for *S. elegans* ( $n=7$ ). With larger sample sizes, it is likely that more groups would show greater niche separation, particularly if lower  $SEA_B$  estimates were followed.

Lastly, another limitation of this study is that cephalopod and crustacean samples were not collected from precisely the same locations within the English Channel, resulting in uncertainty regarding whether these species genuinely share resources. Similar isotopic signatures can be widespread across large areas without necessarily indicating any direct interactions among the studied species. Therefore, although isotopic niche overlap suggests potential resource sharing, it alone cannot conclusively confirm direct dietary competition due to the potential spatial separation in sampling. Despite this limitation, comparing the isotopic niches of these cephalopods and crustaceans remains valuable for understanding their ecological roles and potential trophic interactions at broader, regional scales. Even with spatial uncertainties, isotopic analyses provide essential baseline information about resource use patterns in *S. officinalis*, *S. elegans*, *C. pagurus*, and *H. gammarus*, forming an initial step towards identifying possible trophic overlaps. Subsequent investigations should aim to sample these species from shared foraging grounds and validate the findings through similar methods applied in this study.

### 3.4.4 Conclusions

This study highlights the importance of careful interpretation when assessing isotopic niche overlap, as overlap does not necessarily indicate direct competition. Various ecological factors and interactions can influence niche dynamics, and the context in which overlap occurs must be considered. Nonetheless, the methods used in this study, including Layman's metrics for analysing isotopic data structure, provide

valuable insights into the organisation of species within communities. The use of standard ellipses for presenting and quantifying isotopic niches offers a simple yet effective way to compare different organisms.

The relatively broad isotopic niches observed across all species suggest a diverse prey base, which could enhance their resilience to environmental change. However, the strong basis for competition among the four species co-occurring in the English Channel point to the need for a comprehensive approach in conservation and fisheries management. Such an approach should consider the interconnectedness of these species and the prey they depend on to ensure sustainable management of the ecosystem.

While common challenges in stable isotope analysis, such as annual baseline variability, can complicate interpretations, this study has accounted for these issues where possible. The findings offer meaningful insights into the trophic ecology of the target species, paving the way for future research with robust experimental designs to build on these results.



## Chapter 4 Future Directions

The findings of this thesis provide valuable insights into the trophic ecology and ecological interactions of *Sepia officinalis*, a species of considerable ecological and commercial importance in the English Channel. By exploring stable isotopic differences among tissues, including eye lenses, beaks, and muscle, this study revealed variations in  $\delta^{13}\text{C}$  and  $\delta^{15}\text{N}$  values, shedding light on the trophic ecology of *S. officinalis* throughout its life cycle. Furthermore, the isotopic niche overlap between *S. officinalis* and crustaceans indicated shared dietary and habitat resources with potential for interspecific competition.

Moving forward, experimental research could be key to addressing some of the key gaps in cephalopod trophic ecology. Controlled feeding studies in laboratory settings can investigate estimates of isotopic incorporation rates and tissue-specific fractionation, especially the differences among beaks and eye lenses. Moreover, varying experimental parameters such as temperature, acidity, prey type and availability could clarify how environmental changes influence isotopic assimilation and, as a result, improve isotope-based ecological interpretations (Cherel and Hobson, 2005).

Another direction for future work is the integration of environmental DNA (eDNA) with SIA. Comparing prey community data from eDNA analysis with isotopic signatures, studies could achieve greater taxonomic resolution in diet reconstructions and potentially uncover spatial foraging patterns, by allowing researchers to cross-reference prey spatial distribution and the isotopic signatures within their cephalopod consumers (Saccò et al., 2019). Further works in the field of genetics could also help make sense of the nuances within cephalopod ecology that SIA struggles to answer

on its own. Furthermore, the integration of genomic data with stable isotopes could assess the influence of genetic variations on isotopic fractionation of tissues among sub-populations, sex or maturity, to exemplify a few, and not only could it enhance the resolution of dietary tracing but also allow researchers to identify and target critical life stages more effectively. Genetic variation could also indicate the existence of distinct isotopic niches (indicative of different ecological niches) within *S. officinalis* populations. It is possible for genetic markers to identify diversity within populations of marine organisms and reveal different foraging strategies or the pool of resources they may draw from (Tennesen et al., 2023). Not only does this help contextualise results from isotopic niche studies, but it can be particularly useful for targeted fisheries management.

Direct evidence, such as tagging and stomach content analysis, are also valuable tools to complement stable isotope analysis. A combined isotopic niche data with stomach content analysis can provide a detailed understanding of prey presence and proportions within consumer diets, offering robust insights into consumer-prey interactions. Studies like Hunter et al. (2013) on the movement of *Cancer pagurus* in the English Channel provided direct evidence of habitat preferences. Tagging *S. officinalis* would allow for similar tracking of habitat use. Combining tagging with SIA would not only yield direct evidence of shared habitats but also address limitations in isotopic niche studies, such as the assumption of isotopic homogeneity of prey and basal resources across the environment (Rubenstein and Hobson, 2004).

Compound-specific isotope analysis (CSIA) offers another advanced approach. By targeting specific compounds (e.g., lipids and amino acids) within tissues, the method may provide a more accurate representation of the stable isotope ratios of different

dietary sources (Wu et al., 2018). CSIA provides a more accurate representation of the stable isotope ratios of dietary sources compared to bulk SIA, which gives only average isotope ratios of whole tissues (Wu et al., 2018). For instance, applying CSIA to cephalopod beaks or muscle tissues could yield more precise insights into dietary contributions. It would also enable researchers to detect how specific compounds, such as proteins, influence isotopic signatures, like the effect of chitin on nitrogen isotope ratios. This approach may validate genuine resource-use patterns or identify misleading isotopic signals, such as those arising from lipid content affecting carbon isotope values (Wu et al., 2018).

Additionally, increasing isotopic dimensionality through integrating isotopes like  $\delta^{18}\text{O}$  (oxygen isotopes), which reflect environmental factors such as temperature, could provide broader context for interpreting movement and habitat use. Methods like nicheROVER in R, extending beyond bivariate data ( $\delta^{13}\text{C}$  and  $\delta^{15}\text{N}$ ), could enhance niche overlap and resource partitioning studies (Swanson et al., 2015).

Models such as Ecopath with Ecosim, which integrate fisheries catch data and species interactions, have become important tools for addressing fisheries management questions (Christensen and Walters, 2004). Data derived from isotopic ecology studies can significantly enhance these models by accurately capturing the complexities of species interactions and food web dynamics. Advances in computational methods, including machine learning, are now facilitating the development of more comprehensive ecosystem models. These enhanced models provide researchers with tools to answer complex ecological questions rapidly, offering considerable promise for securing biodiversity and fisheries sustainability in the face of a changing climate.

Stable isotope analysis continues to prove its effectiveness as a powerful ecological research tool, particularly when combined with novel approaches. Continued methodological advances will be essential in overcoming current limitations and enhancing ecological interpretations derived from isotopic data. By integrating stable isotope analysis with these emerging and complementary approaches, researchers can achieve a more complete understanding of cephalopod ecology.

Ultimately, we hope that the findings from this thesis can contribute to guiding the management and conservation of *S. officinalis* and related species. The novel insights gained into isotopic differences or correction factors between tissues can enhance comparisons across different studies of *S. officinalis*. Furthermore, understanding the complexities of multi-tissue analysis is crucial for addressing challenges in interpreting ecological data in stable isotope studies. This research also emphasizes the value of an ecosystem-based management approach, particularly in dynamic and critical ecosystems like the English Channel, which are increasingly impacted by climate change.





## Appendices

Table 2: Age-specific correction factors for  $\delta^{13}\text{C}$  and  $\delta^{15}\text{N}$  values in the archival tissues of *S. officinalis* where age had a significant effect. Correction factors (‰) are provided for each age class (0.75, 1.00, and 2.00 years) in both beak and eye lens tissues. A significant effect ( $p < 0.05$ ) was observed for  $\delta^{13}\text{C}$  and  $\delta^{15}\text{N}$  in beaks, and for  $\delta^{15}\text{N}$  in eye lenses, while  $\delta^{13}\text{C}$  in eye lenses showed no significant age-related variation ( $p > 0.05$ ).

Archival tissue	Isotope	Age class (years)	Correction Value (‰)	p-value
Beak	$\delta^{13}\text{C}$	0.75	+1.65	<0.05
Beak	$\delta^{13}\text{C}$	1.00	+2.05	<0.05
Beak	$\delta^{13}\text{C}$	2.00	+3.01	<0.05
Beak	$\delta^{15}\text{N}$	0.75	+2.44	<0.05
Beak	$\delta^{15}\text{N}$	1.00	+3.02	<0.05
Beak	$\delta^{15}\text{N}$	2.00	+3.95	<0.05
Eye Lens	$\delta^{15}\text{N}$	0.75	+3.98	<0.05
Eye Lens	$\delta^{15}\text{N}$	1.00	+4.77	<0.05
Eye Lens	$\delta^{15}\text{N}$	2.00	+5.12	<0.05
Eye Lens	$\delta^{13}\text{C}$	0.75	0.00	>0.05
Eye Lens	$\delta^{13}\text{C}$	1.00	0.00	>0.05
Eye Lens	$\delta^{13}\text{C}$	2.00	0.00	>0.05

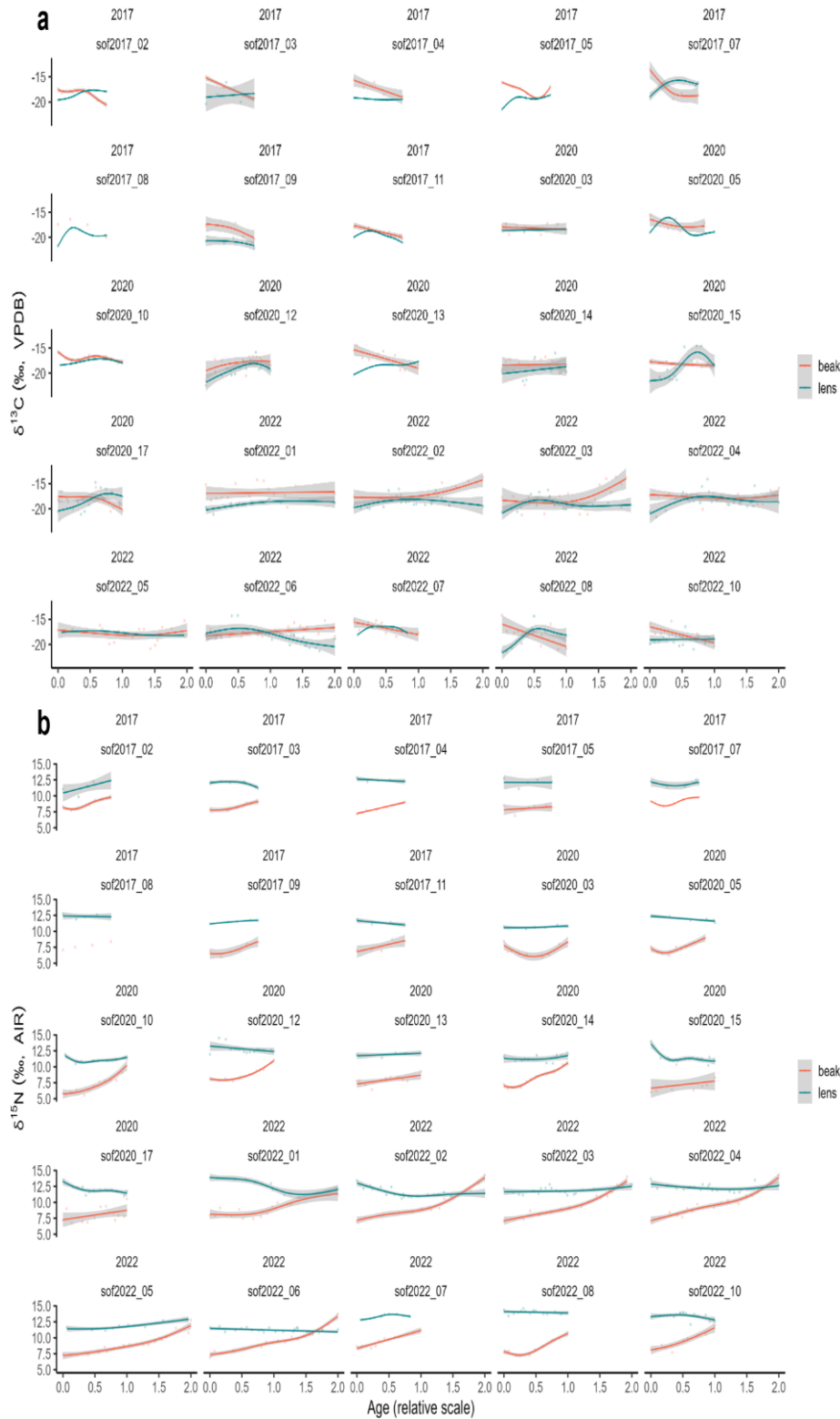


Fig. 11: *Sepia officinalis* lifetime chronological records of  $\delta^{13}\text{C}$  (a) and  $\delta^{15}\text{N}$  (b) for each individual specimen analysed in this study are shown using beak (red) and eye lens (turquoise) isotope data. To visualize trends for each archival tissue, a LOESS smoother was applied to the data using ggplot in R.



## References

- AGNALT, A. et al. (2009) Population characteristics of the world's northernmost stocks of European lobster (*Homarus gammarus*) in Tysfjord and Nordfolda, northern Norway. *New Zealand Journal of Marine and Freshwater Research*, 43(1), pp. 47–57.
- AGUS, B. et al. (2024) Age Estimation in *Sepia officinalis* Using Beaks and Statoliths. *Animals*, 14(15), p. 2230.
- ALVITO, P.M. et al. (2015) Cephalopods in the diet of nonbreeding black-browed and grey-headed albatrosses from South Georgia. *Polar Biology*, 38(5), pp. 631–641.
- ANDERSON, S.C. et al. (2011) Rapid Global Expansion of Invertebrate Fisheries: Trends, Drivers, and Ecosystem Effects. *PLOS ONE*, 6(3), p. e14735.
- ARKHIPKIN, A. (2016) Octopus and squid populations are booming – here's why. [Online] The Conversation. Available from : <http://theconversation.com/octopus-and-squid-populations-are-booming-heres-why-59830> [Accessed 25/01/24].
- ARMELLONI, E.N. et al. (2020) Exploring the embryonic development of upper beak in *Octopus vulgaris* Cuvier, 1797: New findings and implications for age estimation. *Fisheries Research*, 221, p. 105375.
- AUER, S.K. et al. (2016) Flexibility in metabolic rate and activity level determines individual variation in overwinter performance. *Oecologia*, 182(3), pp. 703– 712.
- BARRAT, I. and ALLCOCK, L. (2012) *Rhombosiphon elegans* (Elegant Cuttlefish). [Online] *Sepia elegans*. The IUCN Red List of Threatened Species 2012. Available from : <https://www.iucnredlist.org/species/162579/920760> [Accessed 26/08/24].
- BARRETT, C.J. et al. (2022) Cuttlefish conservation: a global review of methods to ameliorate unwanted fishing mortality and other anthropogenic threats to sustainability. *ICES Journal of Marine Science*, 79(10), pp. 2579–2596.
- BELL-TILCOCK, M. et al. (2021) Advancing diet reconstruction in fish eye lenses. *Methods in Ecology and Evolution*, 12(3), pp. 449–457.
- BEN-TZVI, O. et al. (2007) The inclusion of sub-detection limit LA-ICPMS data, in the analysis of otolith microchemistry, by use of a palindrome sequence analysis (PaSA). *Limnology and Oceanography: Methods*, 5(3), pp. 97–105.
- BETTENCOURT, V. and GUERRA, A. (1999) Carbon- and oxygen-isotope composition of the cuttlebone of *Sepia officinalis*: a tool for predicting ecological information? *Marine Biology*, 133(4), pp. 651–657.
- BINNEY, F. et al. (2024) European Lobster (*Homarus gammarus*) in Jersey, Channel Islands. Summary Report 2024. Government of Jersey.

BLAMPIED, S.R. et al. (2022) Value of coastal habitats to commercial fisheries in Jersey, English Channel, and the role of marine protected areas. *Fisheries Management and Ecology*, 29(5), pp. 734–744.

BLANC, A. and DAGUZAN, J. (1998) Artificial surfaces for cuttlefish eggs (*Sepia officinalis* L.) in Morbihan Bay, France. *Fisheries Research*, 38(3), pp. 225–231.

BLOOR, I.S.M. et al. (2013) Movements and behaviour of European common cuttlefish *Sepia officinalis* in English Channel inshore waters: First results from acoustic telemetry. *Journal of Experimental Marine Biology and Ecology*, 448,

BLOOR, I.S.M., ATTRILL, M.J. and JACKSON, E.L. (2013) A Review of the Factors Influencing Spawning, Early Life Stage Survival and Recruitment Variability in the Common Cuttlefish (*Sepia officinalis*). In: *Advances in Marine Biology*. Elsevier, pp. 1–65.

BOAVIDA-PORTUGAL, J. et al. (2022a) Global Patterns of Coastal Cephalopod Diversity Under Climate Change. *Frontiers in Marine Science*, 8, [Online] Available from: <https://www.frontiersin.org/articles/10.3389/fmars.2021.740781> [Accessed 03/01/2024].

BOAVIDA-PORTUGAL, J. et al. (2022b) Global Patterns of Coastal Cephalopod Diversity Under Climate Change. *Frontiers in Marine Science*, 8, [Online] Available from: [doi.org/10.3389/fmars.2021.740781](https://doi.org/10.3389/fmars.2021.740781) [Accessed 28/09/2024].

BOBOWSKI, B.T.C. et al. (2023) Cephalopods, a gap in the European Marine Strategy Framework Directive and their future integration. *Marine Biology*, 170(3), p. 26.

BORGES, F.O. et al. (2023) Climate-Change Impacts on Cephalopods: A Meta-Analysis. *Integrative and Comparative Biology*, 63(6), pp. 1240–1265.

BOUDREAU, S.A. and WORM, B. (2012) Ecological role of large benthic decapods in marine ecosystems: a review. *Marine Ecology Progress Series*, 469, pp. 195–213.

BOYLE, P. and RODHOUSE, P. (2008) *Cephalopods: Ecology and Fisheries*. John Wiley & Sons.

BUSS, D. et al. (2022) Evidence of resource partitioning between fin and sei whales during the twentieth-century whaling period. *Marine Biology*, 169, [Online] Available from: [doi.org/10.1007/s00227-022-04131-x](https://doi.org/10.1007/s00227-022-04131-x).

CARLETON, S.A. and DEL RIO, C.M. (2010) Growth and catabolism in isotopic incorporation: a new formulation and experimental data. *Functional Ecology*, 24(4), pp. 805–812.

CARTER, W.A., BAUCHINGER, U. and MCWILLIAMS, S.R. (2019) The Importance of Isotopic Turnover for Understanding Key Aspects of Animal Ecology and Nutrition. *Diversity*, 11(5), p. 84.

CASTRO, B.G. and GUERRA, Á. (1990) The diet of *Sepia officinalis* (Linnaeus, 1758) and *Sepia elegans* (D'Orbigny, 1835) (Cephalopoda, Sepioidea) from the Ría de Vigo (NW Spain). [Online] Available from: <https://digital.csic.es/handle/10261/25072> [Accessed 23/08/2024].

CHASE, J.M. and LEIBOLD, M.A. (2003) *Ecological Niches: Linking Classical and Contemporary Approaches*. University of Chicago Press.

CHEN, C.S. et al. (2006) The apparent disappearance of *Loligo forbesi* from the south of its range in the 1990s: Trends in *Loligo* spp. abundance in the northeast Atlantic and possible environmental influences. *Fisheries Research*, 78(1), pp. 44–54.

CHEN, P. et al. (2021) Interannual Abundance Fluctuations of Two Oceanic Squids in the Pacific Ocean Can Be Evaluated Through Their Habitat Temperature Variabilities. *Frontiers in Marine Science*, 8, [Online] Available from: [doi.org/10.3389/fmars.2021.770224](https://doi.org/10.3389/fmars.2021.770224) [Accessed 25/03/2024].

CHEN, X. et al. (2012) Relationship between beak morphological variables and body size and mantle length of male and female Argentine shortfin squid (*Illex argentinus*). *Journal of Ocean University of China*, 11(4), pp. 539–546.

CHEREL, Y. and HOBSON, K.A. (2005) Stable isotopes, beaks and predators: a new tool to study the trophic ecology of cephalopods, including giant and colossal squids. *Proceedings of the Royal Society B: Biological Sciences*, 272(1572), pp. 1601–1607.

CHEREL, Y. et al. (2009) Tissue, ontogenic and sex-related differences in  $\delta^{13}\text{C}$  and  $\delta^{15}\text{N}$  values of the oceanic squid *Todarodes filippovae* (Cephalopoda: Ommastrephidae). *Marine Biology*, 156(4), pp. 699–708.

CHEREL, Y., BUSTAMANTE, P. and RICHARD, P. (2019) Amino acid  $\delta^{13}\text{C}$  and  $\delta^{15}\text{N}$  from sclerotized beaks: a new tool to investigate the foraging ecology of cephalopods, including giant and colossal squids. *Marine Ecology Progress Series*, 624, pp. 89–102.

CHEUNG, W.W.L. et al. (2012) Review of climate change impacts on marine fisheries in the UK and Ireland. *Aquatic Conservation: Marine and Freshwater Ecosystems*, 22(3), pp. 368–388.

CHOUVELON, T. et al. (2011) Inter-specific and ontogenic differences in  $\delta^{13}\text{C}$  and  $\delta^{15}\text{N}$  values and Hg and Cd concentrations in cephalopods. *Marine Ecology Progress Series*, 433, pp. 107–120.

CHRISTENSEN, V. and WALTERS, C.J. (2004) Ecopath with Ecosim: methods, capabilities and limitations. *Ecological Modelling*, 172(2), pp. 109–139.

CHUNG, M.-T. et al. (2020) Elemental Ratios in Cuttlebone Indicate Growth Rates in the Cuttlefish *Sepia pharaonis*. *Frontiers in Marine Science*, 6, [Online] Available from: [doi.org/10.3389/fmars.2019.00796](https://doi.org/10.3389/fmars.2019.00796) [Accessed 14/10/2024].

CHUNG, M.-T. et al. (2021) Metabolic proxy for cephalopods: Stable carbon isotope values recorded in different biogenic carbonates. *Methods in Ecology and Evolution*, 12(9), pp. 1648–1657.

COOPER, R.N. and WISSEL, B. (2012) Loss of trophic complexity in saline prairie lakes as indicated by stable-isotope based community-metrics. *Aquatic Biosystems*, 8(1), p. 6.

COSTA-PEREIRA, R. et al. (2019) Competition and resource breadth shape niche variation and overlap in multiple trophic dimensions. *Proceedings of the Royal Society B: Biological Sciences*, 286(1902), p. 20190369.

CURTIS, J.S. et al. (2020) Stable isotope analysis of eye lenses from invasive lionfish yields record of resource use. *Marine Ecology Progress Series*, 637, pp. 181– 194.

DAUVIN, J.-C. (2019) Chapter 6 - The English Channel: La Manche. In: SHEPPARD, C. (ed.) *World Seas: an Environmental Evaluation* (Second Edition). Academic Press, pp. 153–188.

DAVIES, D. et al. (2018) Supporting sustainable *Sepia* stocks. Inshore Fisheries and Conservation Authority.

DENIRO, M.J. and EPSTEIN, S. (1978) Influence of diet on the distribution of carbon isotopes in animals. *Geochimica et Cosmochimica Acta*, 42(5), pp. 495–506.

DENNIS, R.L.H. et al. (2011) The generalism–specialism debate: the role of generalists in the life and death of species. *Biological Journal of the Linnean Society*, 104(4), pp. 725–737.

DEVRIES, M.S. et al. (2015) Isotopic Incorporation Rates and Discrimination Factors in Mantis Shrimp Crustaceans. *PLOS ONE*, 10(4), p. e0122334.

DILLON, K.S. et al. (2021) Stable Isotopic Niche Variability and Overlap across Four Fish Guilds in the North-Central Gulf of Mexico. *Marine and Coastal Fisheries*, 13(3), pp. 213–227.

DOMINGUES, P.M., SYKES, A. and ANDRADE, J.P. (2002) The effects of temperature in the life cycle of two consecutive generations of the cuttlefish *Sepia officinalis* (Linnaeus, 1758), cultured in the Algarve (South Portugal). *Aquaculture International*, 10(3), pp. 207–220.

DOREY, N. et al. (2013) Ocean acidification and temperature rise: effects on calcification during early development of the cuttlefish *Sepia officinalis*. *Marine Biology*, 160(8), pp. 2007–2022.

DOUBLEDAY, Z.A. et al. (2016) Global proliferation of cephalopods. *Current Biology*, 26(10), pp. R406–R407.

DU, J. et al. (2020) Comparing trophic levels estimated from a tropical marine food web using an ecosystem model and stable isotopes. *Estuarine, Coastal and Shelf Science*, 233, p. 106518.

DUNN, M.R. (1999) Aspects of the stock dynamics and exploitation of cuttlefish, *Sepia officinalis* (Linnaeus, 1758), in the English Channel. *Fisheries Research*, 40(3), pp. 277–293.

EATON, T. (2019) Cephalopod Diet. In: VONK, J. and SHACKELFORD, T. (eds.) *Encyclopedia of Animal Cognition and Behavior*. Cham: Springer International Publishing, pp. 1–7.

FRANZOI, A. (2016) ANIMAL ECOLOGY THROUGH STABLE ISOTOPE ANALYSIS. [Online] Available from: <https://iris.unipv.it/handle/11571/1203350> [Accessed 19/03/2025].

FRY, B. (2006a) *Stable Isotope Ecology*. New York, NY: Springer.

FRY, B. (2006b) Using Stable Isotope Tracers. In: FRY, B. (ed.) *Stable Isotope Ecology*. New York, NY: Springer, pp. 40–75.

FRY, B. and ARNOLD, C. (1982) Rapid  $^{13}\text{C}/^{12}\text{C}$  turnover during growth of brown shrimp (*Penaeus aztecus*). *Oecologia*, 54(2), pp. 200–204.

FRY, B. and SHERR, E.B. (1989)  $\delta^{13}\text{C}$  Measurements as Indicators of Carbon Flow in Marine and Freshwater Ecosystems. In: RUNDEL, P.W., EHLERINGER, J.R. and NAGY, K.A. (eds.) *Stable Isotopes in Ecological Research*. New York, NY: Springer, pp. 196–229.

GANIAS, K. et al. (2021) Fishing for cuttlefish with traps and trammel nets: A comparative study in Thermaikos Gulf, Aegean Sea. *Fisheries Research*, 234, p. 105783.

GIBSON, R.N., ATKINSON, R.J.A. and GORDON, J.D.M. (eds.) (2016) Cephalopods in the north-eastern Atlantic: species, biogeography, ecology, exploitation and conservation. In: *Oceanography and Marine Biology*. CRC Press, pp. 123–202.

GLEGG, G., JEFFERSON, R. and FLETCHER, S. (2015) Marine governance in the English Channel (La Manche): Linking science and management. *Marine Pollution Bulletin*, 95(2), pp. 707–718.

GOFF, R.L. and DAGUZAN, J. (1991) Growth and Life Cycles of the Cuttlefish *Sepia Officinalis* L. (Mollusca: Cephalopoda) in South Brittany (France). *Bulletin of Marine Science*, 49(1–2), pp. 341–348.



- GRAS, M. et al. (2016) Stock structure of the English Channel common cuttlefish *Sepia officinalis* (Linnaeus, 1758) during the reproduction period. *Journal of the Marine Biological Association of the United Kingdom*, 96(1), pp. 167–176.
- GRAY, M.J. (1996) The coastal fisheries of England and Wales, part III: a review of their status 1992-1994. *Oceanographic Literature Review*, 9(43), p. 936.
- GUERRA, Á. (2006) Ecology of *sepia officinalis*. [Online] Available from: <https://digital.csic.es/handle/10261/51142> [Accessed 18/03/2025].
- GUERRA, A. and CASTRO, B.G. (1988) On the life cycle of *Sepia officinalis* (Cephalopoda, Sepioidea) in the ria de Vigo (NW Spain). *On the life cycle of Sepia officinalis* (Cephalopoda, Sepioidea) in the ria de Vigo (NW Spain), 29(3), pp. 395–405.
- GUERRA, Á. et al. (2010) Life-history traits of the giant squid *Architeuthis dux* revealed from stable isotope signatures recorded in beaks. *ICES Journal of Marine Science*, 67(7), pp. 1425–1431.
- GUERRA-MARRERO, A. et al. (2023) Age validation in early stages of *Sepia officinalis* from beak microstructure. *Marine Biology*, 170(2), p. 24.
- HABITAT FOR FISHERY SPECIES. In: *Oceanography and Marine Biology*. CRC Press.
- HANLON, R.T. and MESSENGER, J.B. (2018) *Cephalopod Behaviour*. Cambridge University Press.
- HARRISON, M.K. (1997) The evolution of size-dependent habitat use in Cancer crabs : evidence from phylogenetics, natural selection analysis, and behavioural ecology.
- HAYDEN, B. et al. (2013) Interactions between invading benthivorous fish and native whitefish in subarctic lakes. *Freshwater Biology*, 58(6), pp. 1234–1250.
- HERNANDEZ FARINAS, T. et al. (2014) Temporal changes in the phytoplankton community along the French coast of the eastern English Channel and the southern Bight of the North Sea. *Ices Journal Of Marine Science*, 71(4), pp. 821–833.
- HETTE-TRONQUART, N. (2019) Isotopic niche is not equal to trophic niche. *Ecology Letters*, 22(11), pp. 1987–1989.
- HEWITT, D.E. et al. (2021) Diet-tissue discrimination and turnover of  $\delta^{13}\text{C}$  and  $\delta^{15}\text{N}$  in muscle tissue of a penaeid prawn. *Rapid Communications in Mass Spectrometry*, 35(19), p. e9167.
- HILBORN, R. et al. (2023) Evaluating the sustainability and environmental impacts of trawling compared to other food production systems RAICEVICH, S. (ed.). *ICES Journal of Marine Science*, 80(6), pp. 1567–1579.

- HOBSON, K.A. (1999) Tracing origins and migration of wildlife using stable isotopes: a review. *Oecologia*, 120(3), pp. 314–326.
- HOBSON, K.A. (2008) Applying Isotopic Methods to Tracking Animal Movements. In: *Terrestrial Ecology. Tracking Animal Migration with Stable Isotopes*. Elsevier, pp. 45–78.
- HOBSON, K.A. and CHEREL, Y. (2006) Isotopic reconstruction of marine food webs using cephalopod beaks: new insight from captively raised *Sepia officinalis*. *Canadian Journal of Zoology*, 84(5), pp. 766–770.
- HOBSON, K.A. and CLARK, R.G. (1992) Assessing Avian Diets Using Stable Isotopes I: Turnover of  $^{13}\text{C}$  in Tissues. *The Condor*, 94(1), pp. 181–188.
- HOBSON, K.A. and WASSENAAR, L.I. (2018) *Tracking Animal Migration with Stable Isotopes*. Academic Press.
- HOEINGHAUS, D.J. and III, S.E.D. (2007) Size-based trophic shifts of saltmarsh dwelling blue crabs elucidated by dual stable C and N isotope analyses. *Marine Ecology Progress Series*, 334, pp. 199–204.
- HUNSICKER, M. et al. (2010) Predatory role of the commander squid *Beryteuthis magister* in the eastern Bering Sea: insights from stable isotopes and food habits. *Marine Ecology Progress Series*, 415, pp. 91–108.
- HUNSICKER, M.E. et al. (2011) Functional responses and scaling in predator–prey interactions of marine fishes: contemporary issues and emerging concepts. *Ecology Letters*, 14(12), pp. 1288–1299.
- HUNTER, E. et al. (2013) Edible Crabs “Go West”: Migrations and Incubation Cycle of *Cancer pagurus* Revealed by Electronic Tags. *PLOS ONE*, 8(5), p. e63991.
- HUTCHINSON, G.E. (1978) *An introduction to population ecology*. Yale University Press New Haven.
- HYSLOP, E.J. (1980) Stomach contents analysis—a review of methods and their application. *Journal of Fish Biology*, 17(4), pp. 411–429.
- ICES (2023) Working Group on Cephalopod Fisheries and Life History (WGCEPH; Outputs from 2022 meeting). ICES Scientific Reports.
- Influencing Spawning, Early Life Stage Survival and Recruitment Variability in the Common Cuttlefish (*Sepia officinalis*). In: *Advances in Marine Biology*.
- JACKSON, A.L. et al. (2011) Comparing isotopic niche widths among and within communities: SIBER – Stable Isotope Bayesian Ellipses in R. *Journal of Animal Ecology*, 80(3), pp. 595–602.

- JACKSON, G.D. et al. (2007) Applying new tools to cephalopod trophic dynamics and ecology: perspectives from the Southern Ocean Cephalopod Workshop, February 2–3, 2006. *Reviews in Fish Biology and Fisheries*, 17(2), pp. 79–99.
- JEREB, P. and ROPER, C.F.E. (2010) *Cephalopods of the world: an annotated and illustrated catalogue of cephalopod species known to date*. Rome: FAO.
- JONES, K.A. et al. (2020) Intra-specific Niche Partitioning in Antarctic Fur Seals, *Arctocephalus gazella*. *Scientific Reports*, 10(1), p. 3238.
- KELLER, S. et al. (2014) Influence of environmental parameters on the life-history and population dynamics of cuttlefish *Sepia officinalis* in the western Mediterranean. *Estuarine, Coastal and Shelf Science*, 145, pp. 31–40.
- KNIGHT, T.M. et al. (2005) Trophic cascades across ecosystems. *Nature*, 437(7060),
- KOCH, P.L. (2007) Isotopic Study of the Biology of Modern and Fossil Vertebrates. *Stable Isotopes in Ecology and Environmental Science*, 2, pp. 99–154.
- KOUETA, N. and BOUCAUD-CAMOU, E. (2003) Combined effects of photoperiod and feeding frequency on survival and growth of juvenile cuttlefish *Sepia officinalis*
- KRUMSICK, K.J. and FISHER, J.A.D. (2019) Spatial and ontogenetic variation in isotopic niche among recovering fish communities revealed by Bayesian modeling. *PLOS ONE*, 14(4), p. e0215747.
- L.JACKSON, E. et al. (2001) THE IMPORTANCE OF SEAGRASS BEDS AS A HABITAT FOR FISHERY SPECIES. In: *Oceanography and Marine Biology*. CRC Press.
- LANCASTER, L.T., MORRISON, G. and FITT, R.N. (2017) Life history trade-offs, the intensity of competition, and coexistence in novel and evolving communities under climate change. *Philosophical Transactions of the Royal Society B: Biological Sciences*, 372(1712), p. 20160046.
- LAWTON, P. (1989) Predatory interaction between the brachyuran crab *Cancer pagurus* and decapod crustacean prey. *Marine Ecology Progress Series*, 52, pp. 169–179.
- LAWTON, P. (1995) Postlarval, juvenile, adolescent, and adult ecology. *Biology of the Lobster Homarus americanus*, [Online] Available from: <https://cir.nii.ac.jp/crid/1571980075553989504> [Accessed 18/03/2025].
- LAYMAN, C.A. et al. (2007) Can Stable Isotope Ratios Provide for Community-Wide Measures of Trophic Structure? *Ecology*, 88(1), pp. 42–48.
- LAYMAN, C.A. et al. (2012) Applying stable isotopes to examine food-web structure: an overview of analytical tools. *Biological Reviews*, 87(3), pp. 545–562.

LEVIS, N.A. et al. (2017) Intraspecific adaptive radiation: Competition, ecological opportunity, and phenotypic diversification within species. *Evolution*, 71(10), pp. 2496–2509.

LISHCHENKO, F. et al. (2021) A review of recent studies on the life history and ecology of European cephalopods with emphasis on species with the greatest commercial fishery and culture potential. *Fisheries Research*, 236, p. 105847.

MACAVOY, S.E., ARNESON, L.S. and BASSETT, E. (2006) Correlation of metabolism with tissue carbon and nitrogen turnover rate in small mammals. *Oecologia*, 150(2), pp. 190–201.

MACNEIL, M., SKOMAL, G. and FISK, A. (2005) Stable isotopes from multiple tissues reveal diet switching in sharks. *Marine Ecology Progress Series*, 302, pp.

MARSHALL, H.H. et al. (2019) Stable isotopes are quantitative indicators of trophic niche. *Ecology Letters*, 22(11), pp. 1990–1992.

MARTÍNEZ DEL RIO, C. et al. (2009) Isotopic ecology ten years after a call for more laboratory experiments. *Biological Reviews*, 84(1), pp. 91–111.

MCCLELLAN, C.M. et al. (2014) Understanding the Distribution of Marine Megafauna in the English Channel Region: Identifying Key Habitats for Conservation within the Busiest Seaway on Earth. *PLOS ONE*, 9(2), p. e89720.

MCINTYRE, P.B. and FLECKER, A.S. (2006) Rapid turnover of tissue nitrogen of primary consumers in tropical freshwaters. *Oecologia*, 148(1), pp. 12–21.

MEATH, B. et al. (2019) Stable isotopes in the eye lenses of *Doryteuthis plei* (Blainville 1823): Exploring natal origins and migratory patterns in the eastern Gulf of Mexico. *Continental Shelf Research*, 174, pp. 76–84.

MICHAEL HARAMIS, G. et al. (2007) Stable isotope and pen feeding trial studies confirm the value of horseshoe crab *Limulus polyphemus* eggs to spring migrant shorebirds in Delaware Bay. *Journal of Avian Biology*, 38(3), pp. 367–376.

MIDANI, F.S., WYNN, M.L. and SCHNELL, S. (2017) The importance of accurately correcting for the natural abundance of stable isotopes. *Analytical biochemistry*, 520, pp. 27–43.

MIDANI, F.S., WYNN, M.L. and SCHNELL, S. (2017) The importance of accurately correcting for the natural abundance of stable isotopes. *Analytical biochemistry*, 520, pp. 27–43.

MILLER, J., MILLAR, J. and LONGSTAFFE, F. (2008) Carbon- and nitrogen-isotope tissue-diet discrimination and turnover rates in deer mice, *Peromyscus maniculatus*. *Canadian Journal of Zoology*, 86, pp. 685–691.

MINAGAWA, M. and WADA, E. (1984) Stepwise enrichment of  $^{15}\text{N}$  along food chains: Further evidence and the relation between  $\delta^{15}\text{N}$  and animal age. *Geochimica et Cosmochimica Acta*, 48(5), pp. 1135–1140.

MISEREZ, A. et al. (2008) The Transition from Stiff to Compliant Materials in Squid Beaks. *Science*, 319(5871), pp. 1816–1819.

MMO (2022) UK Sea Fisheries Statistics 2022. Marine Management Organisation. MMO.

MORISSETTE, L., CHRISTENSEN, V. and PAULY, D. (2012) Marine Mammal Impacts in Exploited Ecosystems: Would Large Scale Culling Benefit Fisheries? *PLOS ONE*, 7(9), p. e43966.

NEVES, A. et al. (2009) Feeding habits of the cuttlefish *Sepia officinalis* during its life cycle in the Sado estuary (Portugal). *Hydrobiologia*, 636(1), pp. 479–488.

NEWSOME, S.D. et al. (2007) A niche for isotopic ecology. *Frontiers in Ecology and the Environment*, 5(8), pp. 429–436.

OBERLE, F.K.J., STORLAZZI, C.D. and HANEBUTH, T.J.J. (2016) What a drag: *Oecologia*, 144(4), pp. 598–606.

OESTERWIND, D. et al. (2022) Climate change-related changes in cephalopod biodiversity on the North East Atlantic Shelf. *Biodiversity and Conservation*, 31(5), pp. 1491–1518.

OGLOFF, W.R. et al. (2019) Diet and isotopic niche overlap elucidate competition potential between seasonally sympatric phocids in the Canadian Arctic. *Marine Biology*, 166(8), p. 103.

ONDERZ. FORM. B. et al. (2022) The role of the European lobster (*Homarus gammarus*) in the ecosystem : An inventory as part of a feasibility study for passive fisheries on European lobster *Homarus gammarus* in offshore wind farms. IJmuiden: Wageningen Marine Research.

ONTHANK, K.L. (2013) Exploring the life histories of cephalopods using stable isotope analysis of an archival tissue. Ph.D. United States -- Washington: Washington State University.

PELAGE, L. et al. (2022) Competing with each other: Fish isotopic niche in two resource availability contexts. *Frontiers in Marine Science*, 9, [Online] Available from: [doi.org/10.3389/fmars.2022.975091](https://doi.org/10.3389/fmars.2022.975091) [Accessed 08/08/2024].

PERGA, M.E. and GERDEAUX, D. (2005) 'Are fish what they eat' all year round? *Oecologia*, 144(4), pp. 598–606.

PIERCE, G.J. et al. (2008) A review of cephalopod–environment interactions in European Seas. *Hydrobiologia*, 612(1), pp. 49–70.

PIERCE, R. and O'DOR, R. (2013) *Advances in Squid Biology, Ecology and Fisheries. Part I, Myopsid Squids*. New York, NY: Nova Publishers, [Online] Available from: <https://cir.nii.ac.jp/crid/1130282268688703744> [Accessed 29/04/2024].

PLANQUE, Y. et al. (2021) Trophic niche overlap between sympatric harbour seals (*Phoca vitulina*) and grey seals (*Halichoerus grypus*) at the southern limit of their European range (Eastern English Channel). *Ecology and Evolution*, 11(15), pp. 10004–10025.

PONCE, T. et al. (2021) Isotopic niche and niche overlap in benthic crustacean and demersal fish associated to the bottom trawl fishing in south-central Chile. *Journal of Sea Research*, 173, p. 102059.

POST, D.M. (2002) The long and short of food-chain length. *Trends in Ecology & Evolution*, 17(6), pp. 269–277.

QUAECK-DAVIES, K. et al. (2018) Teleost and elasmobranch eye lenses as a target for life-history stable isotope analyses. *PeerJ*, 6, p. e4883.

QUEIRÓS, J.P. et al. (2018) Ontogenic changes in habitat and trophic ecology in the Antarctic squid *Kondakovia longimana* derived from isotopic analysis on beaks. *Polar Biology*, 41(12), pp. 2409–2421.

QUEIRÓS, J.P. et al. (2020) Cephalopod beak sections used to trace mercury levels throughout the life of cephalopods: The giant warty squid *Moroteuthopsis longimana* as a case study. *Marine Environmental Research*, 161, p. 105049.

REES, A., SHEEHAN, E.V. and ATTRILL, M.J. (2021) Optimal fishing effort benefits fisheries and conservation. *Scientific Reports*, 11(1), p. 3784.

REPOLHO, T. et al. (2014) Developmental and physiological challenges of octopus (*Octopus vulgaris*) early life stages under ocean warming. *Journal of Comparative Physiology B*, 184(1), pp. 55–64.

RODHOUSE, P.G.K. et al. (2014) Chapter Two - Environmental Effects on Cephalopod Population Dynamics: Implications for Management of Fisheries. In: VIDAL, E.A.G. (ed.) *Advances in Marine Biology. Advances in Cephalopod Science: Biology, Ecology, Cultivation and Fisheries*. Academic Press, pp. 99–233.

RODRÍGUEZ-DOMÍNGUEZ, A. et al. (2013) Validation of growth increments in stylets, beaks and lenses as ageing tools in *Octopus maya*. *Journal of Experimental Marine Biology and Ecology*, 449, pp. 194–199.

ROSA, R., O'DOR, R. and PIERCE, G.J. (2013) *Advances in Squid Biology, Ecology and Fisheries. Part I: Myopsid Squids*. Nova Science Publishers Inc.

- ROYER, J. et al. (2006) The English Channel stock of *Sepia officinalis*: Modelling variability in abundance and impact of the fishery. *Fisheries Research*, 78(1), pp. 96–106.
- RUBENSTEIN, D.R. and HOBSON, K.A. (2004) From birds to butterflies: animal movement patterns and stable isotopes. *Trends in Ecology & Evolution*, 19(5), pp. 256–263.
- SACCÒ, M. et al. (2019) New light in the dark - a proposed multidisciplinary framework for studying functional ecology of groundwater fauna. *Science of The Total Environment*, 662, pp. 963–977.
- SAJIKUMAR, K.K. et al. (2020) Distribution, age and growth of the diamondback squid, *Thysanoteuthis rhombus* (Cephalopoda: Thysanoteuthidae) from the tropical Arabian Sea. *Fisheries Research*, 224, p. 105478.
- SAKAMOTO, T. et al. (2023) Stable isotopes in eye lenses reveal migration and mixing patterns of diamond squid in the western North Pacific and its marginal seas. *ICES Journal of Marine Science*, 80(9), pp. 2313–2328.
- SCOWEN, M. et al. (2021) The current and future uses of machine learning in ecosystem service research. *Science of The Total Environment*, 799, p. 149263.
- SHELTON, R.G.J. and HALL, W.B. (1981) A comparison of the efficiency of the Scottish creel and the inkwell pot in the capture of crabs and lobsters. *Fisheries Research*, 1, pp. 45–53.
- SHIPLEY, O.N. and MATICH, P. (2020) Studying animal niches using bulk stable isotope ratios: an updated synthesis. *Oecologia*, 193(1), pp. 27–51.
- SIEGENTHALER, A. et al. (2022) Niche separation between two dominant crustacean predators in European estuarine soft-bottom habitats. *Ecological Indicators*, 138, p. 108839.
- SMITH, I. et al. (2001) Movement of wild European lobsters *Homarus gammarus* in natural habitat. *Marine Ecology Progress Series*, 222, pp. 177–186.
- STAMP, T. et al. (2022) Large-scale historic habitat loss in estuaries and its implications for commercial and recreational fin fisheries. *ICES Journal of Marine Science*, 79(7), pp. 1981–1991.
- STEWART, J.S. et al. (2012) Marine predator migration during range expansion: Humboldt squid *Dosidicus gigas* in the northern California Current System. *Marine Ecology Progress Series*, 471, pp. 135–150.
- STOWASSER, G. et al. (2006) Experimental study on the effect of diet on fatty acid and stable isotope profiles of the squid *Lolliguncula brevis*. *Journal of Experimental Marine Biology and Ecology*, 333(1), pp. 97–114.

STURBOIS, A. et al. (2022) Stomach content and stable isotope analyses provide complementary insights into the trophic ecology of coastal temperate benthodemersal assemblages under environmental and anthropogenic pressures.

SUMAILA, U.R. and TAI, T.C. (2020) End Overfishing and Increase the Resilience of the Ocean to Climate Change. *Frontiers in Marine Science*, 7, [Online] Available from: [doi.org/10.3389/fmars.2020.00523](https://doi.org/10.3389/fmars.2020.00523) [Accessed 22/08/2024].

SURING, E. and WING, S.R. (2009) Isotopic turnover rate and fractionation in multiple tissues of red rock lobster (*Jasus edwardsii*) and blue cod (*Parapercis colias*): Consequences for ecological studies. *Journal of Experimental Marine Biology and Ecology*, 370(1), pp. 56–63.

SWANSON, H.K. et al. (2015) A new probabilistic method for quantifying n-dimensional ecological niches and niche overlap. *Ecology*, 96(2), pp. 318–324.

TENNESSEN, J.B. et al. (2023) Divergent foraging strategies between populations of sympatric matrilineal killer whales. *Behavioral Ecology*, 34(3), pp. 373–386.

Terrestrial Ecology. Tracking Animal Migration with Stable Isotopes. Elsevier, the north-eastern Atlantic: species, biogeography, ecology, exploitation and conservation. In: *Oceanography and Marine Biology*. CRC Press, pp. 123–202.

TILCOCK, M.N. (2019) Isotope Tools To Track Floodplain Rearing of Juvenile Chinook Salmon. M.S. United States -- California: University of California, Davis.

TONDER, A. VAN et al. (2021) Ecology of *Moroteuthopsis longimana* at the sub-Antarctic Prince Edward Islands, revealed through stable isotope analysis of squid beaks. *Marine Ecology Progress Series*, 658, pp. 105–115.

TRUEMAN, C.N., MACKENZIE, K.M. and PALMER, M.R. (2012) Identifying migrations in marine fishes through stable-isotope analysis. *Journal of Fish Biology*, 81(2), pp. 826–847.

VALDOVINOS, F.S., BODINI, A. and JORDÁN, F. (2024) Connected interactions: enriching food web research by spatial and social interactions. *Philosophical Transactions of the Royal Society B: Biological Sciences*, 379(1909), p.

VINAGRE, C. et al. (2011) Effect of body size and body mass on  $\delta^{13}\text{C}$  and  $\delta^{15}\text{N}$  in coastal fishes and cephalopods. *Estuarine, Coastal and Shelf Science*, 95(1), pp. 264–267.

WANG, J. et al. (2003) Spatial and temporal patterns of cuttlefish (*Sepia officinalis*) abundance and environmental influences – a case study using trawl fishery data in French Atlantic coastal, English Channel, and adjacent waters. *ICES Journal of Marine Science*, 60(5), pp. 1149–1158.



WEBER, S., CULLEN, J.A. and FUENTES, M.M.P.B. (2023) Isotopic niche overlap among foraging marine turtle species in the Gulf of Mexico. *Ecology and Evolution*, 13(11), p. e10741.

WINTER, E.R. et al. (2019) Estimating stable isotope turnover rates of epidermal mucus and dorsal muscle for an omnivorous fish using a diet-switch experiment. *Hydrobiologia*, 828(1), pp. 245–258.

WOOD, S.L.R. et al. (2022) Missing Interactions: The Current State of Multispecies Connectivity Analysis. *Frontiers in Ecology and Evolution*, 10, [Online] Available from: [doi.org/10.3389/fevo.2022.830822](https://doi.org/10.3389/fevo.2022.830822) [Accessed 24/03/2024].

WU, L. et al. (2018) Compound-specific  $^{15}\text{N}$  analysis of amino acids: A tool to estimate the trophic position of tropical seabirds in the South China Sea. *Ecology and Evolution*, 8(17), pp. 8853–8864.

X. PAYNE, L. and W. MOORE, J. (2006) Mobile scavengers create hotspots of freshwater productivity. *Oikos*, 115(1), pp. 69–80.

XAVIER, J.C. et al. (2022) The significance of cephalopod beaks as a research tool: An update. *Frontiers in Physiology*, 13, [Online] Available from: [doi.org/10.3389/fphys.2022.1038064](https://doi.org/10.3389/fphys.2022.1038064) [Accessed 17/03/2024].

XU, W. et al. (2019) Inter-individual variation in trophic history of *Dosidicus gigas*, as indicated by stable isotopes in eye lenses. *Aquaculture and Fisheries*, 4(6),

ZHANG, J. et al. (2022) Ontogenetic Trophic Shifts by *Ommastrephes bartramii* in the North Pacific Ocean Based on Eye Lens Stable Isotopes. *Fishes*, 7(5), p. 295.

ZIEGLER, A., MILLER, A. and NAGELMANN, N. (2021) Novel insights into early life stages of finned octopods (Octopoda: Cirrata). *Swiss Journal of Palaeontology*, 140(1), p. 24.

ZIEGLER, A., MILLER, A. and NAGELMANN, N. (2021) Novel insights into early life stages of finned octopods (Octopoda: Cirrata). *Swiss Journal of Palaeontology*, 140(1), p. 24.